Supersonic Aerodynamic Characteristics of a Circular Body Earth-to-Orbit Vehicle

George M. Ware and Walter C. Engelund
Langley Research Center • Hampton, Virginia

Ian O. MacConochie
Lockheed Engineering & Sciences Company • Hampton, Virginia

January 1994

Summary

The circular body configuration was investigated as a generic shape applicable to single- or multi-stage reusable Earth-to-orbit transports. The principal attribute of the configuration is its low structural mass for a given propellant loading. The low mass results from the utilization of a simple cylindrical body having a circular cross section. A thick clipped-delta wing was the major lifting surface. For directional control, three different vertical fin arrangements were investigated: a conventional aft-mounted center fin, wingtip fins, and a nose-mounted fin. The tests were conducted in the Langley Unitary Plan Wind Tunnel at Mach numbers of 1.60, 2.30, 2.96, 3.90, and 4.60.

The results of the investigation indicate that the configuration is longitudinally stable about the estimated center of gravity at 0.72 body length up to a Mach number of about 3.00. Above Mach 3.00, the model is longitudinally unstable at low angles of attack but has a stable secondary trim point at angles of attack around 30°. The model has sufficient pitch control authority with elevator and body flap to produce stable trim over the test range. The aft-center-fin configuration is directionally stable at low angles of attack up to a Mach number of 3.90. The wingtip and nose fins are not intended to produce directional stability.

The rudder-like surfaces on the tip fins and the all-movable nose fin were designed as active controls to produce artificial directional stability. These controls were effective in producing yawing moment. Yawing moments produced by deflecting the rudder on the aft center fin were accompanied by adverse roll. Differential deflection of the aileron surfaces on the wing trailing edge was effective in producing rolling moment but was accompanied by large values of adverse yawing moment. The test, however, was conducted only with the nose fin configuration and the fin was deflected. While an attempt was made to eliminate the effect of fin deflection, there is no assurance that this was successful, and it may be a contributing factor to the large adverse rolling moment.

Introduction

NASA is investigating concepts for use as future space transportation systems. The studies have included single- and multi-stage Earth-to-orbit designs (refs. 1 to 5). Structural weight is a critical factor in the performance and cost of these systems. Therefore, having an efficient lightweight structure is an important consideration. A circular cross-section body was investigated because of its high strength-to-weight and strength-to-volume ratios. The design is a generic configuration that can be used as a single-stage vehicle or as an orbiter or booster element of a multi-stage system. The structural, subsonic aerodynamic, and hypersonic heating characteristics are presented in references 6 to 8, respectively.

The present investigation was made to determine the supersonic aerodynamic characteristics of the circular body vehicle (CBV) during unpowered entry. The model has a large circular fuselage and an aft-mounted clipped-delta wing. The estimated center of gravity of the vehicle was at 72 percent of the body length. (The aft location results from the heavy rocket motors at the base with empty fuel tanks in the forward body.) The aft center of gravity causes control effectiveness problems due to the short moment arms associated with aft-mounted surfaces. Three vertical fins were tested for directional control: a conventional aft-mounted center fin, wingtip fins, and a nose-mounted fin. Pitch and roll control surfaces were mounted on the wing trailing edge. A movable body flap extended aft of the fuselage. The tests were conducted in the Langley Unitary Plan Wind Tunnel for Mach numbers of 1.60, 2.30, 2.96, 3.90, and 4.60.

Symbols

The longitudinal data are referred to the stability-axis system and the lateral-directional data are referred to the body-axis system (fig. 1). The data are normalized by the planform area, span, and mean aerodynamic chord of the wing, excluding the body flap. The moment reference center was located at the proposed vehicle center of gravity, which is at 0.72 body length from the nose.

b body span, in.

C_D drag coefficient, $\text{Drag}/qS_{\text{ref}}$

C_L lift coefficient, $\text{Lift}/qS_{\text{ref}}$

C_l rolling-moment coefficient, Rolling moment$/qS_{\text{ref}}b$

C_{l_β} $\Delta C_l/\Delta\beta$ taken at $\beta = 0°$ and $4°$, per deg

C_m pitching-moment coefficient, Pitching moment$/qS_{\text{ref}}\bar{c}$

C_n yawing-moment coefficient, Yawing moment$/qS_{\text{ref}}b$

C_{n_β} $\Delta C_n/\Delta\beta$, taken at $\beta = 0°$ and $4°$, per deg

C_Y side-force coefficient, Side force$/qS_{\text{ref}}$

C_{Y_β} $\Delta C_Y/\Delta\beta$ taken at $\beta = 0°$ and $4°$, per deg

$\bar{c}$ wing mean aerodynamic chord, in.

L/D	lift-drag ratio
M	Mach number at free-stream conditions
q	free-stream dynamic pressure, lb/in^2
S_{ref}	wing planform area (projected to body centerline including body flap), in^2
X	longitudinal body axis
Y	lateral body axis
Z	vertical body axis
α	angle of attack, deg
β	angle of sideslip, deg
δ_a	aileron control deflection angle $(\delta_{a,L} - \delta_{a,R})/2$, deg
δ_{BF}	body flap deflection angle (positive when deflected downward), deg
δ_e	elevator deflection angle (positive when deflected downward), deg
δ_n	nose-fin deflection angle (positive when deflected with trailing edge to right), deg
δ_r	rudder deflection angle (positive when deflected with trailing edge to left), deg
δ_{SB}	speed brake deflection angle, deg
δ_{TF}	tip-fin controller deflection angle (positive when deflected with trailing edge to left), deg

Subscripts:

max	maximum
L	left
R	right

Description of Model

Figure 2(a) is a photograph of the circular body orbiter model in the Langley Unitary Plan Wind Tunnel, and figure 2(b) is a sketch of the CBV showing the three fin arrangements tested. Dimensional information is given in figure 3 and table I. The configuration consists of a spherically blunted ogive nose blending into a large circular body with a clipped-delta wing mounted on the far aft underside. A movable body flap extends aft from the lower body. The wing is equipped with elevator surfaces on the inboard portion of the trailing edge and small aileron surfaces on the outboard portion. Three vertical control surfaces were investigated for directional control: (1) a large conventional center fin on the upper aft

fuselage, (2) a vertical fin near the fuselage nose, and (3) small fins on each wingtip.

The pitch control study consisted of elevator deflections of $\pm 10°$ and body flap deflection up to 25°. Roll control resulted from differential deflection of the ailerons. Yaw control was accomplished by deflection of surfaces on the aft center fin and wingtip fins. The control surfaces were simulated by wedges of 10°, 20°, and 30° attached to the fins. The wingtip control surfaces, referred to as tip-fin controllers, are designed to be deflected in an outward direction only. Yawing moment from the nose fin was generated by pivoting the fin about its 0.25-chord station. In addition to pitch, roll, and yaw control, various speed brake controls were investigated. Braking action for the model with the aft center fin was accomplished by flaring the split rudder. For the model with tip fins, braking consisted of simultaneous outward deflection of both tip-fin controllers. For the nose-fin configuration, aft side-body-mounted panels were deflected. (See figs. 2(b) and 3(d).)

Apparatus, Tests, and Corrections

Tests were conducted in the Langley Unitary Plan Wind Tunnel. The tunnel is a supersonic closed-circuit design with two test sections. The flow in the low-speed section can be varied from a Mach number of 1.50 to 2.80. The high-speed section produces Mach numbers from 2.30 to 4.60. Reference 9 contains additional information concerning this facility. The current investigation was conducted in the low-speed section at a Mach number of 1.60 and in the high-speed section at Mach numbers of 2.30, 2.96, 3.90, and 4.60. All tests were made at a constant Reynolds number of 2.0×10^6 per foot. The model was sting mounted through its base, and forces and moments were measured with an internally mounted strain-gauge balance.

Model angles of attack and sideslip were corrected for the sting and balance deflection under load. Customary tunnel corrections for flow angularity were applied to the data. In an attempt to produce turbulent flow over the model, transition grit was applied according to the method of reference 10. Two gritting techniques were used. In the low-speed section, No. 50 sand grains were thinly sprinkled in 1/16-in. bands located 1.2 in. aft of the nose and 0.3 in. perpendicular to the leading edge of the wing. The grit was located in the same positions for tests in the high-speed section; however, individual grains of No. 35 grit were applied at regular spacing of 4 grain diameters.

The model pitch range was a nominal $-2°$ to 22°. (Tests at $M = 1.60$ were limited to $\alpha = 18°$ because

2

Table I. Geometric Characteristics of Circular Body Model

Body:
    Length (reference length), in. 26.00
    Base area, in^2 . . . . 16.74
Wing:
    Airfoil . . . . NACA 0010-10
    Mean aerodynamic chord (reference length), in. 8.00
    Span (reference span), in. 17.52
    Area to body centerline (reference area), in^2 . . . . 121.65
    Area, exposed outside of body, in^2 . . . . 76.27
Aft center fin:
    Airfoil . . . . Double wedge
    Area, in^2 . . . . 25.00
Tip fins (each):
    Airfoil . . . . Modified wedge
    Area, in^2 . . . . 2.90
Nose fin:
    Airfoil . . . . Modified flat plate
    Area, in^2 . . . . 1.84
Control surfaces (each):
    Elevons:
        Area, in^2 . . . . 6.39
    Body flap:
        Area, in^2 . . . . 6.24
    Aileron:
        Area, in^2 . . . . 1.46
    Tip-fin controller (speed brake):
        Area, in^2 . . . . 1.27
    Aft-center-fin rudder (speed brake):
        Area, in^2 . . . . 6.15
    Body speedbrake:
        Area, in^2 . . . . 2.43

of model unsteadiness.) The model was tested at angles of sideslip of 0° and 4° over the angle-of-attack range. Data were taken in a pitch-pause manner as the model was moved from negative to positive angles. No base pressure corrections were applied to the data.

Results and Discussion

Longitudinal Characteristics

Baseline characteristics. In figure 4, lift, drag, and pitching-moment coefficients and lift-drag (L/D) ratio are plotted against angle of attack for the model with each of the vertical fin arrangements and with fins off. The data showed that the fin configuration had little effect on longitudinal aerodynamics with the exception of the conventional center fin arrangement. The large aft center fin (68 percent of the

exposed area of a single wing panel) produced more drag than the other fin arrangements. As a result, L/D values were lower and pitching moments were more positive because the drag of the fin acted above the model's center of gravity.

The variation of lift for all configurations was about the same and was relatively linear over the test angle-of-attack range. A high degree of longitudinal stability occurred at $M = 1.60$. As Mach number increased, the stability level decreased. At $M = 2.96$, the configurations were, in general, neutrally stable at low angles of attack and tended to be stable above $\alpha = 20°$. At $M = 3.90$ and above, the configurations were unstable at low angles of attack and again, the pitching-moment curves rotated in the stable direction above $\alpha = 12°$. Extrapolating the data, the configurations would have a stable trim point at

3

angles of attack from 26° to 30°. The untrimmed $(L/D)_{max}$ was about 3.0 at $M = 1.60$ and decreased to about 2.0 at $M = 4.60$ except for the aft-center-fin configuration. For this configuration, $(L/D)_{max}$ was 2.5 at the low Mach number and slightly lower than the others at the high Mach number.

Pitch control characteristics. Elevator effectiveness was studied with the vertical fins off for all Mach numbers except $M = 1.60$. At $M = 1.60$, the CBV model with the aft center fin was used. For consistency across the Mach range, elevator data have been simulated at $M = 1.60$ by adding increments from elevator deflection data from the model with a center fin to data for the model with no fins. The fins-off data (fig. 5) are considered applicable for the nose- and tip-fin configurations. For the aft-center-fin model, however, the difference in longitudinal trim discussed previously must be considered.

Elevator deflections studied were $\delta_e = 0°$ and $\pm 10°$. With $\delta_e = -10°$ at $M = 1.60$, the model was trimmed at a slightly positive angle of attack with low values of positive C_L. At $M = 2.96$ the model is almost neutrally stable. With pitch controls undeflected, a slightly unstable trim point occurs at $\alpha = 13°$ and a slightly stable trim point (extrapolated) at $\alpha = 25°$. At Mach numbers of 3.90 and 4.60, positive elevator deflection of 10° produced a stable trim point at $\alpha = 20°$. Therefore, in the speed range of this study, elevator control is capable of trimming the CBV at positive lift with positive or neutral longitudinal stability. The low lift values at low Mach numbers may make elevator deflections greater than $-10°$ undesirable because of the accompaning loss of lift.

Figure 6 shows the effects of body flap deflection as an additional pitch control. (The data at $M = 1.60$ were derived in a similar manner as for the elevator deflection data.) These data are again for the model with no vertical fins. The body flaps were deflected only in the positive direction (nose down pitch). Positive deflection drove the model trim to lower angles of attack. This effect was detrimental at the lower Mach numbers where stable trim was already at low angles of attack. However, at Mach numbers of 3.90 and 4.60 where the secondary trim point is of interest, positive body flap deflection produced stable trim at angles of attack that are more typical of lifting entry ($\alpha = 15°$ to 30°). Pitch control for the CBV by elevator and body flap deflection thus appears satisfactory in producing stable trim at positive lift across the test range.

Speed brake effects. The effects of the three different speed brake systems tested on the CBV model are given in figures 7 to 9. Speed brakes are used by a gliding unpowered spacecraft as an energy management device to adjust cross range and target the landing site. In figure 7 (the aft-center-fin arrangement), the brake was located on the split rudder of the fin. Data are presented with the brake open 7.5° on either side from the closed position. The brake was effective in increasing drag. However, the effectiveness of the brake decreased with increasing angle of attack and Mach number as the vertical fin became shielded by the wing and body. A large nose-up pitching moment resulted because of the increased drag above the model center of gravity. If speed brakes were used on the CBV in this fashion, a large compensating elevator deflection would have to accompany brake deflection.

Figure 8 shows the effect of tip-fin-mounted speed brakes. Because the surfaces were relatively small, deflections of 20° and 60° were tested. Since the brakes were extended out from the wingtips and were not blanketed by the wing, only a slight loss in effectiveness occurred with changes in angle of attack. The line of action for the drag increment of the tip-fin speed brakes was close enough to the estimated center of gravity that little change in pitching moment resulted.

The speed brakes for the nose-fin model were mounted on the sides of the body over the wing. No data for this configuration was taken at $M = 1.60$. As shown in figure 9, deflecting the side-body speed brakes increased drag only slightly. In fact, lift was decreased about as much as drag was increased. Apparently, the speed brakes decreased the negative pressure over the upper surface of the wing and a loss in lift resulted. There was a slight reduction in L/D values. The largest effect, however, was an introduction of a nose-up pitching-moment increment. In general, the body-mounted speed brakes were not effective.

Lateral Characteristics

Lateral-directional stability. The lateral-directional characteristics of the CBV are presented in figure 10 in the form of the stability parameters C_{Y_β}, C_{n_β}, and C_{l_β} plotted against angle of attack. Data are shown for the model with all fin configurations. The large aft center fin was the only fin configuration designed to give the CBV directional stability (positive C_{n_β}). The small wingtip fins housed rudder-like surfaces (tip-fin controllers) that could be continually deflected to add artificial directional stability. See reference 11 for a description of tip-fin controllers and their use. The all-movable nose-mounted fin was designed to act in a similar

manner. Sensors would detect deviation from the desired flight path and signal the nose fin to deflect to drive the CBV back on course or prevent the vehicle from diverging.

Directional stability of the aft-center-fin configuration decreased with increasing Mach number and angle of attack. For this configuration, the CBV was directionally stable at $M = 1.60$ up to an angle of attack of $14°$. At $M = 3.90$, the model was neutrally stable at $\alpha = 4°$ and unstable over the remainder of the angle-of-attack range. The model was unstable at $M = 4.60$. As expected, the tip-fin and nose-fin configurations were unstable over the Mach and angle-of-attack ranges. Little difference in effective dihedral parameter, $-C_{l_\beta}$, occurred between the fins-off, tip-fins, and nose-fin configurations. The nose fin and tip fins produced $+C_{l_\beta}$ values at low angles of attack and negative values at the higher angles. The aft-center-fin model had negative values of C_{l_β} at all Mach numbers and angles of attack.

Yaw control effects. Figure 11 shows the lateral control characteristics of the aft-center-fin configuration. Although a decrease in effectiveness occurred, deflection of the rudder produced yawing moments across the test Mach number and angle-of-attack ranges. The retention of effectiveness at high angles of attack is probably due to the large size of the aft center fin that placed the rudder high above the blanketing effect of the fuselage and wing. The high placement also caused relatively large adverse rolling moments with rudder deflection. The value of the rolling moment was about two-thirds that of the yawing moments at $M = 1.60$ and almost equal to the yawing moments at $M = 4.60$.

Figure 12 shows the effect of deflecting tip-fin controllers. The data indicate that the controllers were effective. Effectiveness decreased as Mach number increased, but yawing-moment values were almost constant over the angle-of-attack range at each Mach number. Only small adverse rolling moments resulted from controller deflection.

The nose fin was placed forward to take advantage of the long moment arm created by the 0.72-body-length center of gravity. The nose fin was effective over the Mach range (fig. 13). As with the other yaw control devices, effectiveness decreased as Mach number and angle of attack increased except for $M = 1.60$. At this Mach number, yaw effectiveness increased with angle of attack. Yawing moments were accompanied by small proverse rolling moments.

Roll control effects. Roll control tests were made only with the nose-fin model. Control was

produced by differentially deflecting the dedicated aileron control surfaces on the outer wing trailing edge. The effectiveness values are for cases with the control surfaces set at $10°$ and $20°$ on the left and $-10°$ or $-20°$ on the right. In addition, the nose fin was set at $10°$. Since the data presented are increments derived with the aileron deflected and undeflected, yaw control input should not be a factor. The data of figure 14, however, indicate that while the ailerons were relatively effective as a roll control, yawing moments of equal magnitude were produced. The question arises as to whether the source of the yawing moment was caused entirely by the aileron deflection or influenced by the nose-fin deflection. To answer this question, additional tests are required.

Concluding Remarks

Tests of a circular body spacecraft model have been conducted in the Langley Unitary Plan Wind Tunnel at Mach numbers from 1.60 to 4.60. The design is an option considered for single- or multi-stage Earth-to-orbit vehicles. The model had a circular body with a clipped-delta wing. Three vertical fin arrangements were investigated: a conventional aft-mounted center fin, wingtip fins, and a nose-mounted fin.

The results of the investigation indicate that the configuration is longitudinally stable about the estimated center of gravity at 0.72 body length up to a Mach number of about 3.0. Above Mach 3.0, the model is longitudinally unstable at low angles of attack but has a stable secondary trim point at angles of attack around $30°$. The model has sufficient pitch control authority with elevator and body flap to produce stable trim over the test range. The aft-center-fin configuration is directionally stable at low angles of attack up to a Mach number of 3.90. The wingtip and nose fins are not intended to produce directional stability. The rudder-like surfaces on the tip fins and the all-movable nose fin were designed as active controls to produce artificial directional stability. These controls were effective in producing yawing moment. Yawing moment produced by deflecting the rudder on the aft center fin produced yawing moments accompanied by adverse roll.

Differential deflection of the aileron surfaces on the wing trailing edge were effective in producing rolling moment but were accompanied by large values of adverse yawing moment. The test, however, was conducted only with the nose-fin configuration and the fin was deflected. While an attempt was made to eliminate the effect of fin deflection, there is no assurance this was successful, and it may be

5

a contributing factor to the large adverse rolling moment.

NASA Langley Research Center
Hampton, VA 23681-0001
November 10, 1993

References

1. Freeman, Delma C., Jr.: The New Space Transportation Begins Today. *Astronaut. & Aeronaut.*, vol. 21, no. 6, June 1983, pp. 36-37, 48.

2. Martin, James A.: Orbit on Demand: In This Century If Pushed. *Aerosp. America*, vol. 23, no. 2, Feb. 1985, pp. 46-48.

3. Talay, T. A.: Shuttle II. SAE Tech. Paper Ser. 871335, June 1987.

4. Holloway, Paul F.; and Talay, Theodore A.: Space Transportation Systems Beyond 2000. IAF Paper 87-188, Oct. 1987.

5. Talay, Theodore A.; and Morris, W. Douglas: Advanced Manned Launch Systems. Paper presented at AAAF, DGLR, Royal Aeronautical Society, and ESA Second European Aerospace Conference on Progress in Space Transportation (Bonn, Federal Republic of Germany), May 22-24, 1989.

6. MacConochie, I. O.; and Klich, P. J.: Technologies Involved in Configuring and Advanced Earth-to-Orbit Transport for Low Structural Mass. SAWE Paper 1380, May 1980.

7. Lepsch, R. A., Jr.; and MacConochie, I. O.: Subsonic Aerodynamic Characteristics of a Circular Body Earth-to-Orbit Transport. AIAA-86-1801, June 1986.

8. Wells, William L.; MacConochie, Ian O.; Helms, Vernon T.; and Raney, David: Heating Rate Distributions at Mach 10 on a Circular Body Earth-to-Orbit Transport Vehicle. AIAA-85-0974, June 1985.

9. Jackson, Charlie M., Jr.; Corlett, William A.; and Monta, William J.: *Description and Calibration of the Langley Unitary Plan Wind Tunnel.* NASA TP-1905, 1981.

10. Braslow, Albert L.; Hicks, Raymond M.; and Harris, Roy V., Jr.: Use of Grit-Type Boundary-Layer-Transition Trips. *Conference on Aircraft Aerodynamics*, NASA SP-124, 1966, pp. 19-36.

11. Powell, Richard W.; and Freeman, Delma C., Jr.: Application of a Tip-Fin Controller to the Shuttle Orbiter for Improved Yaw Control. AIAA-81-0074, Jan. 1981.
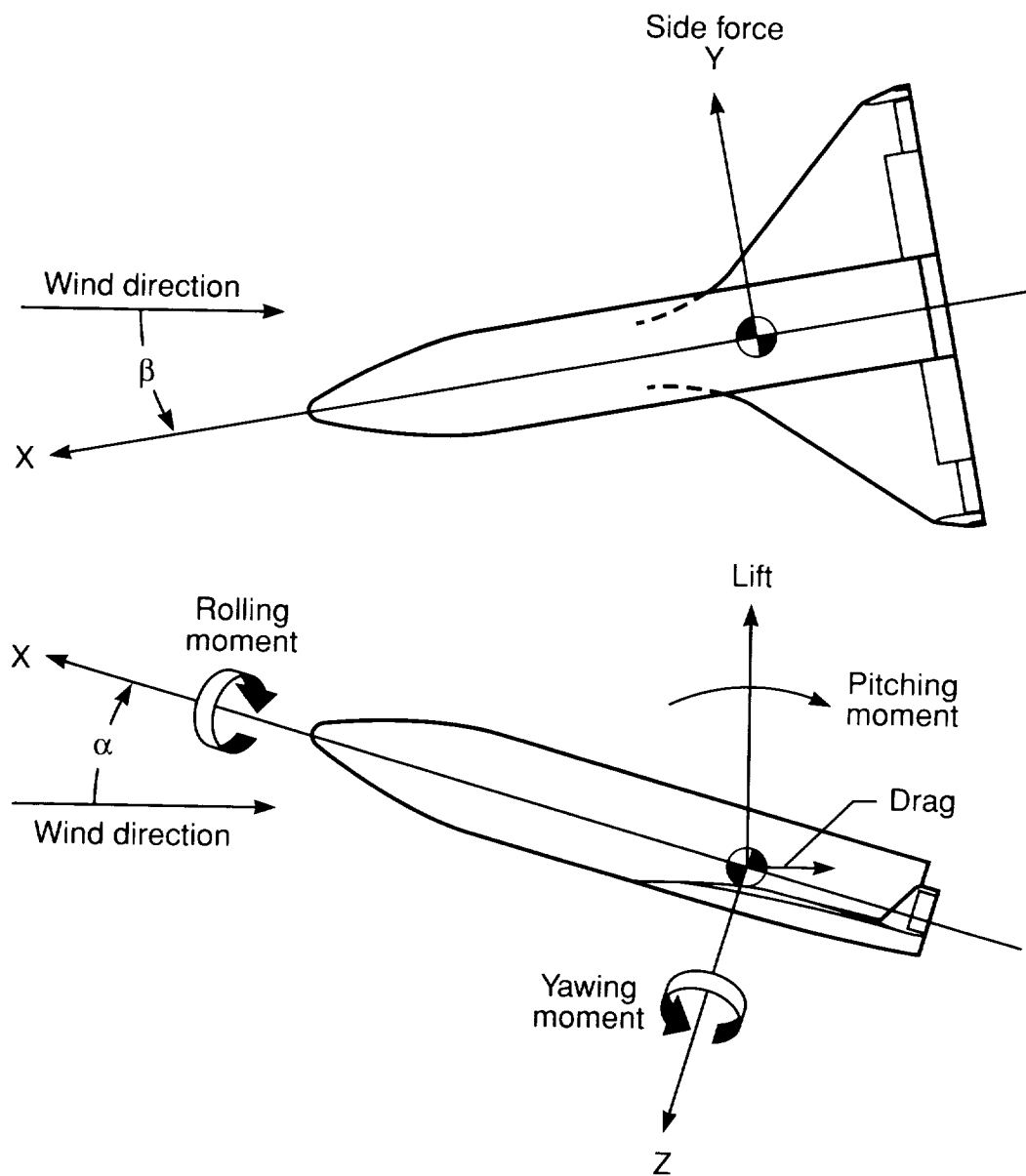
Figure 1. System of axis used in investigation, with positive directions of forces and moments.
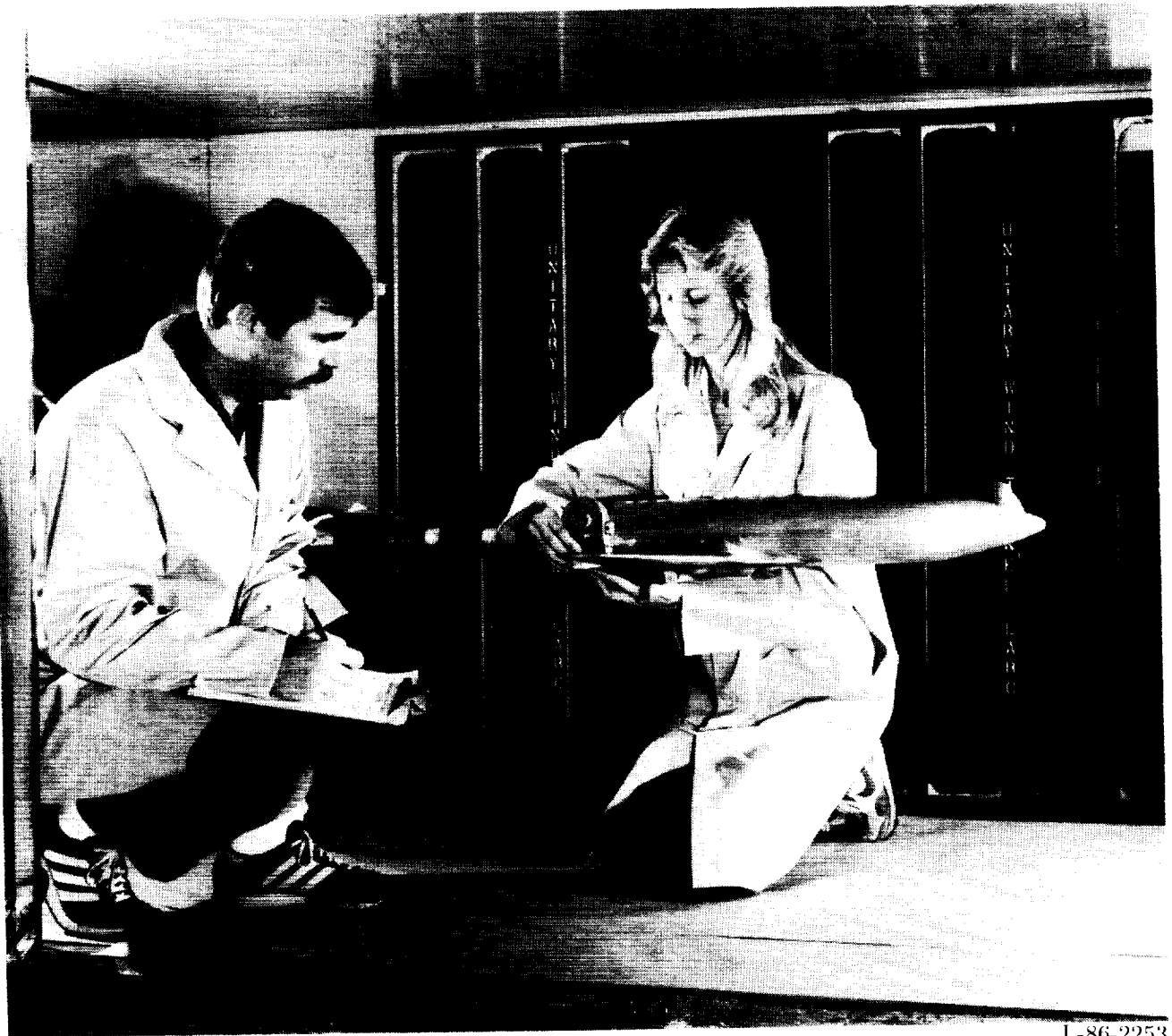
L-86-2253

(a) Photograph of model in the Langley Unitary Plan Wind Tunnel.

Figure 2. Circular body Earth-to-orbit vehicle model.

Aft center fin
(with rudder and
speed brake)

Speed brake
(used with nose-
fin configuration)

Elevator

Aileron

Nose fin

Tip fin
(with controller
and speed brake)
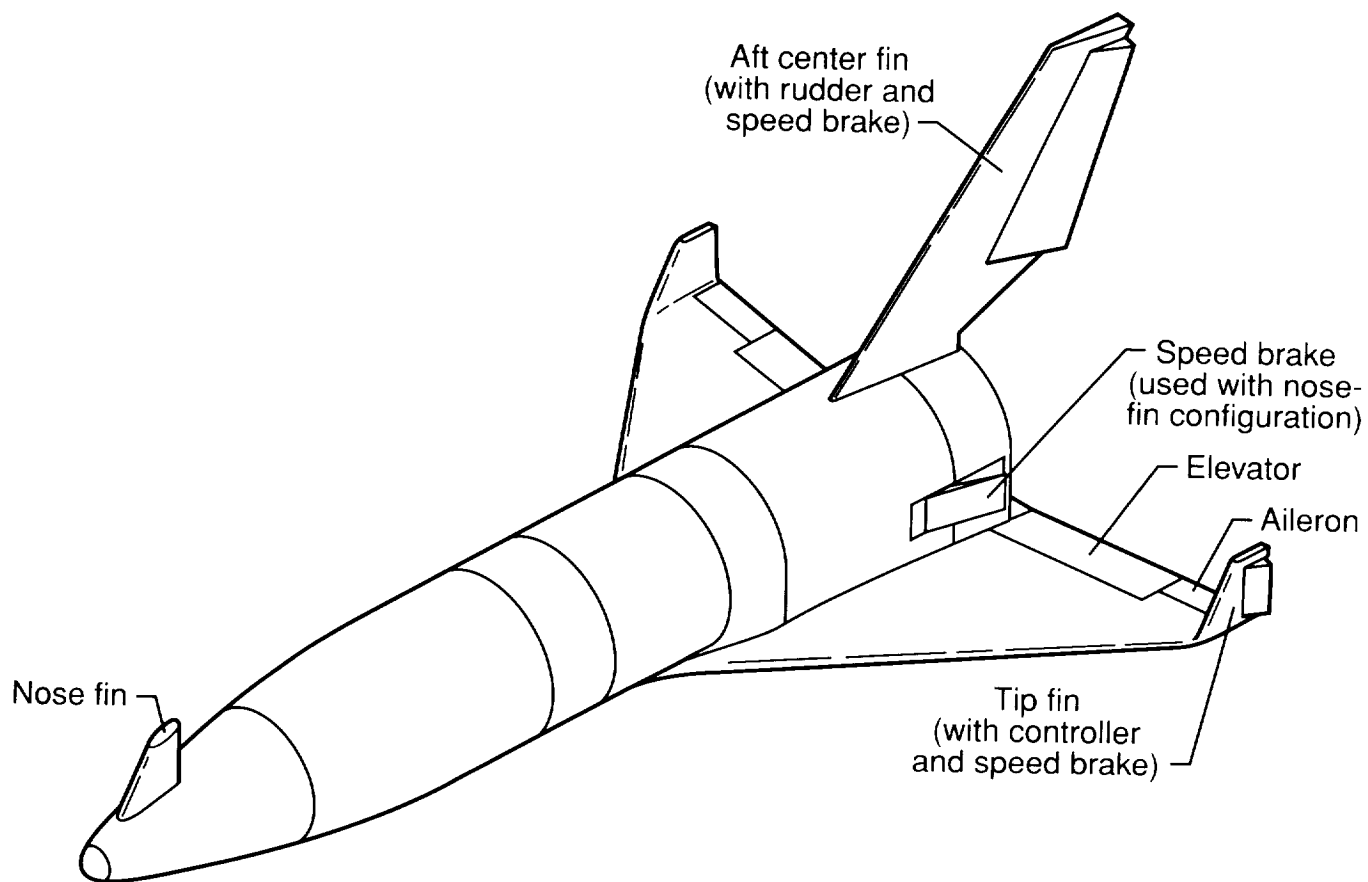
(b) Sketch of model showing three fin arrangements investigated.

Figure 2. Concluded.

9

Tangency point

4.33D

8.12

.50R

18.8R

47°

2.246

.725

1.44

Body flap

4.40

2.00

11.64

7°

4.33 17.52

1.83

26.00

18.72

.78

.25

1.44

S = 121.65 in^2
$\overline{c}$ = 8.00 in.
b = 17.52 in.
L = 26.00 in.

(a) Wing body.

Figure 3. Model used in investigation. All linear dimensions are in inches.

1.5° toe in

10°

.18

.25

.86

.76

.24

30°

1.68

1.96

2.00

(b) Tip fin.

Figure 3. Continued.

11
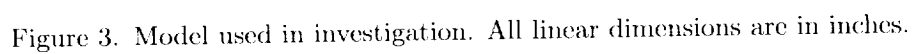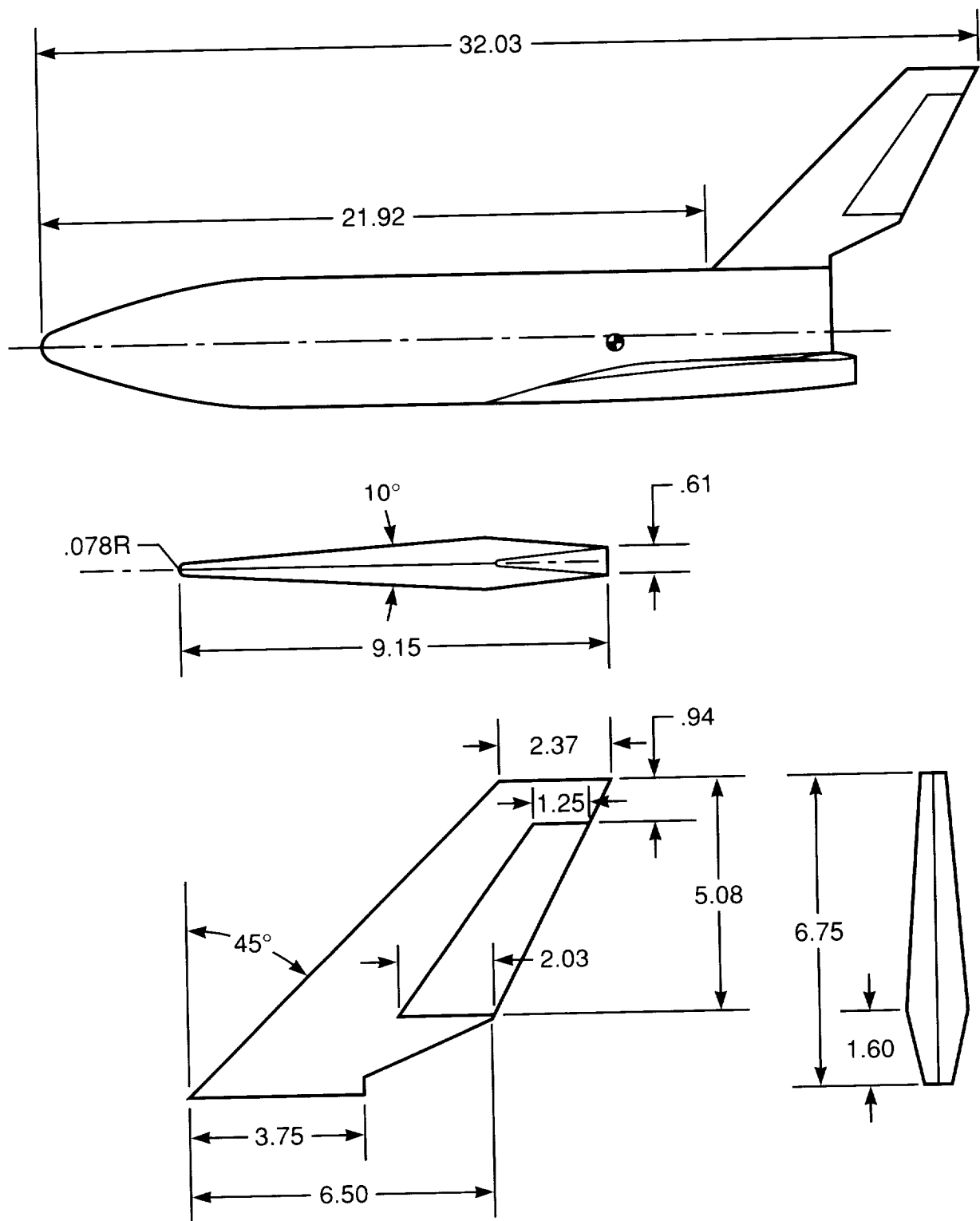
(c) Aft center fin.

Figure 3. Continued.
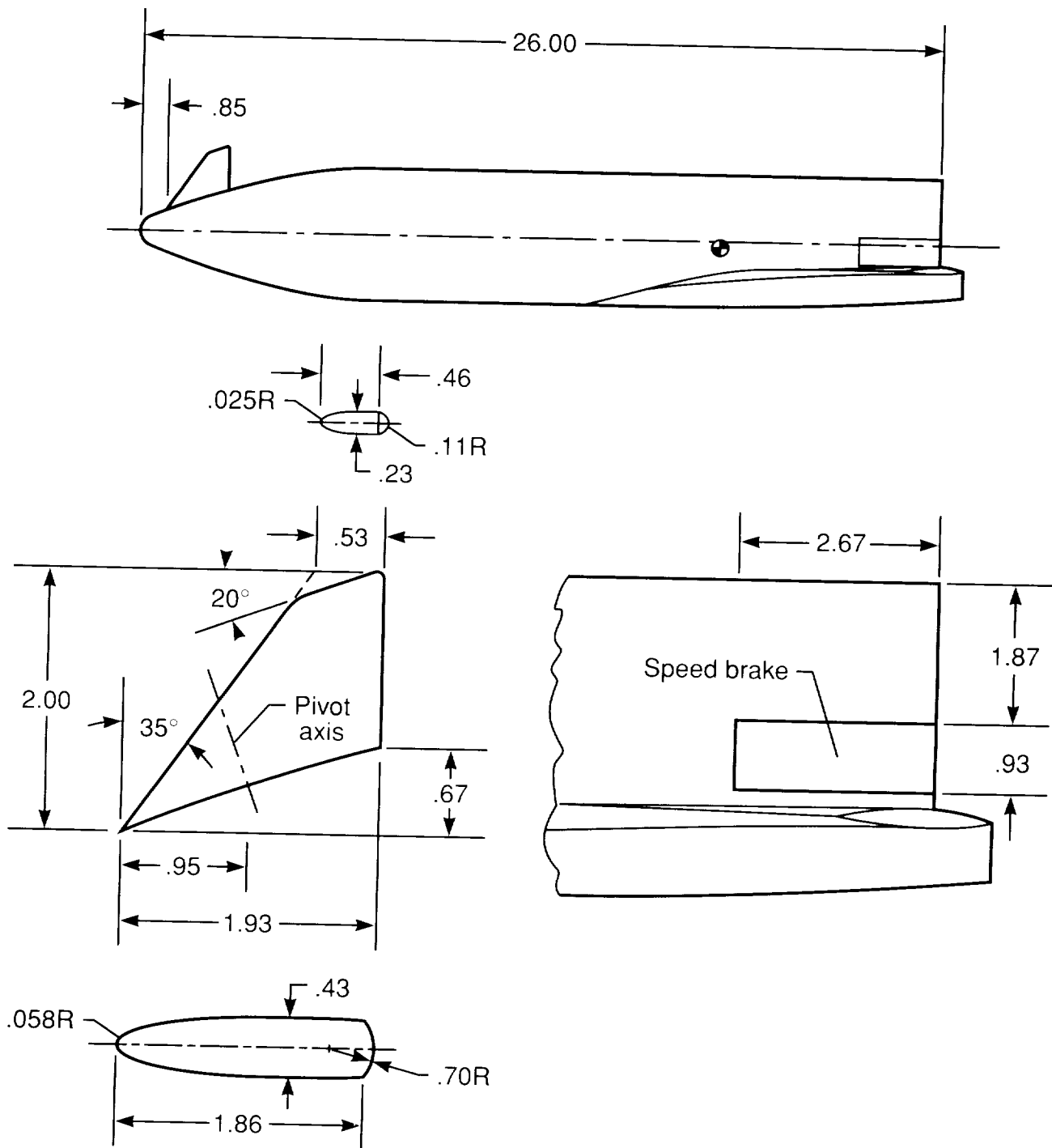
(d) Nose fin.

Figure 3. Concluded.
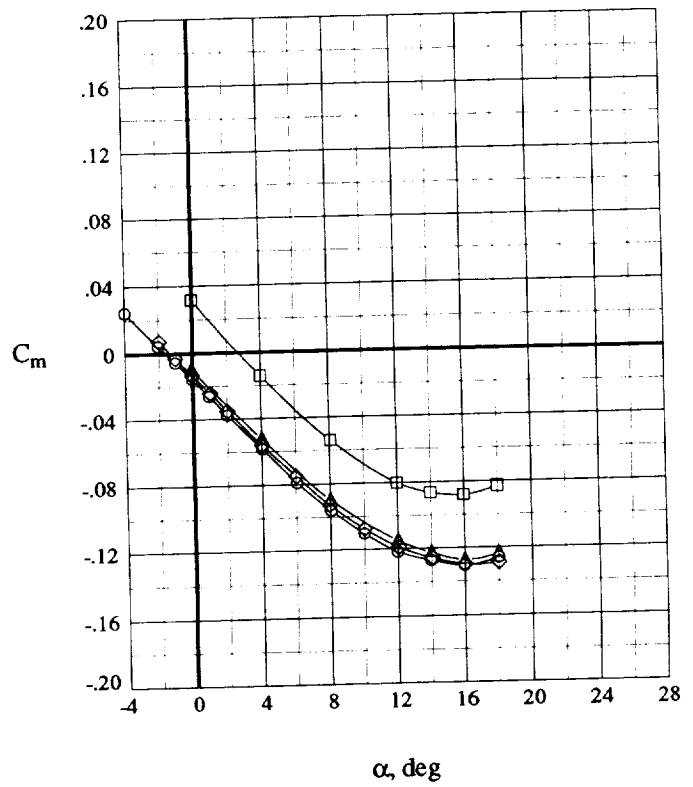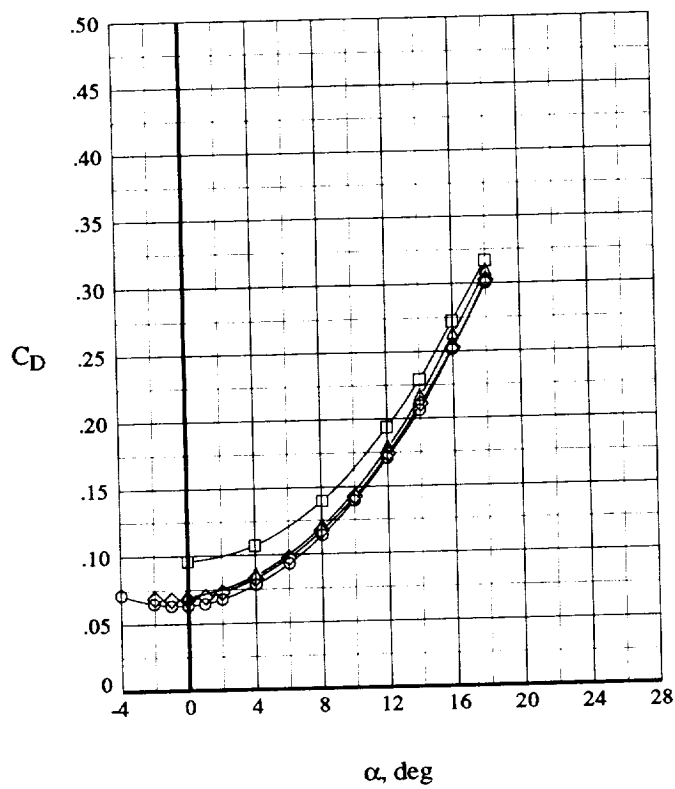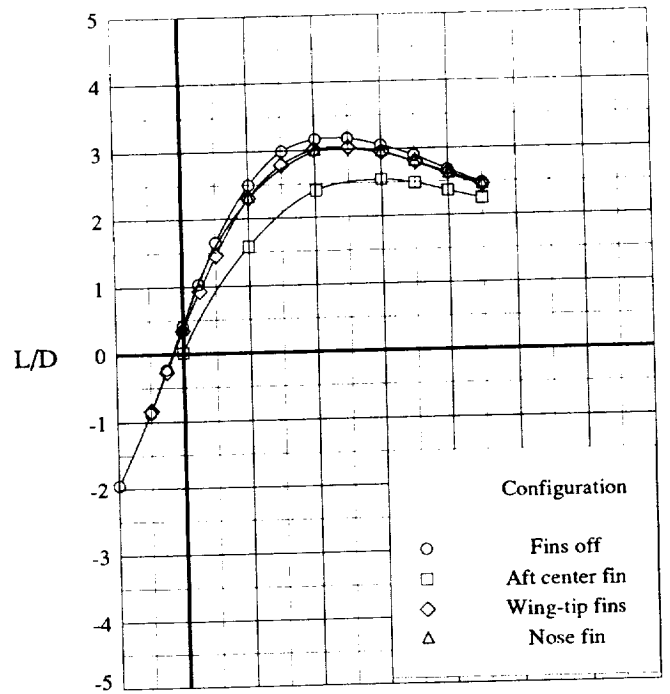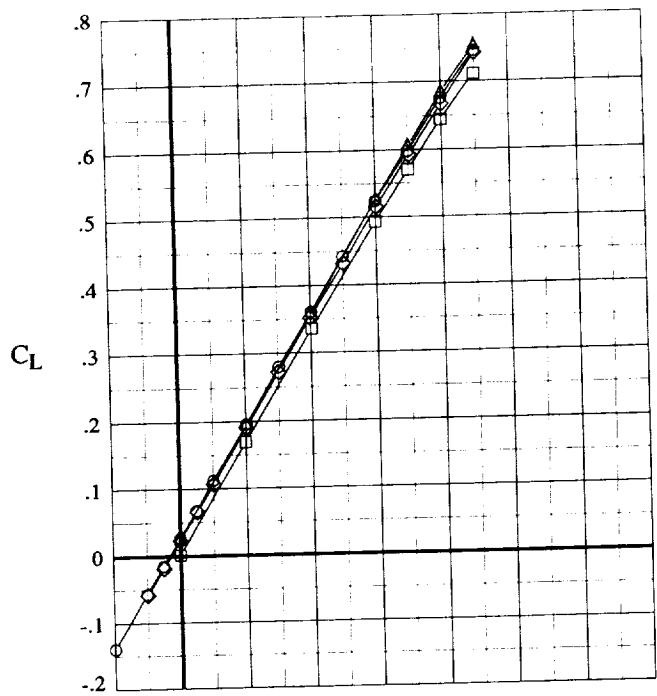
(a) M = 1.60.

Figure 4. Longitudinal characteristics of circular body model with various fin arrangements.

Configuration

|	
○	Fins off
□	Aft center fin
◇	Wing-tip fins
△	Nose fin
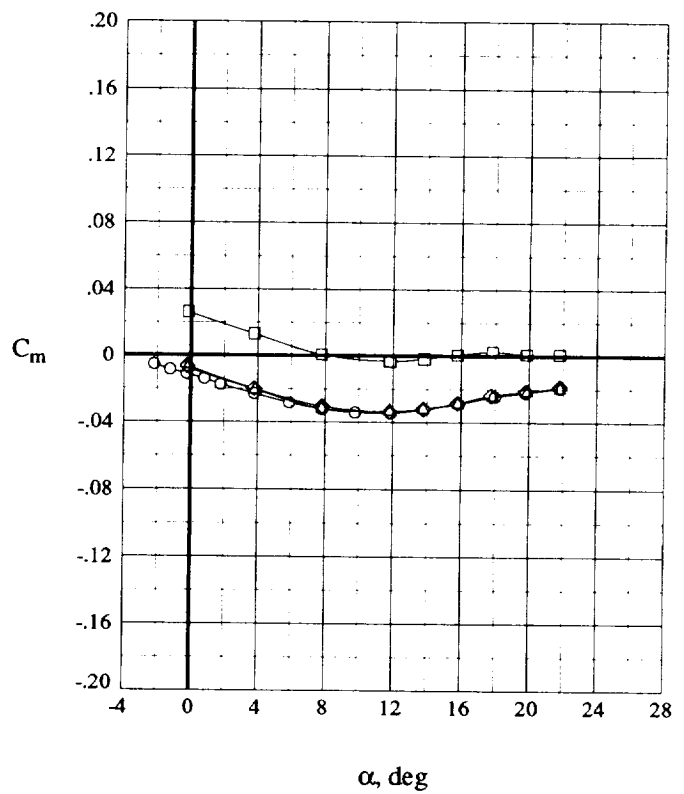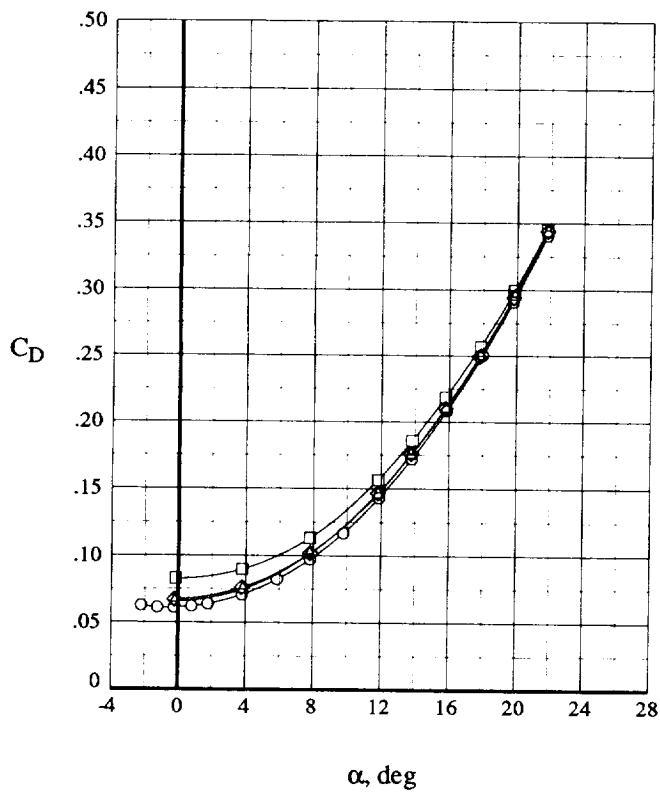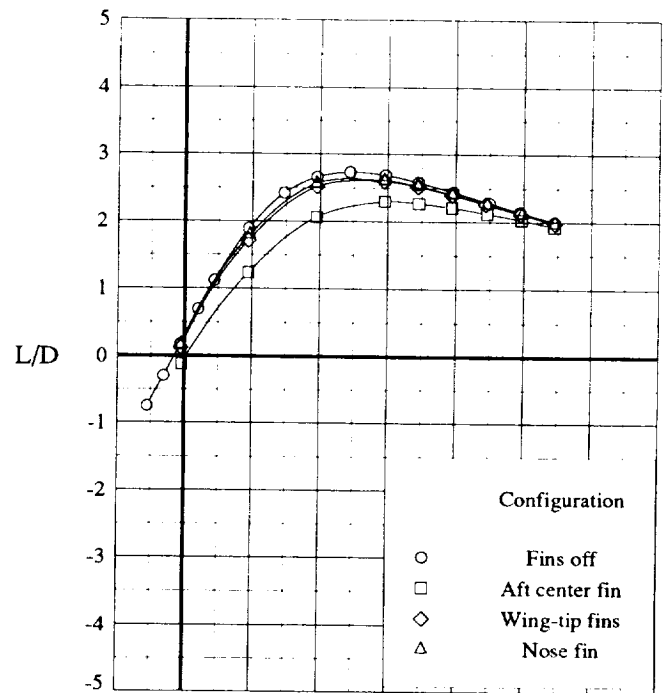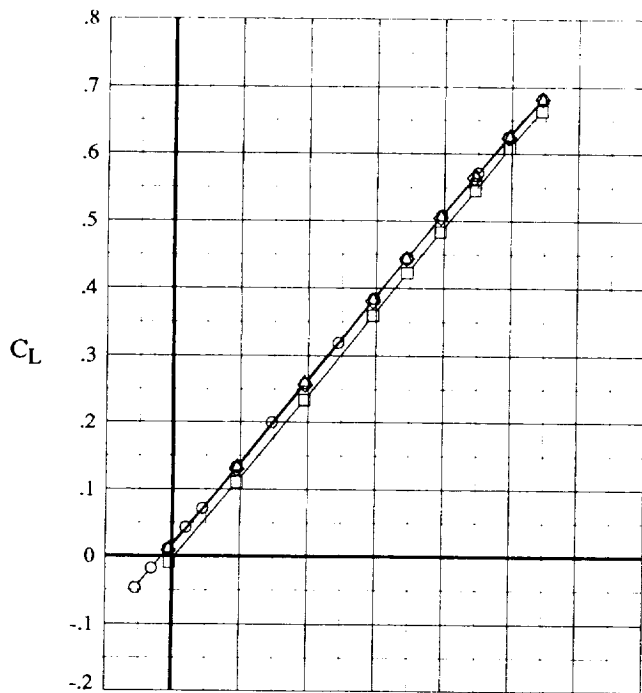
(b) M = 2.30.
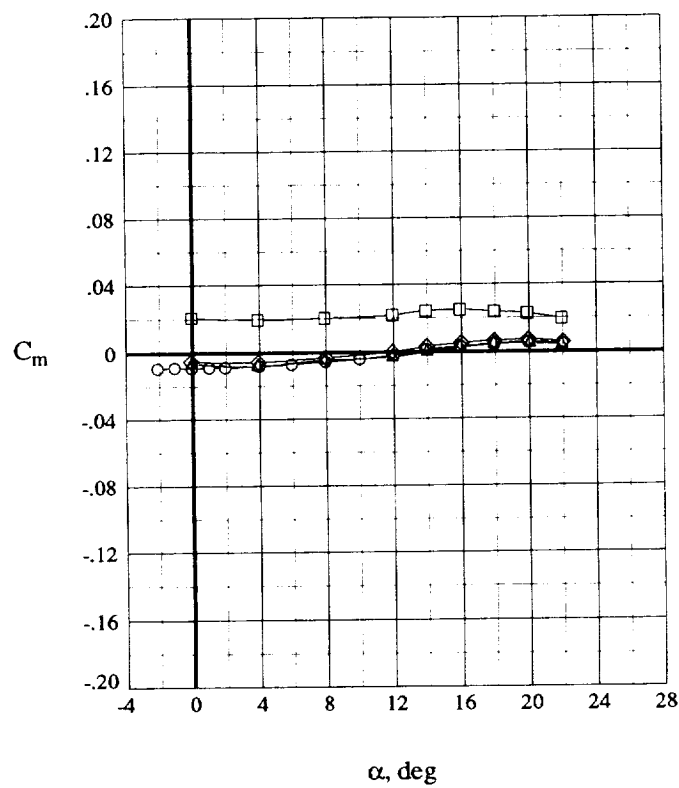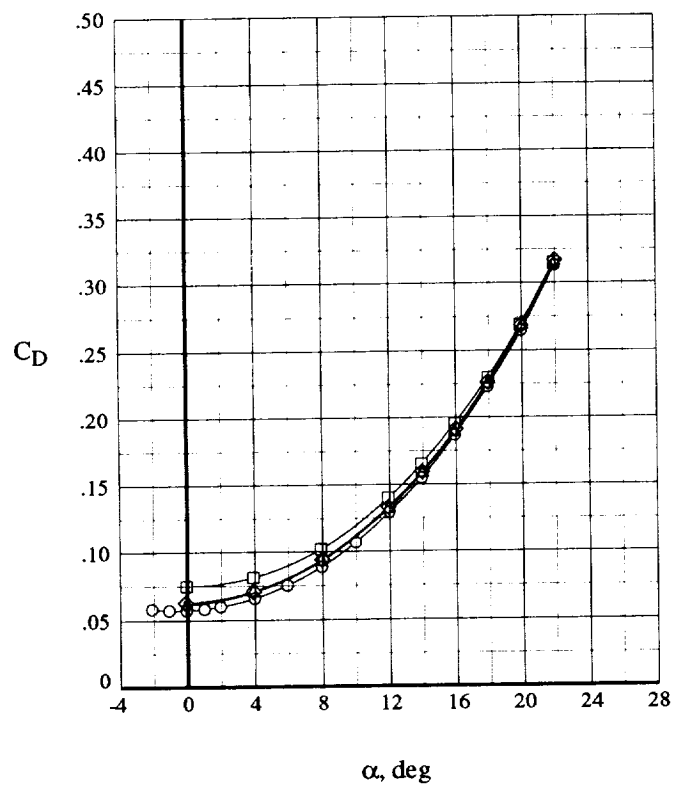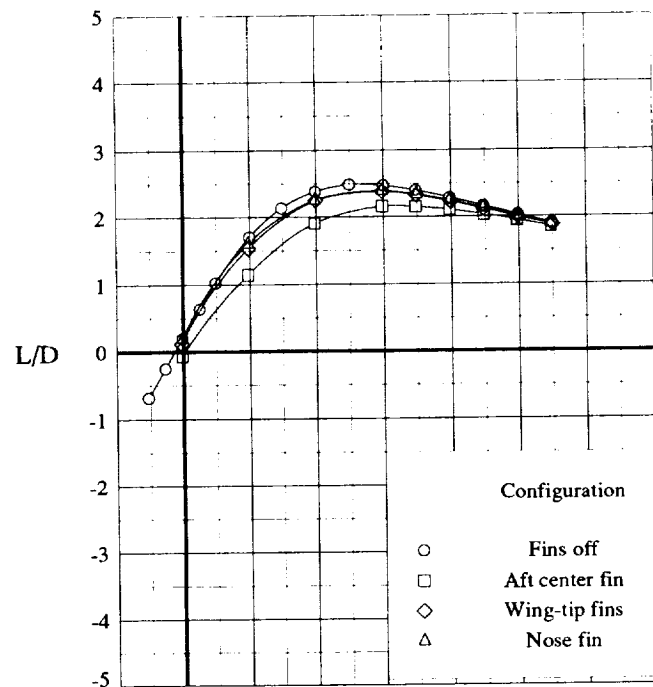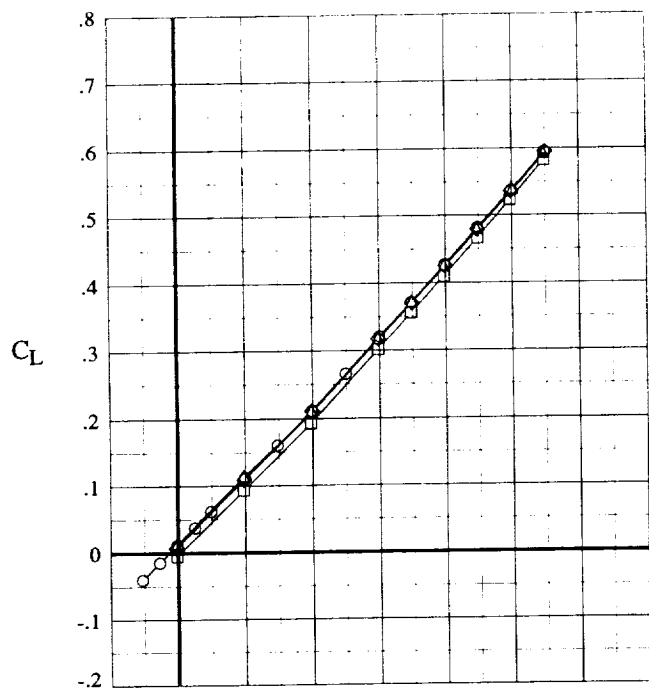
Figure 4. Continued.
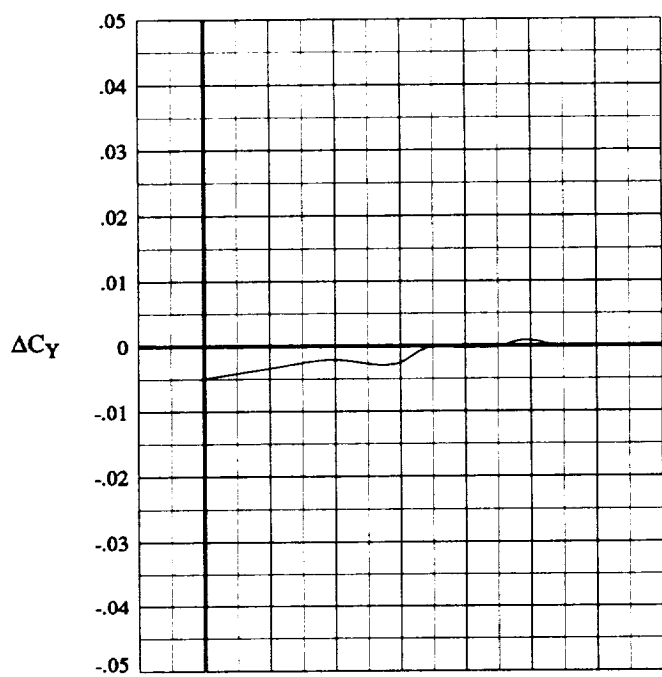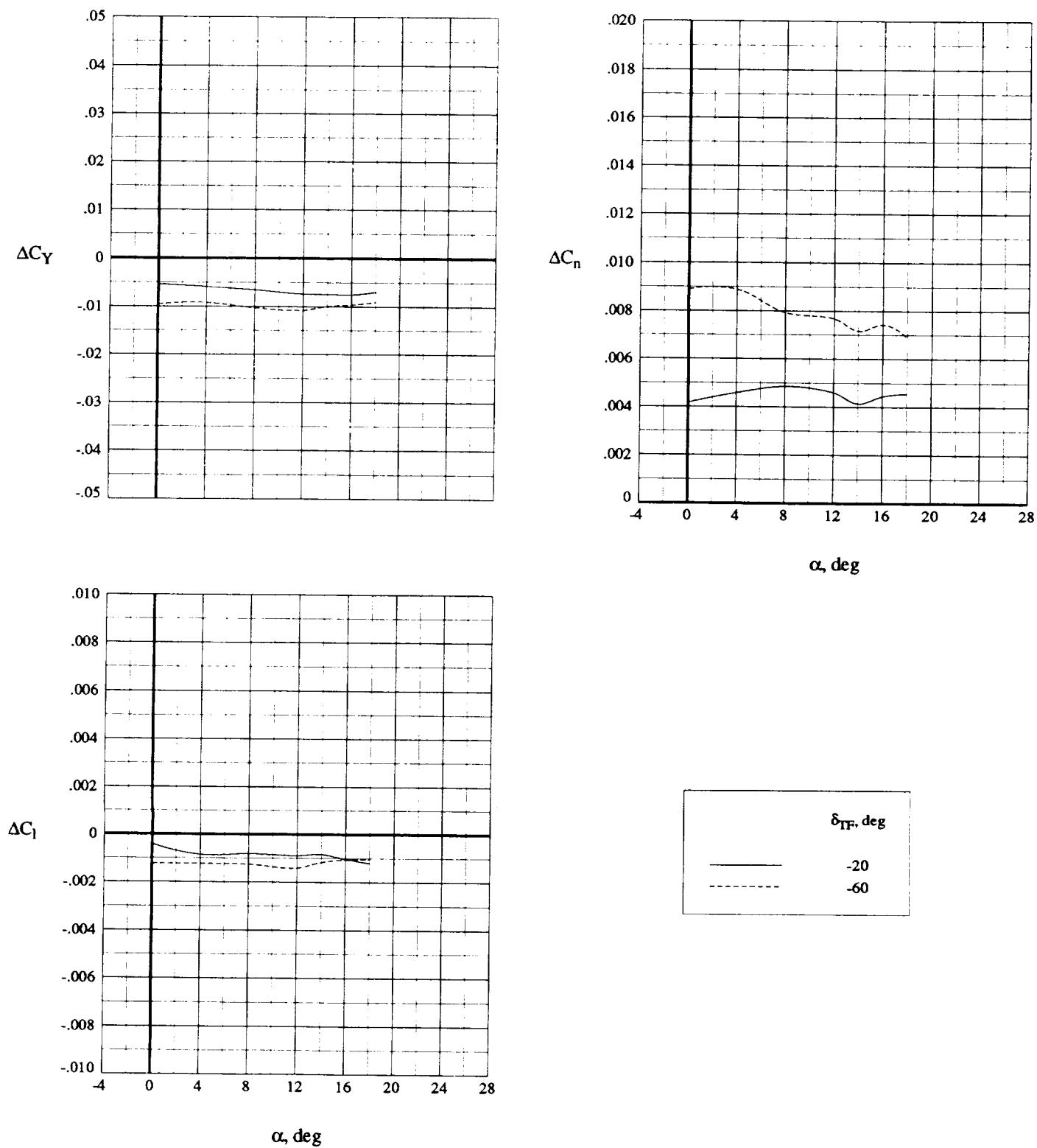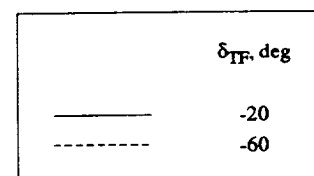
(c) M = 2.96.

Figure 4. Continued.
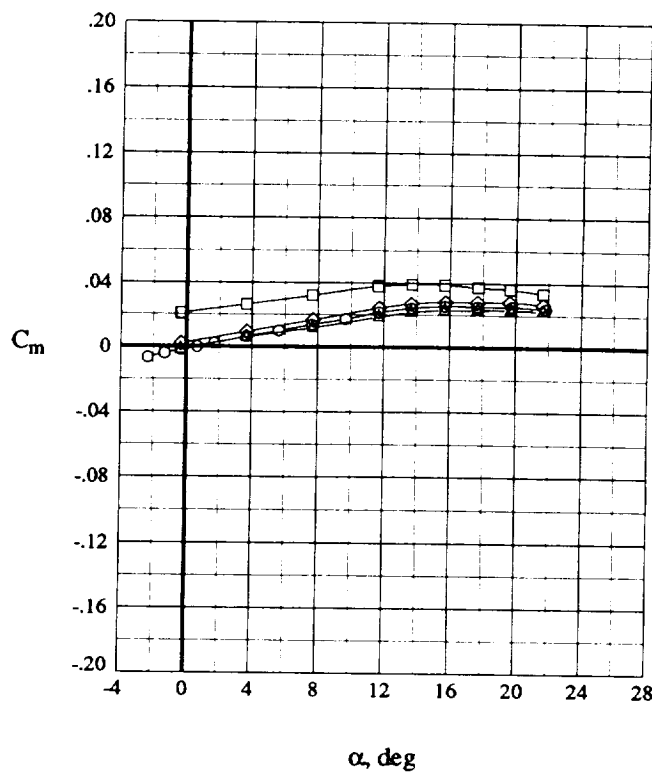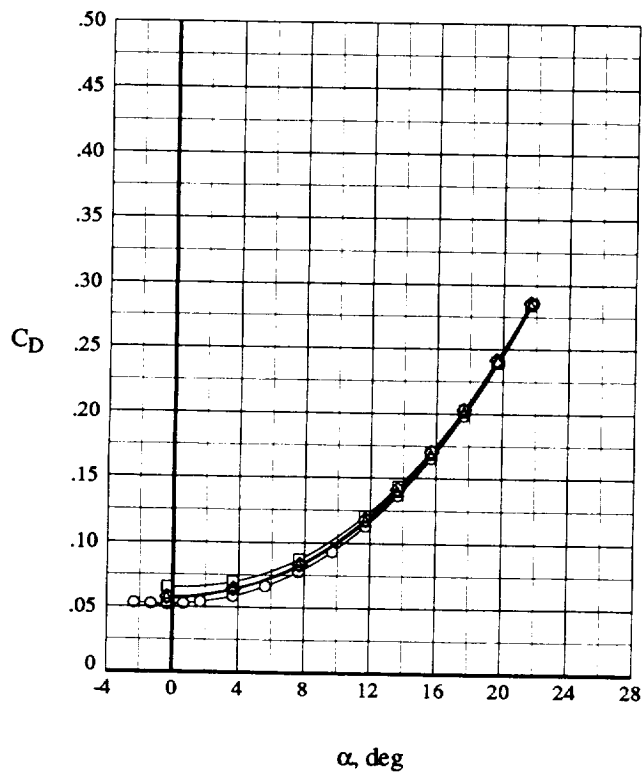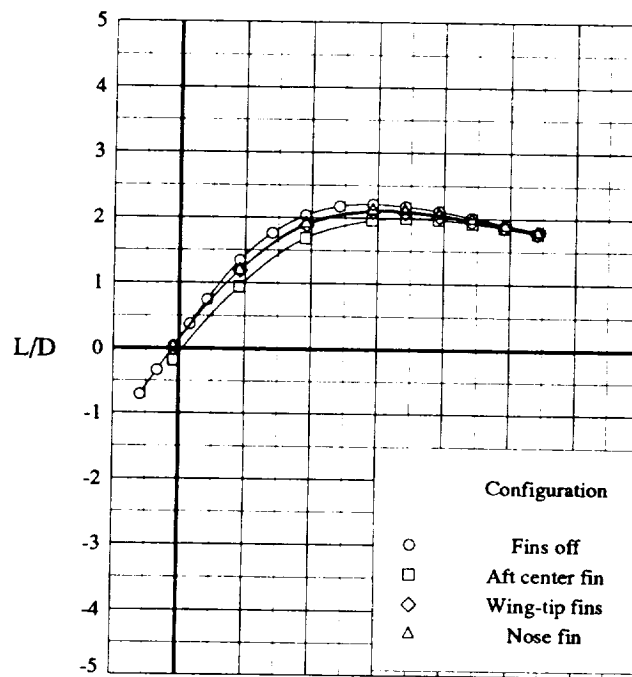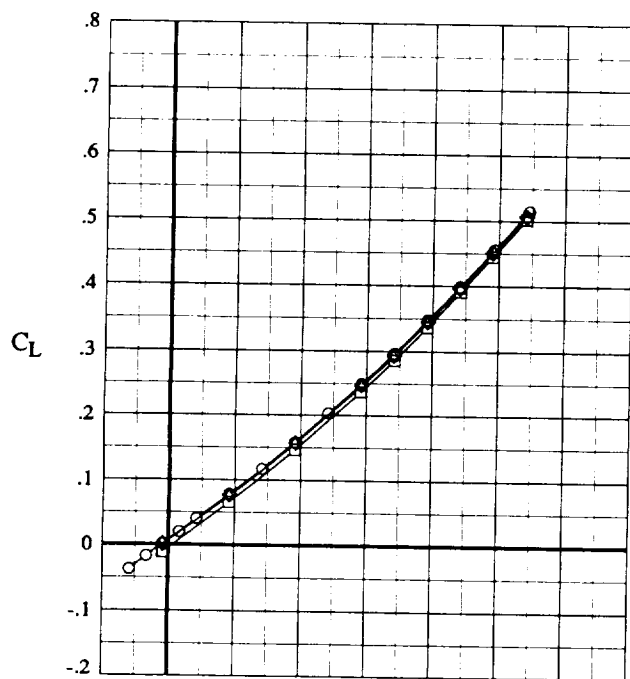
(d) M = 3.90.

Figure 4. Continued.
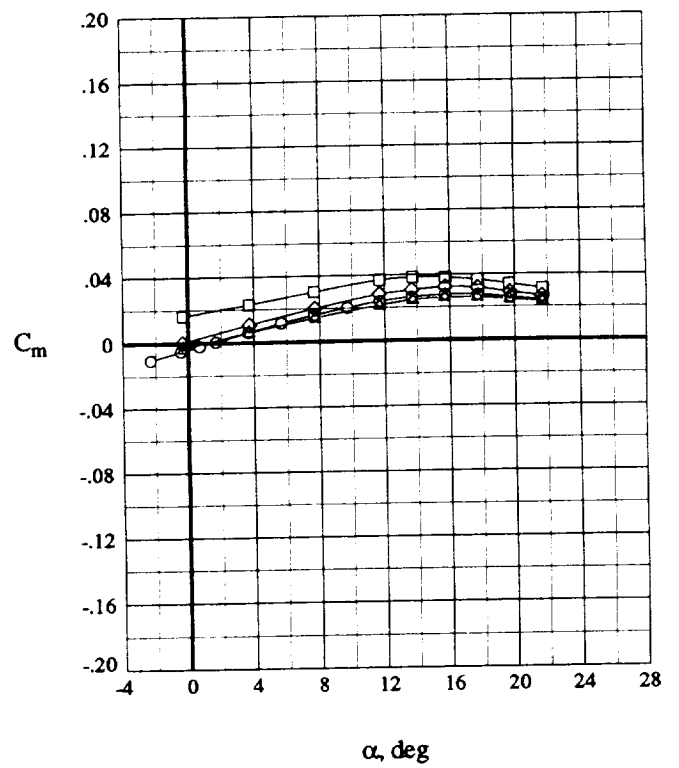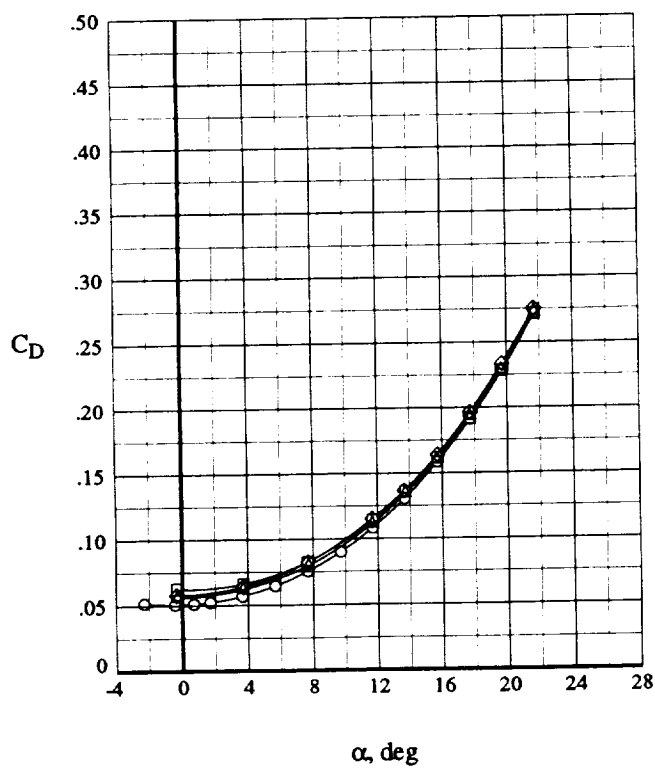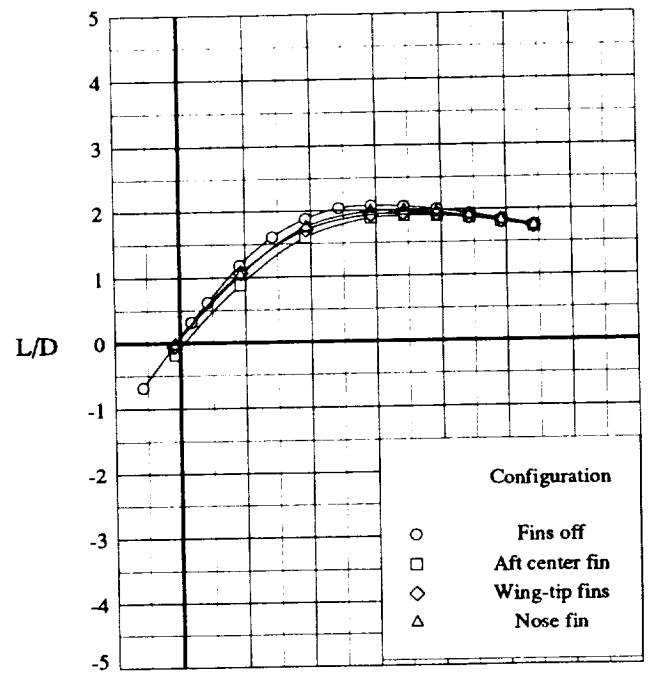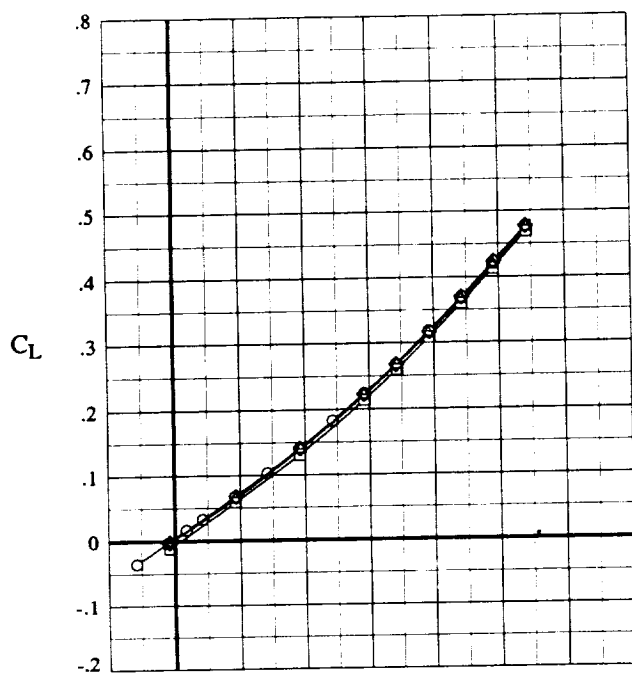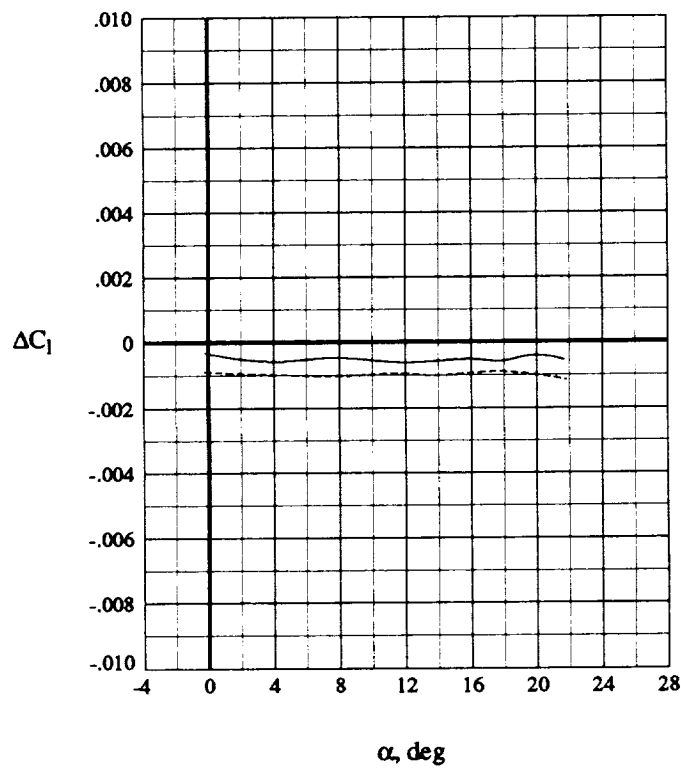
(e) M = 4.60.

Figure 4. Concluded.
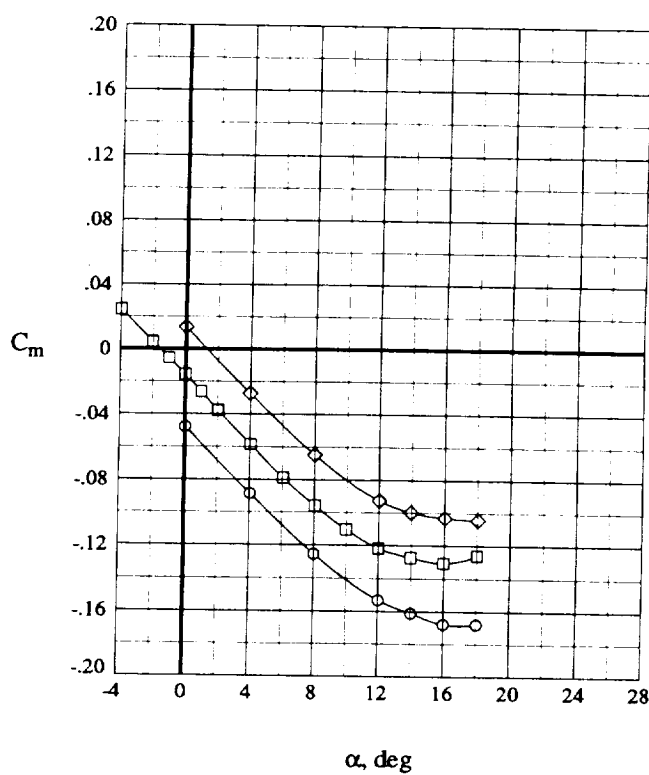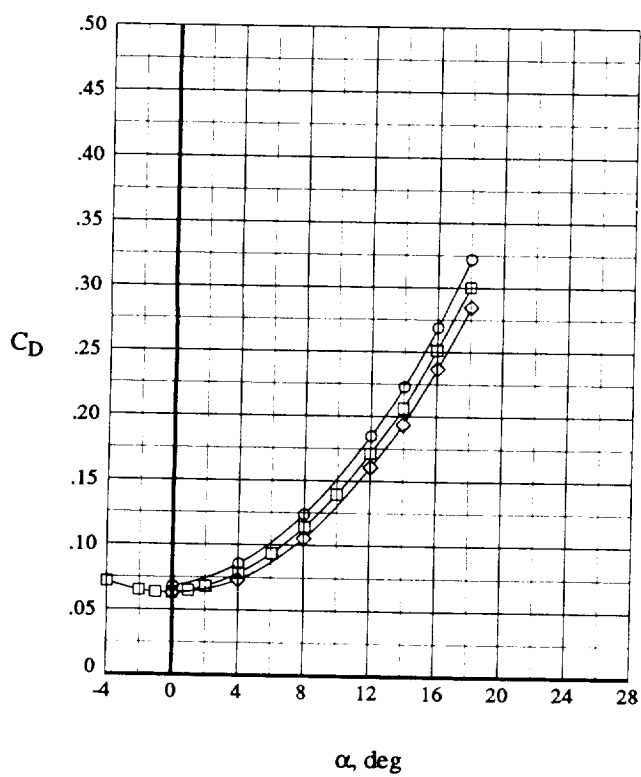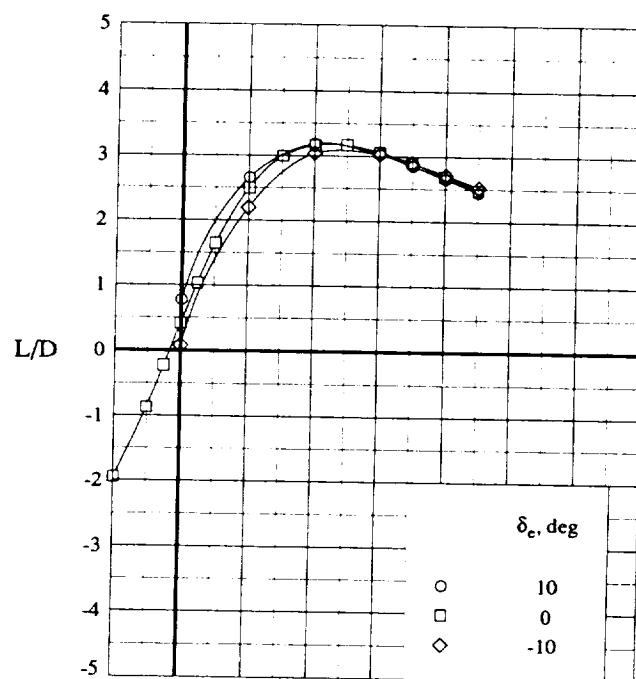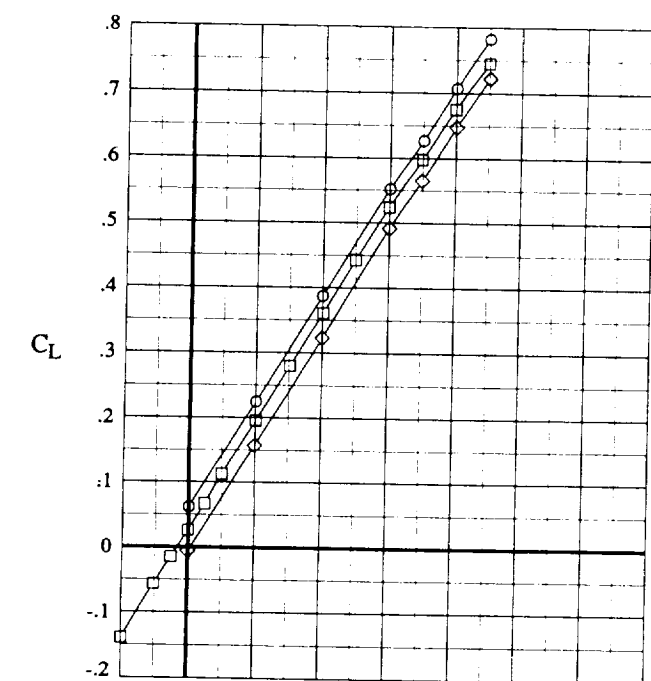
(a) M = 1.60.

Figure 5. Effect of elevator deflection on longitudinal characteristics of circular body model with all vertical fins off.

19
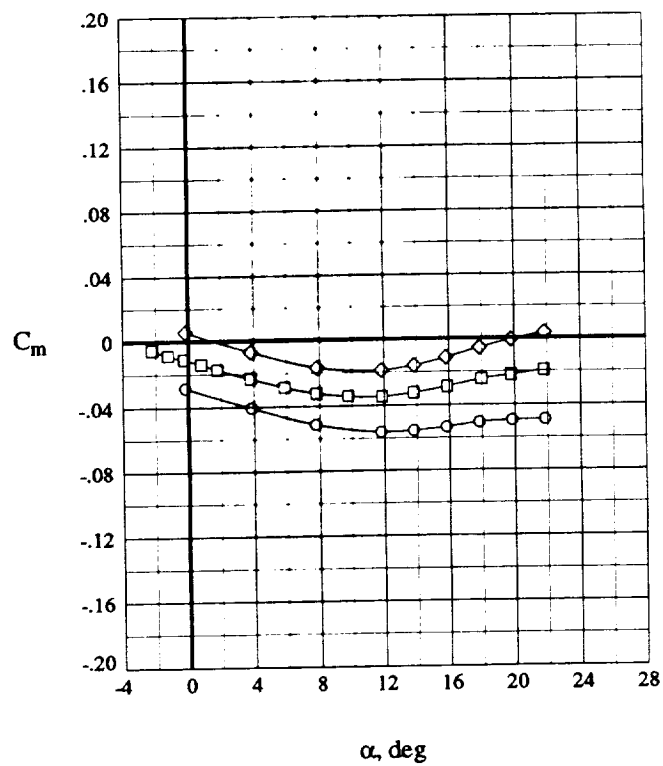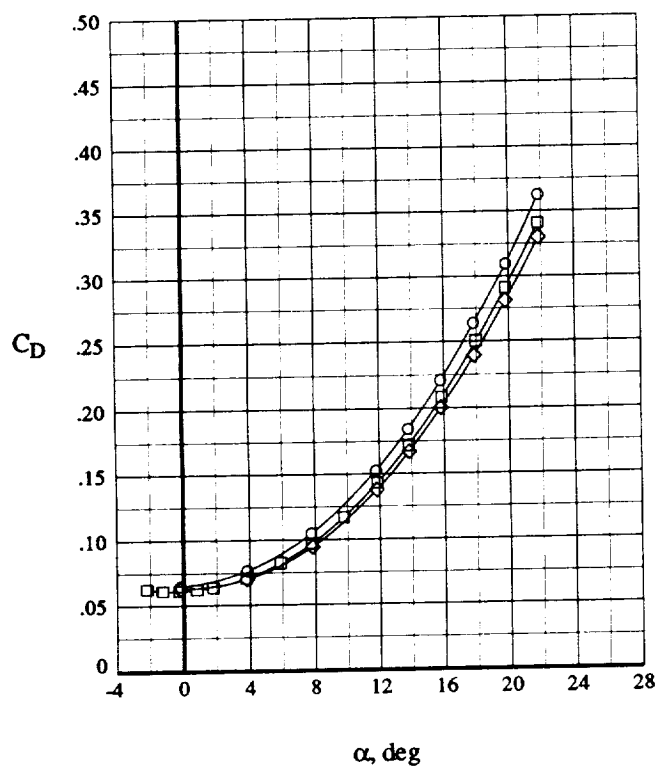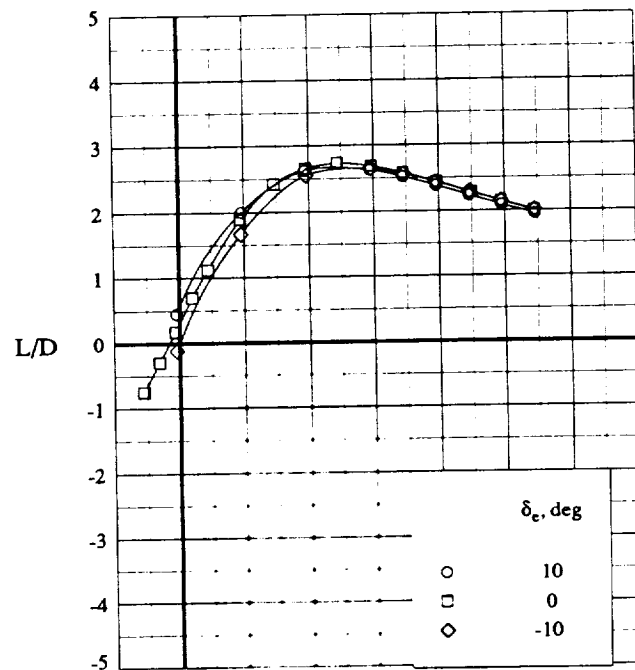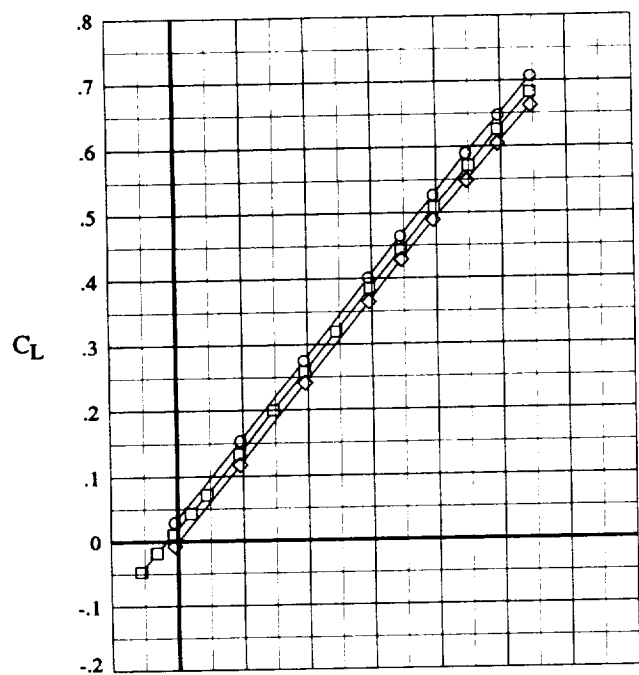
(b) M = 2.30.

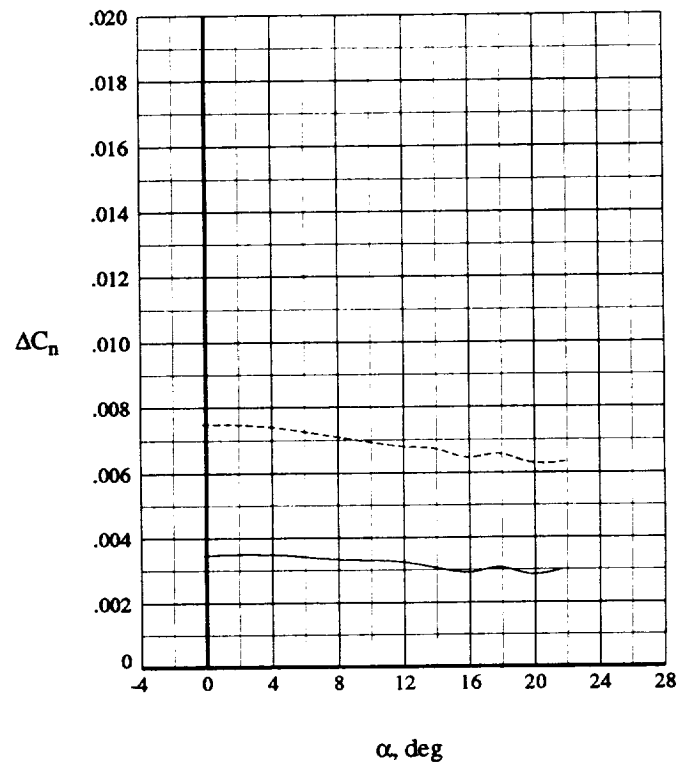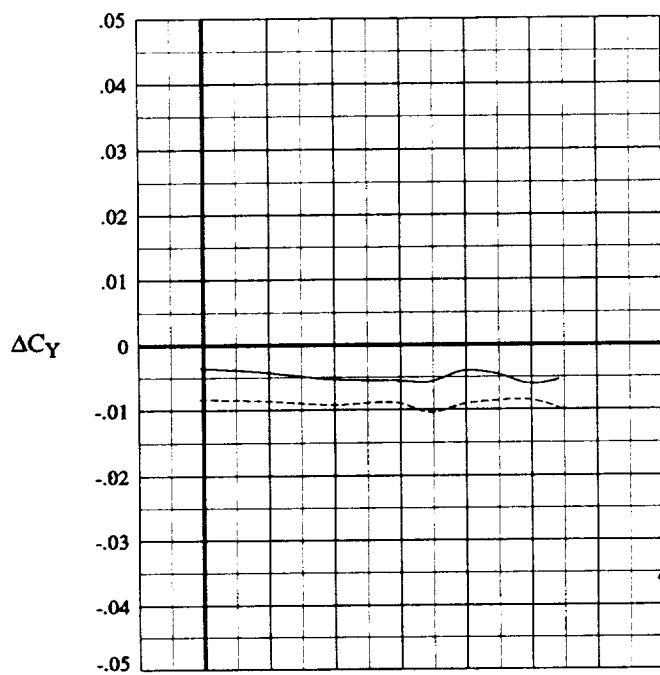Figure 5. Continued.
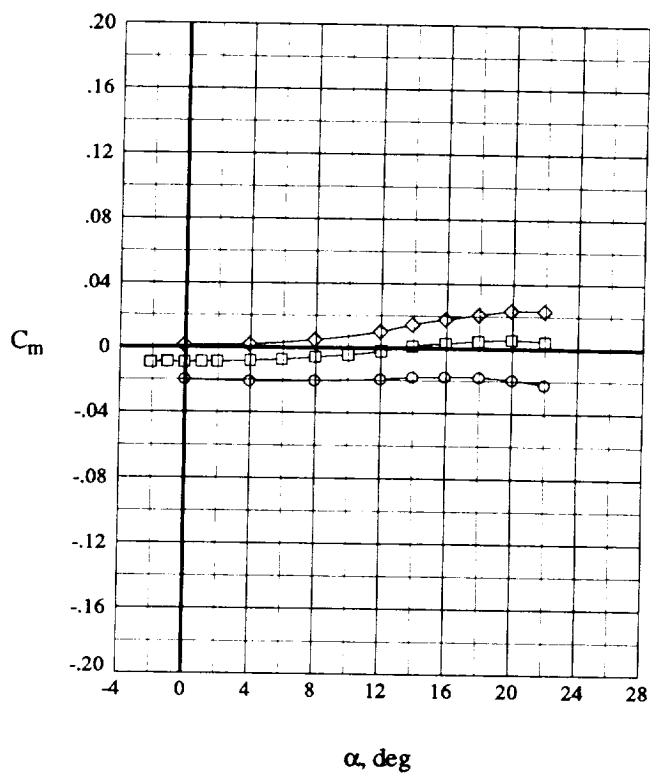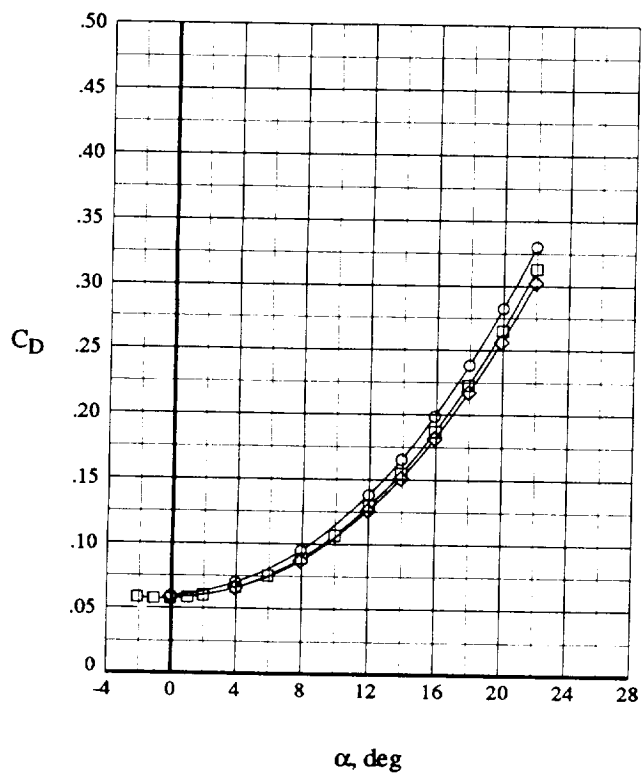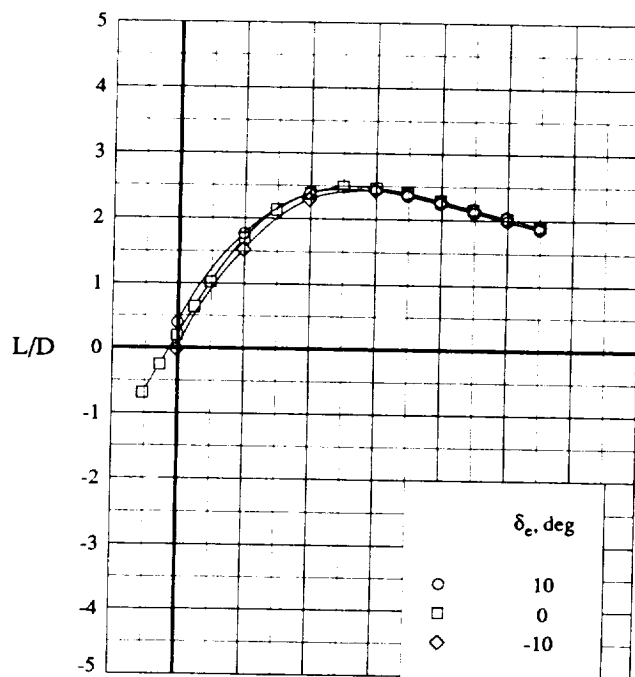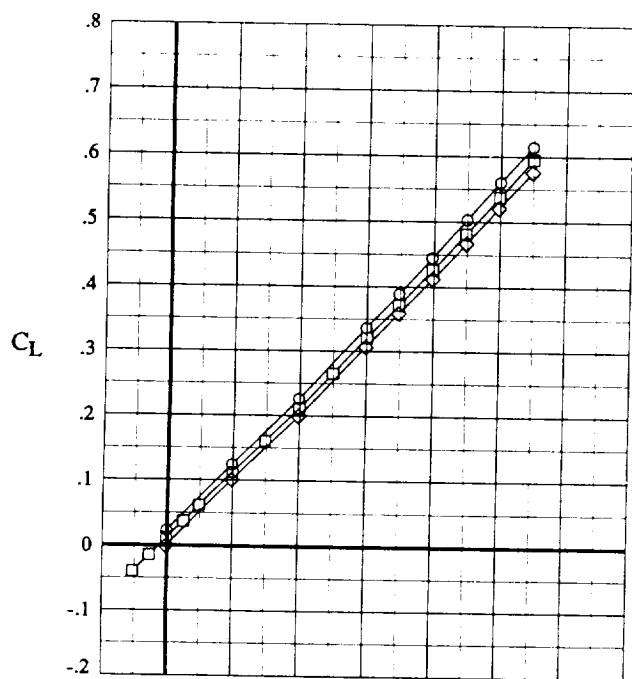
(c) M = 2.96.

Figure 5. Continued.
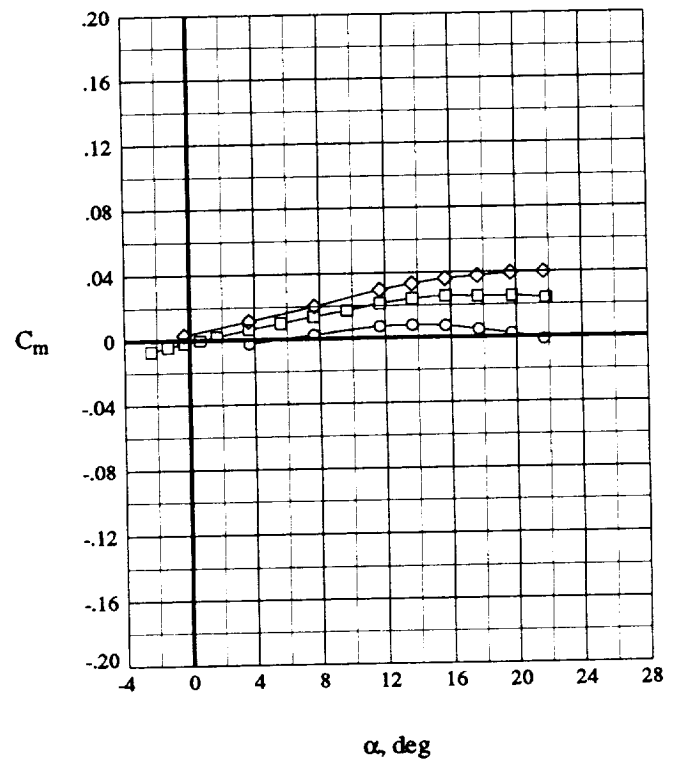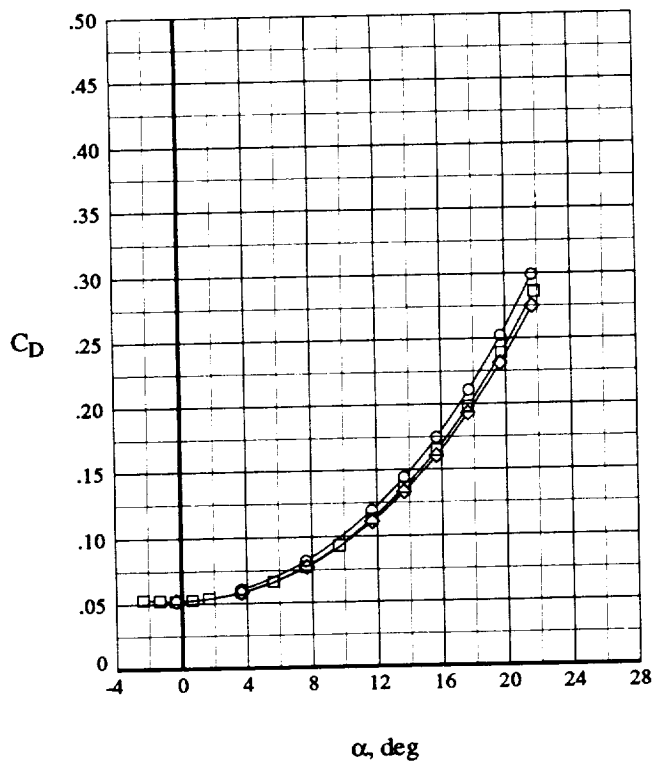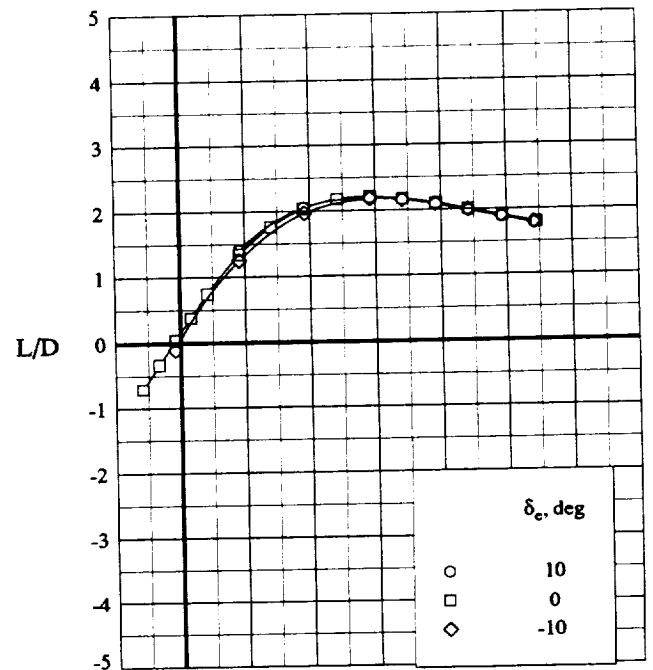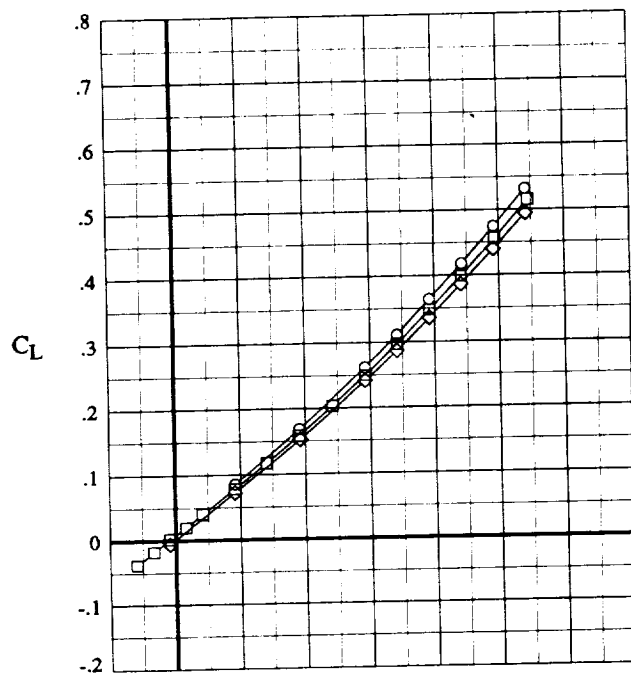
(d) M = 3.90.

Figure 5. Continued.
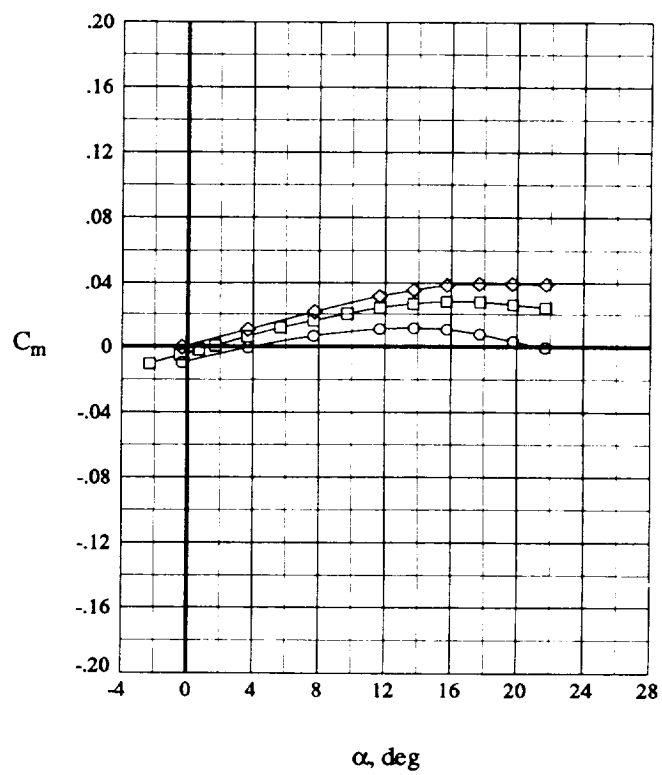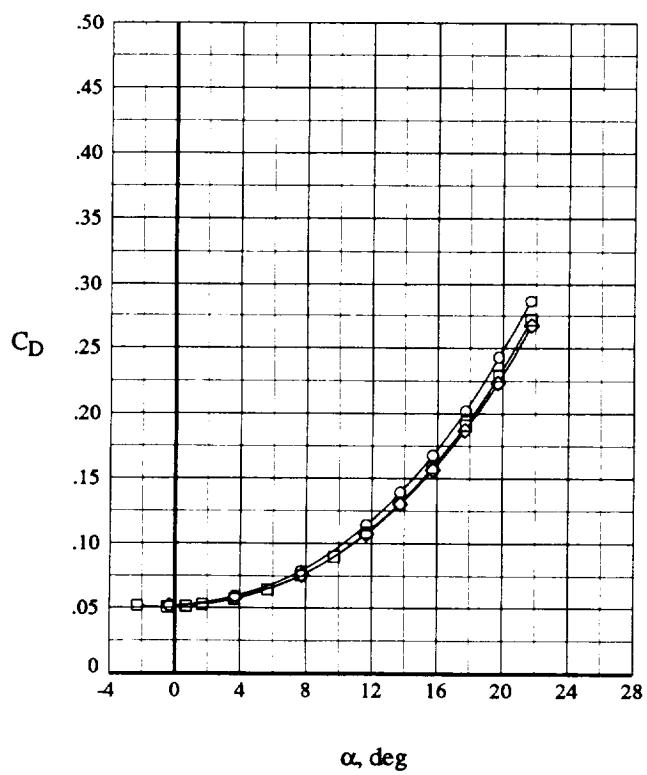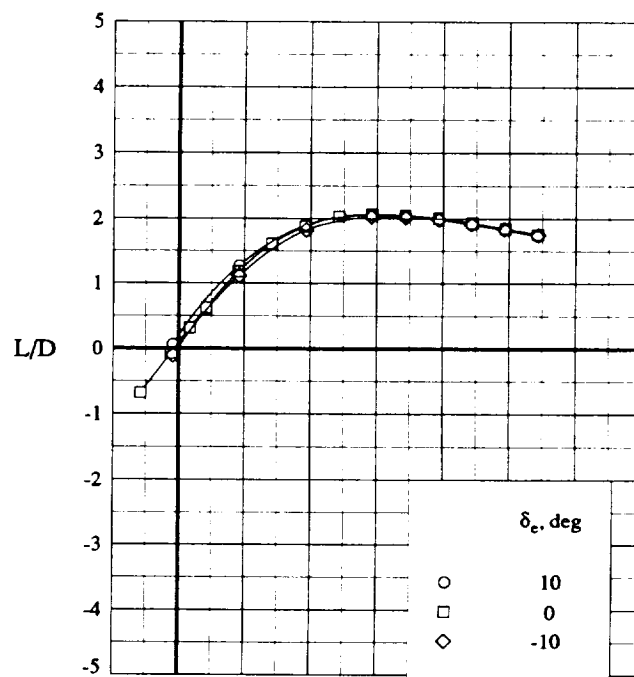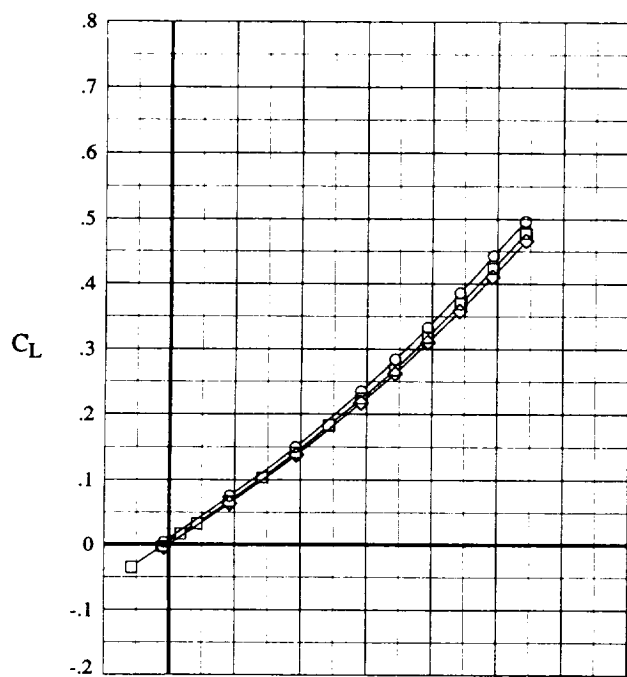
(e) M = 4.60.

Figure 5. Concluded.
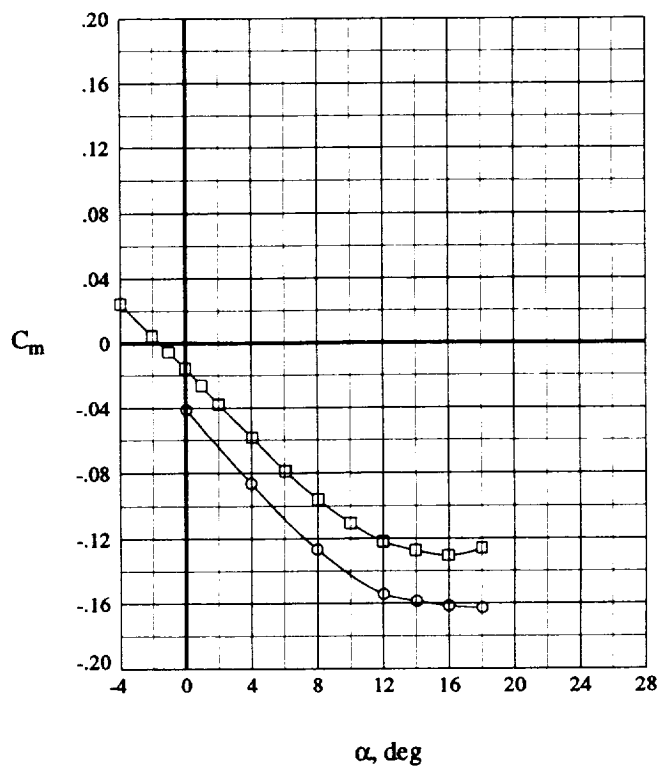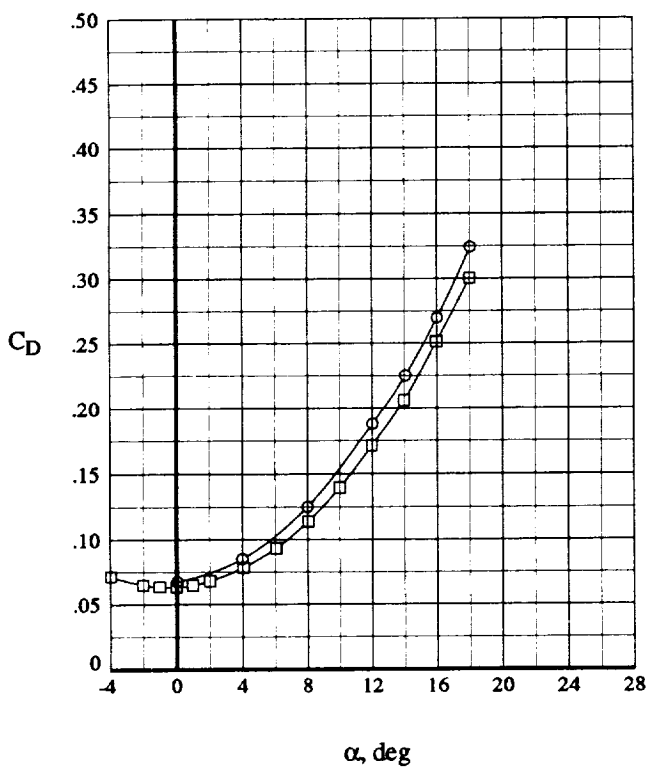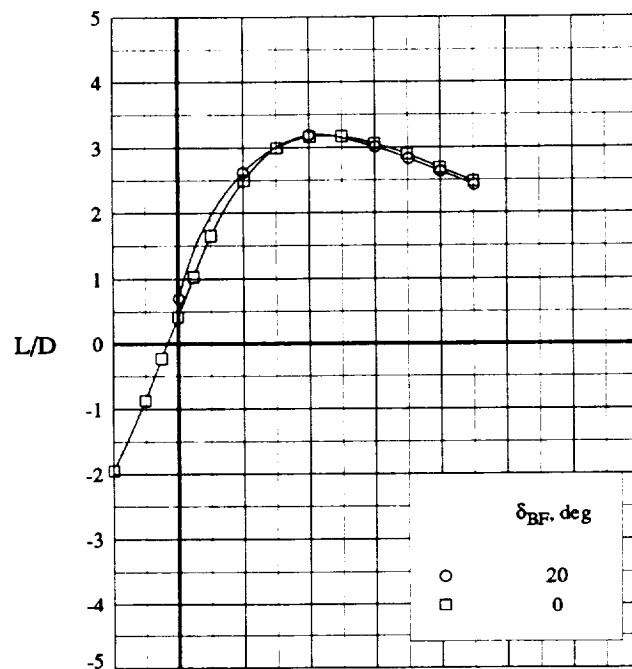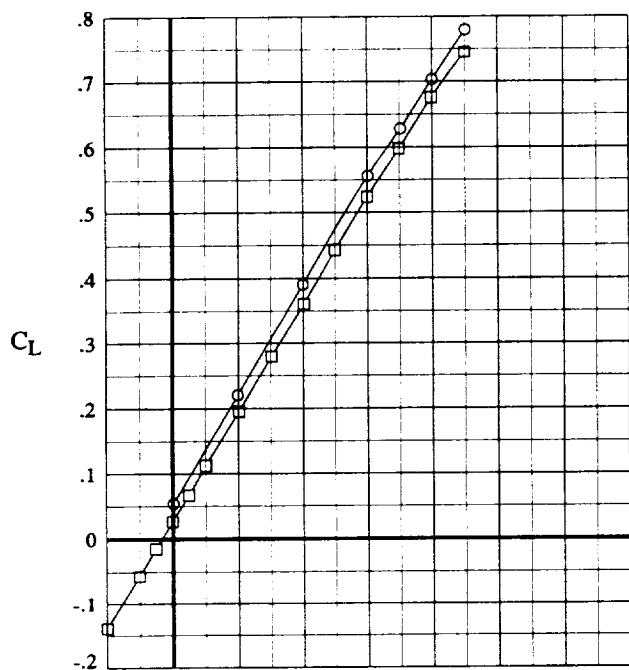
(a) M = 1.60.

Figure 6. Effect of body flap deflection on longitudinal characteristics of circular body model with all vertical fins off.
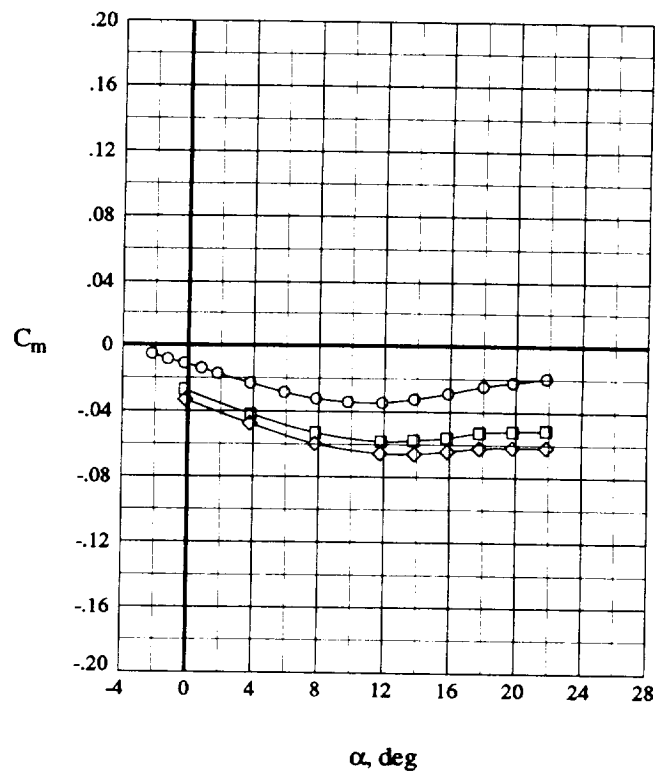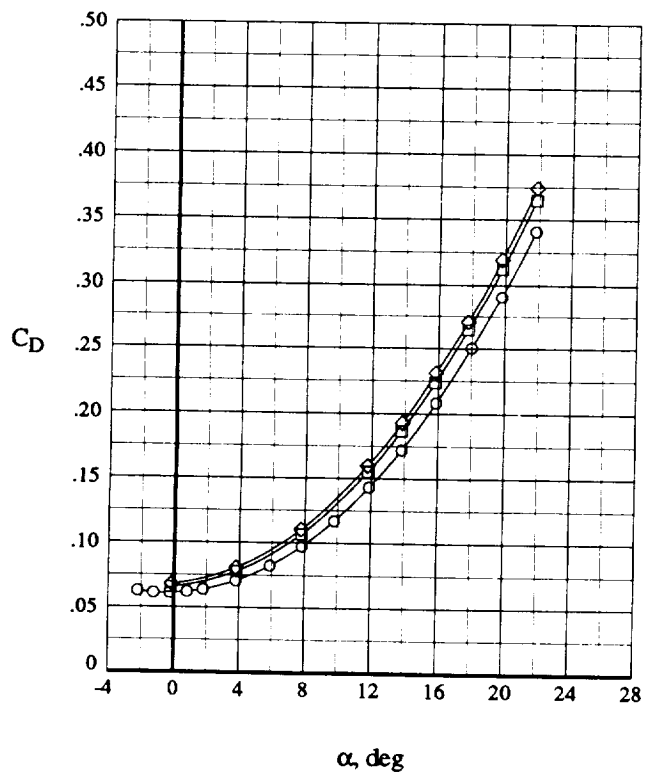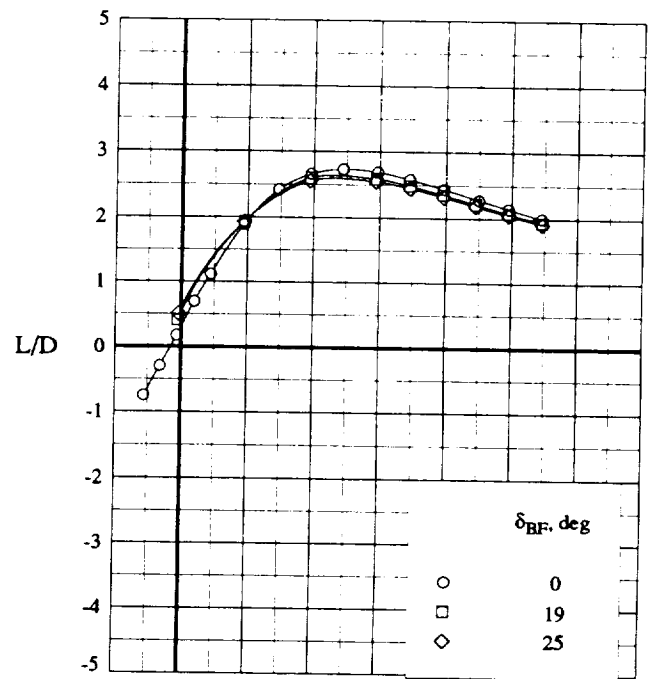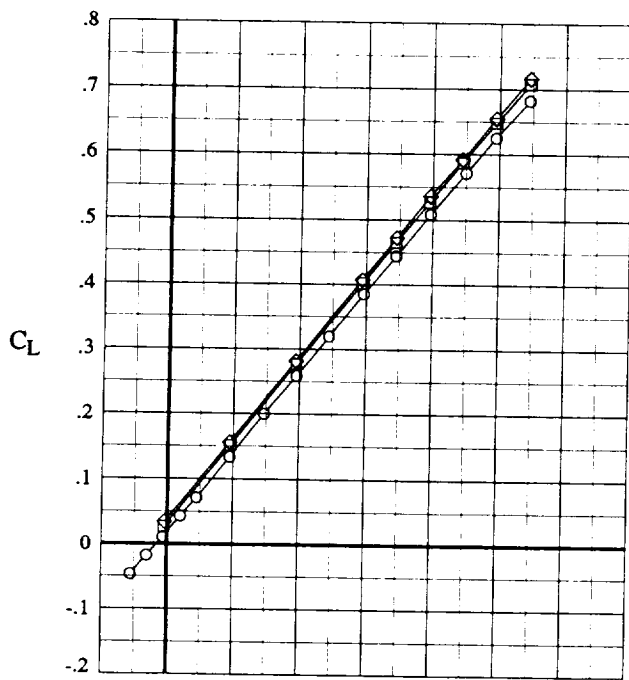
(b) M = 2.30.

Figure 6. Continued.
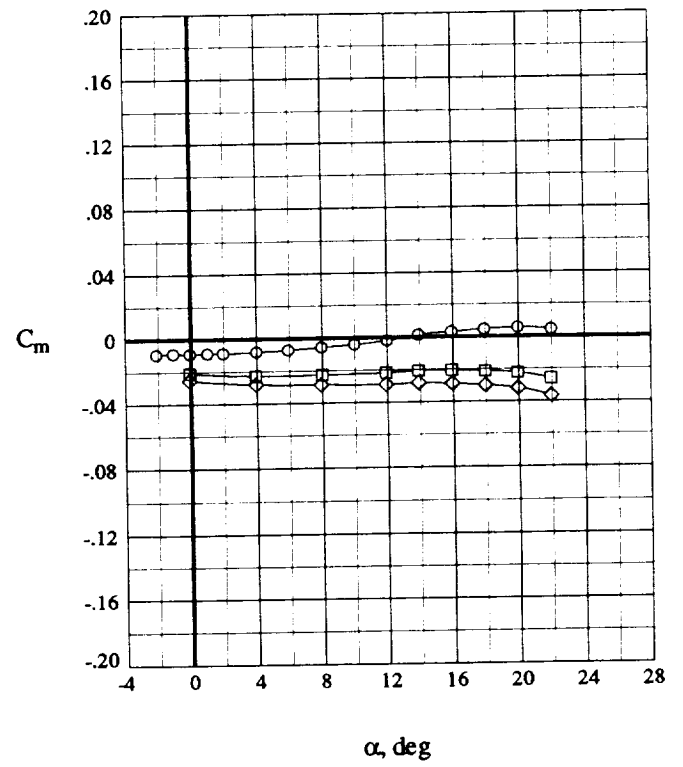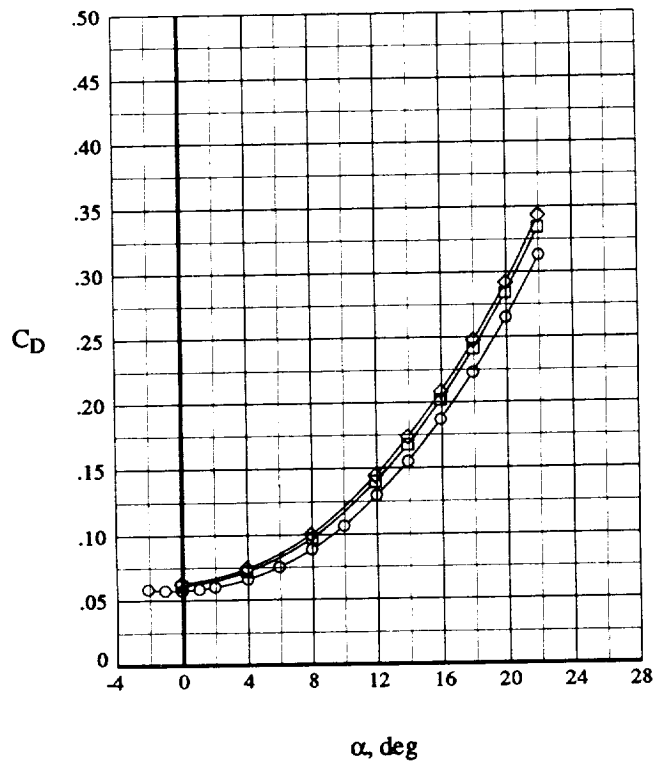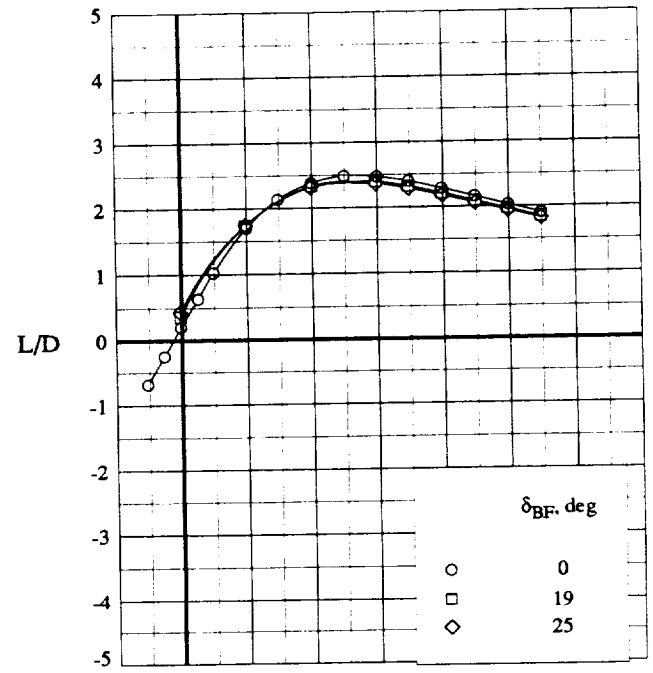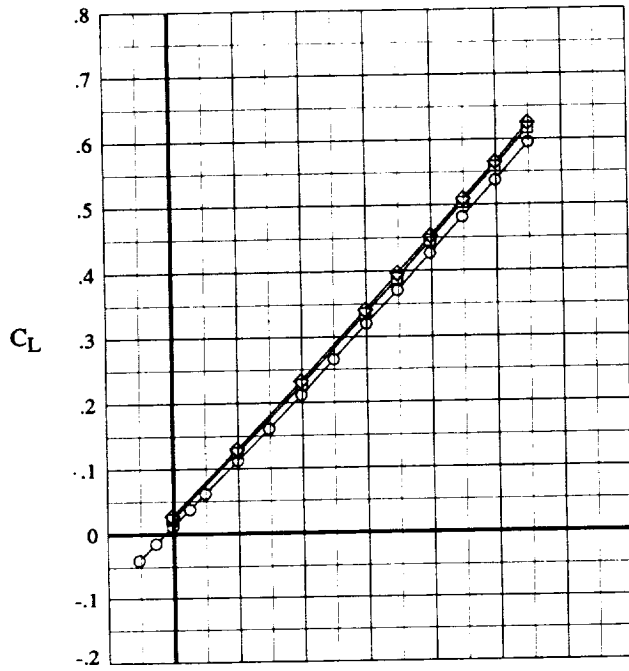
(c) M = 2.96.

Figure 6. Continued.
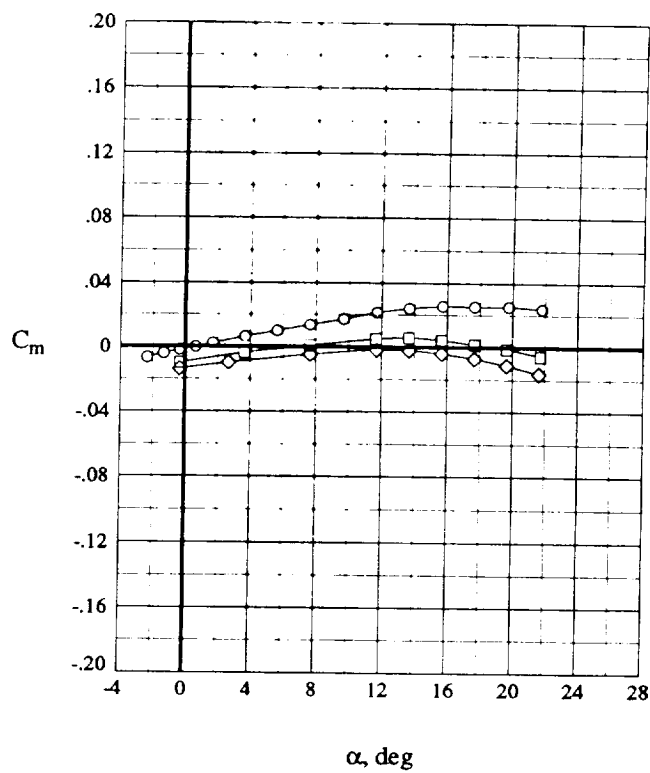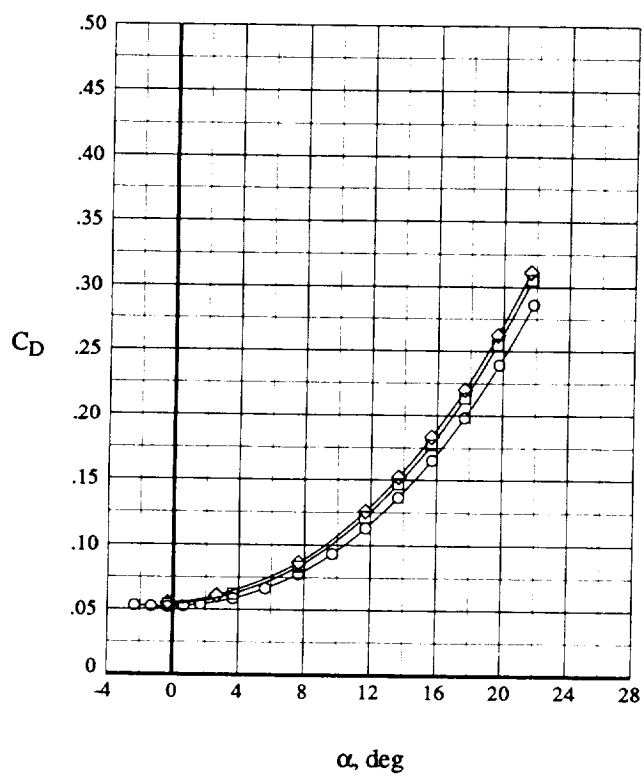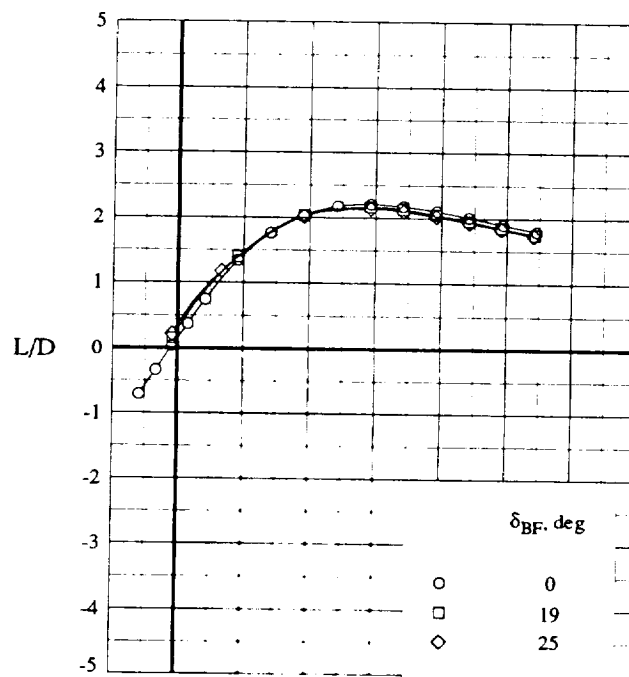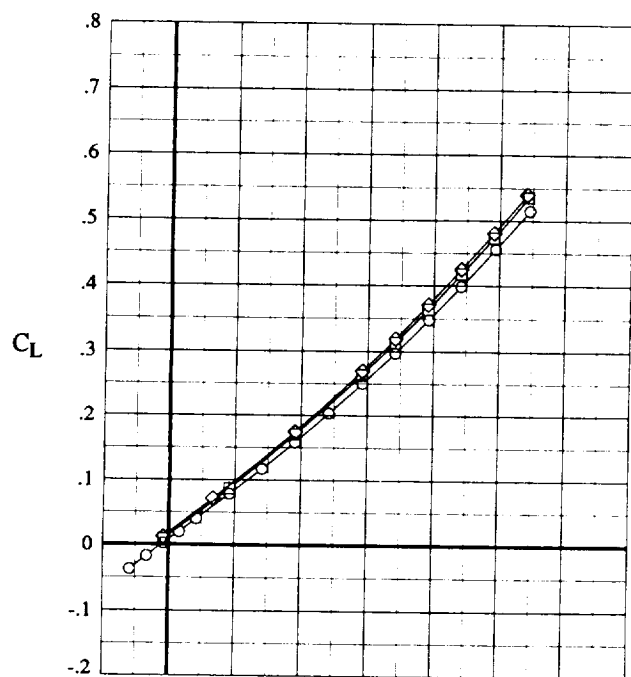
(d) M = 3.90.

Figure 6. Continued.
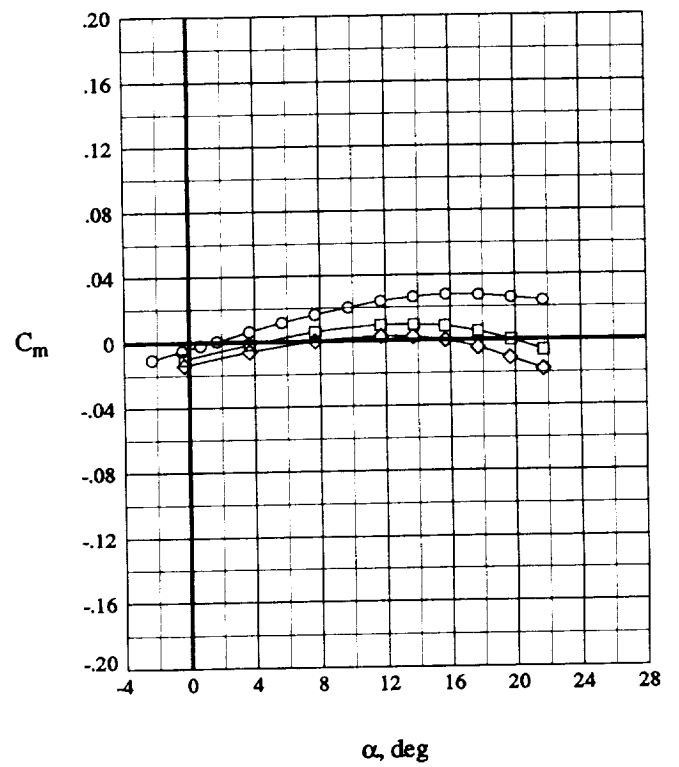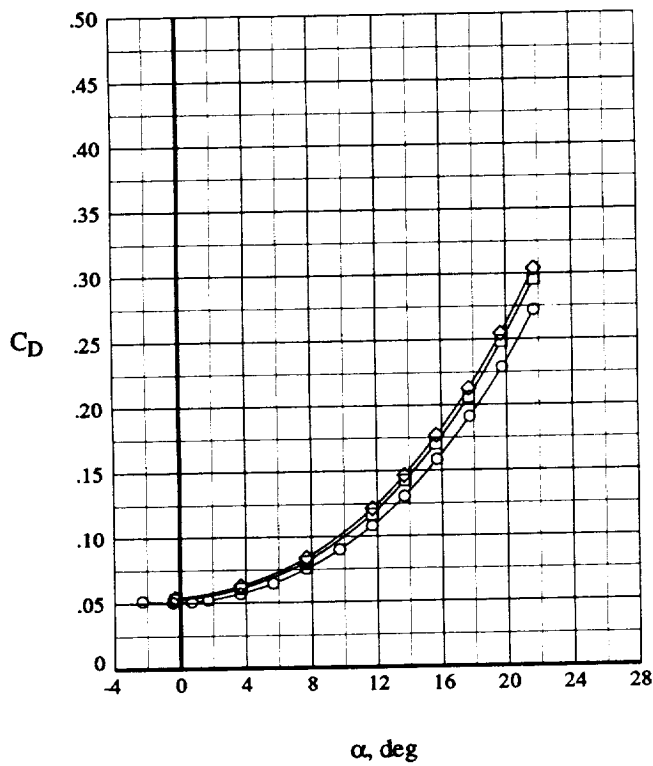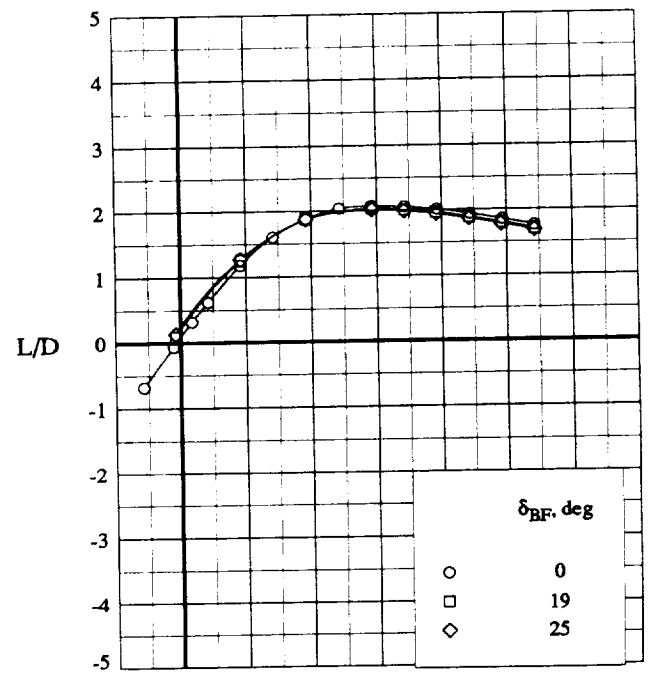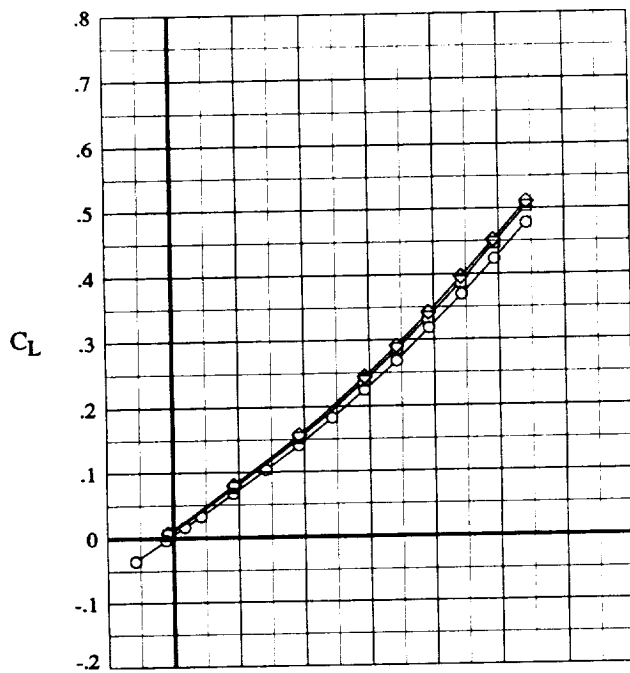
(e) M = 4.60.

Figure 6. Concluded.
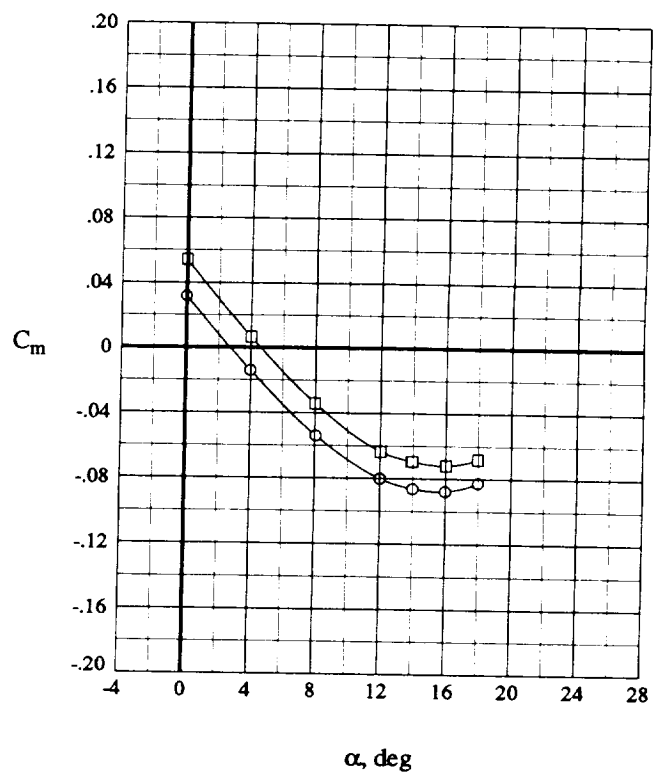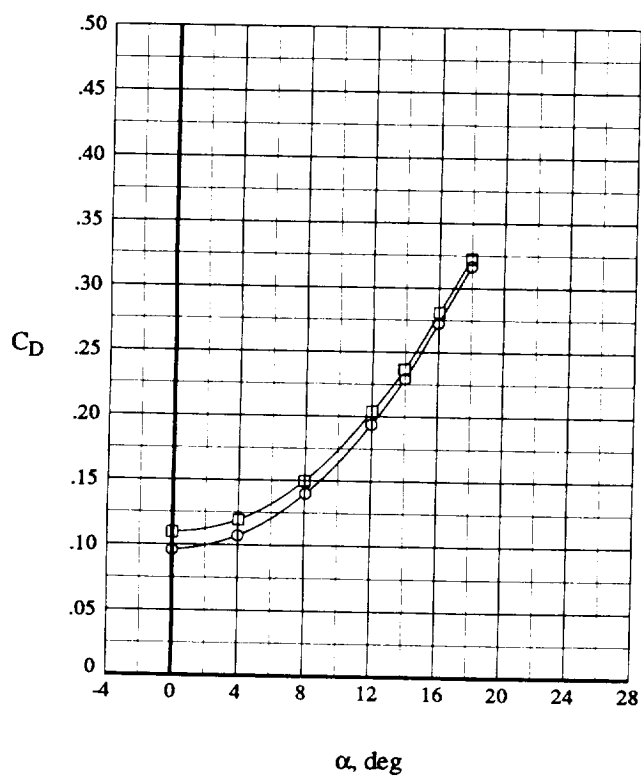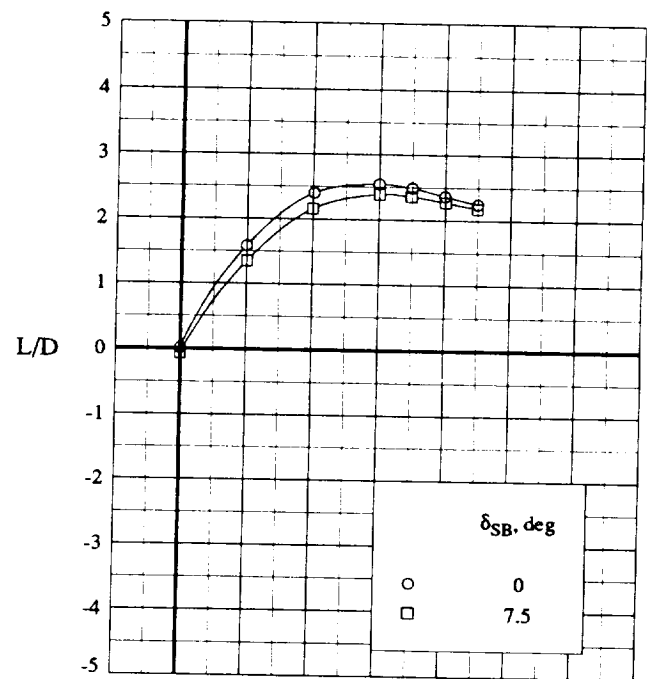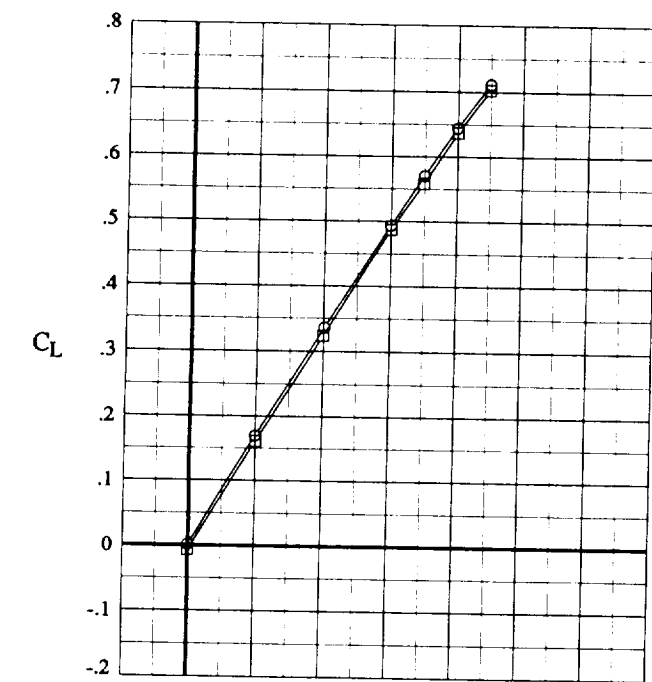
(a) M = 1.60.

Figure 7. Effect of speed brake deflection on longitudinal characteristics of circular body model with aft center fin.

29

α, deg
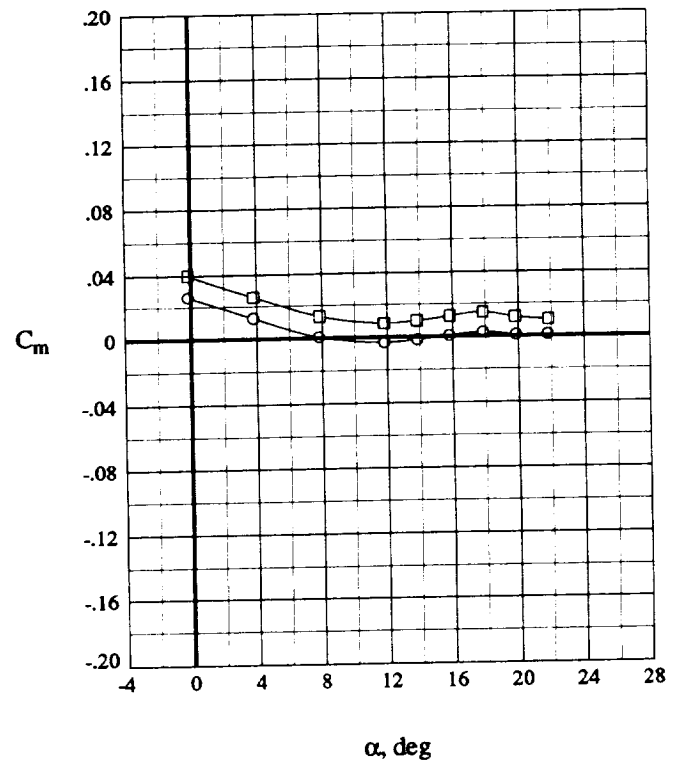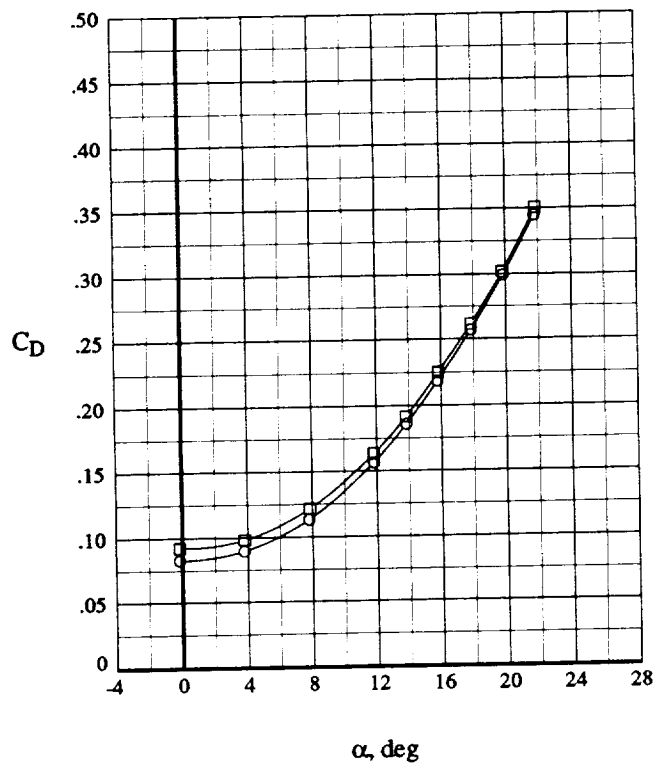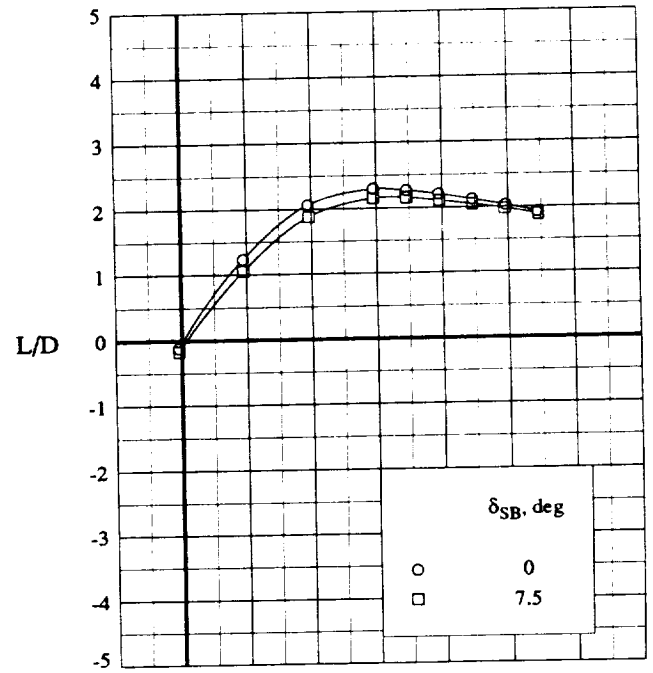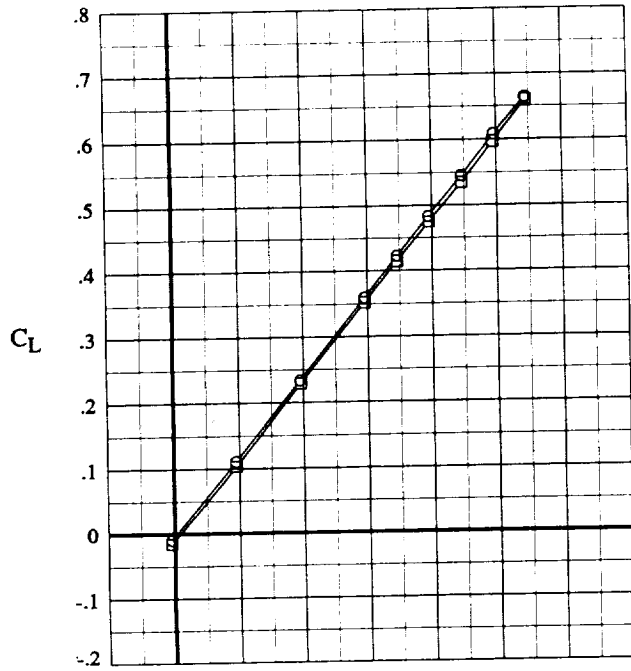
(b) M = 2.30.

Figure 7. Continued.

30
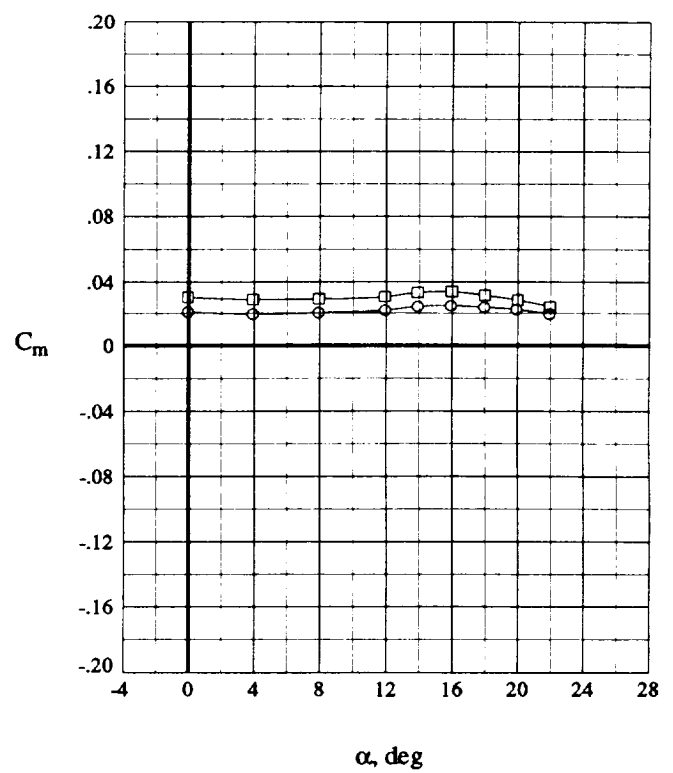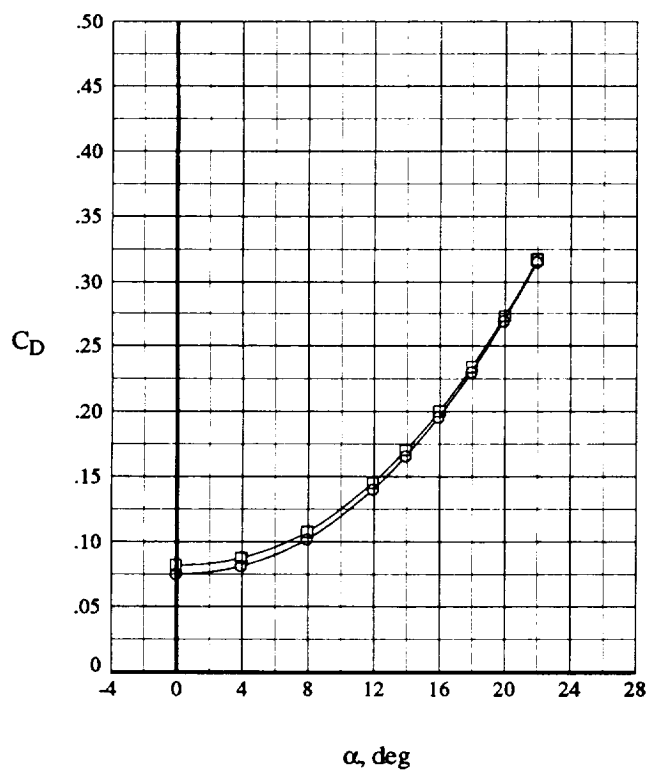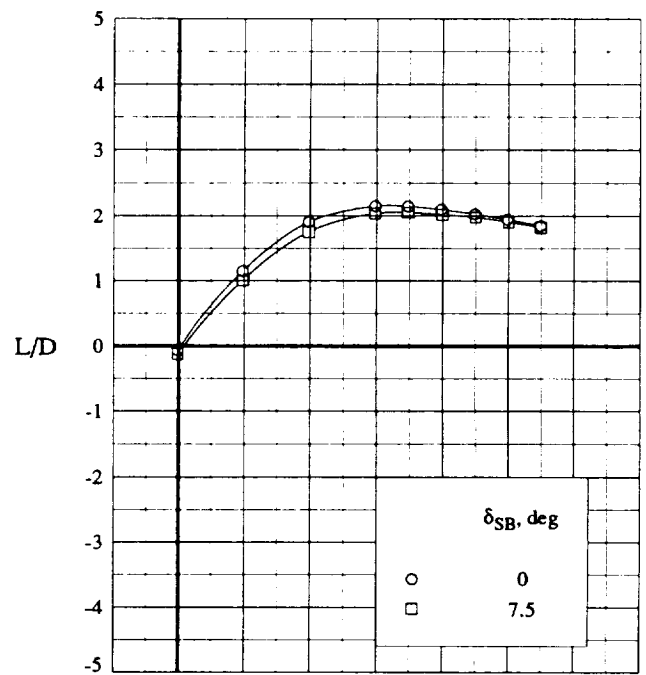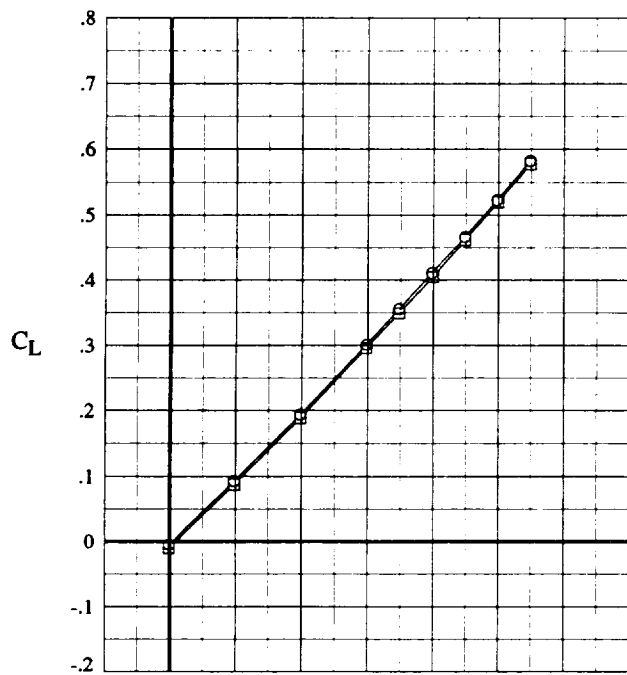
(c) M = 2.96.

Figure 7. Continued.
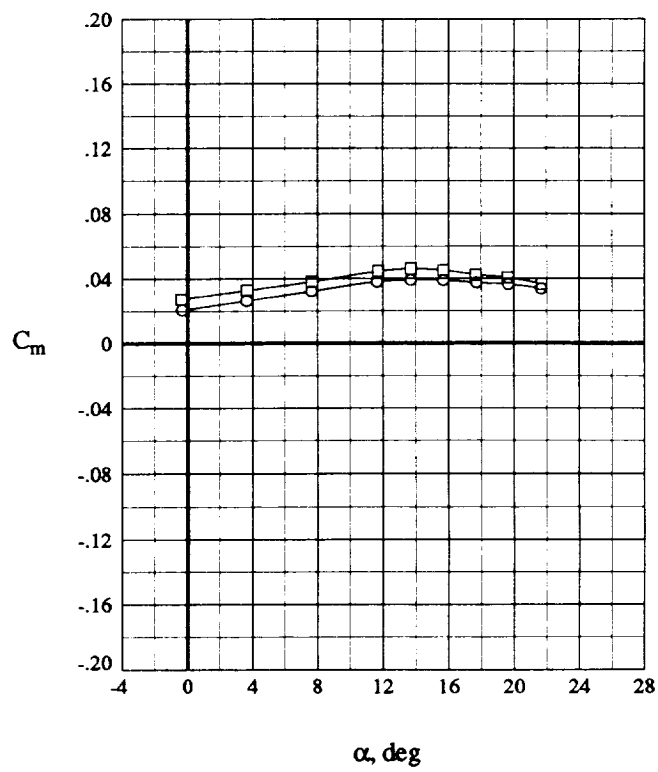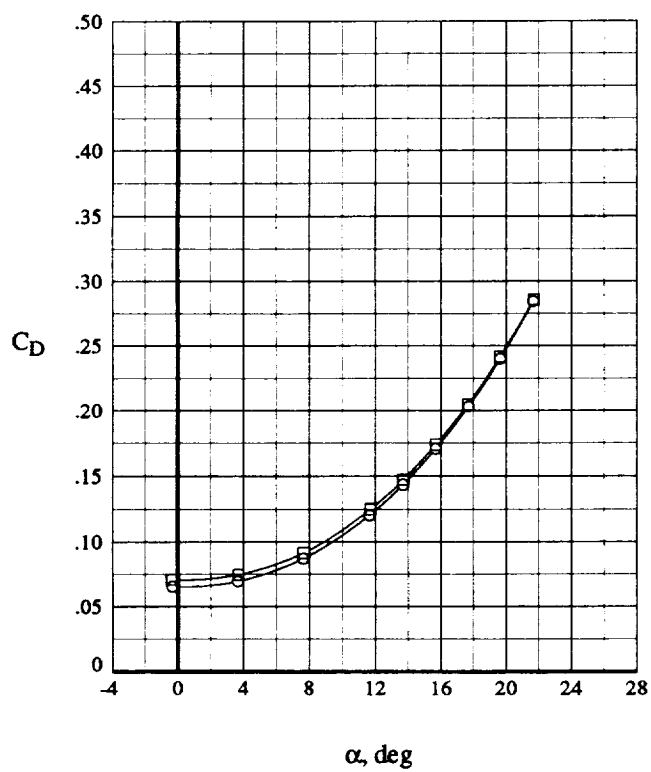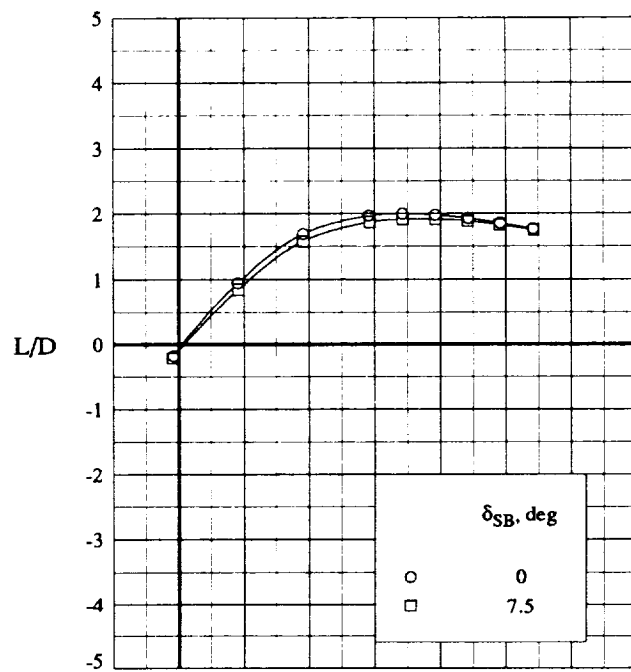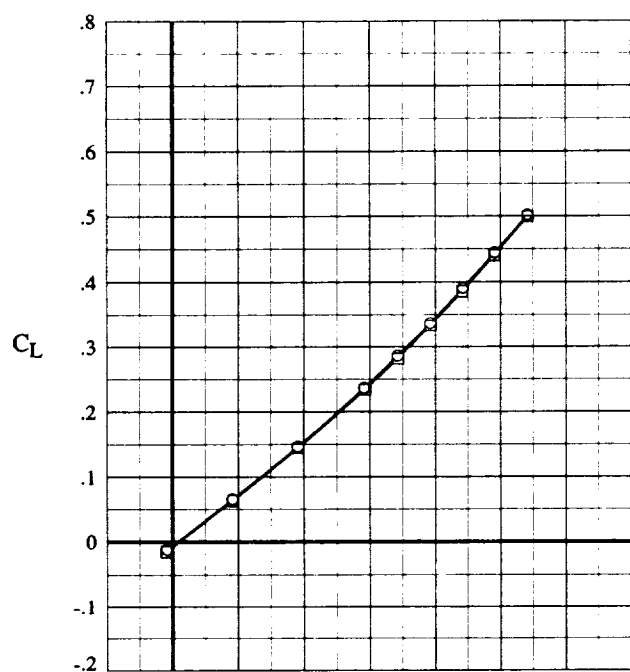
(d) M = 3.90.

Figure 7. Continued.
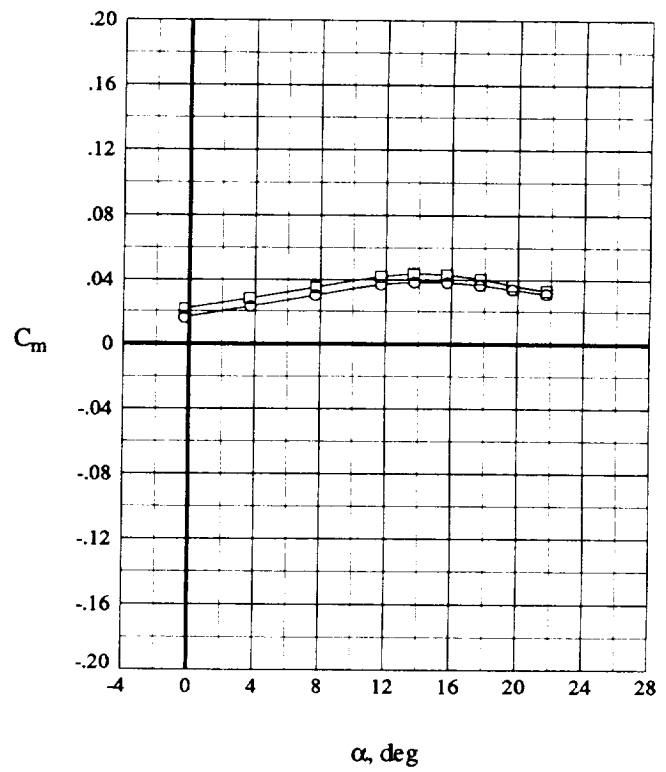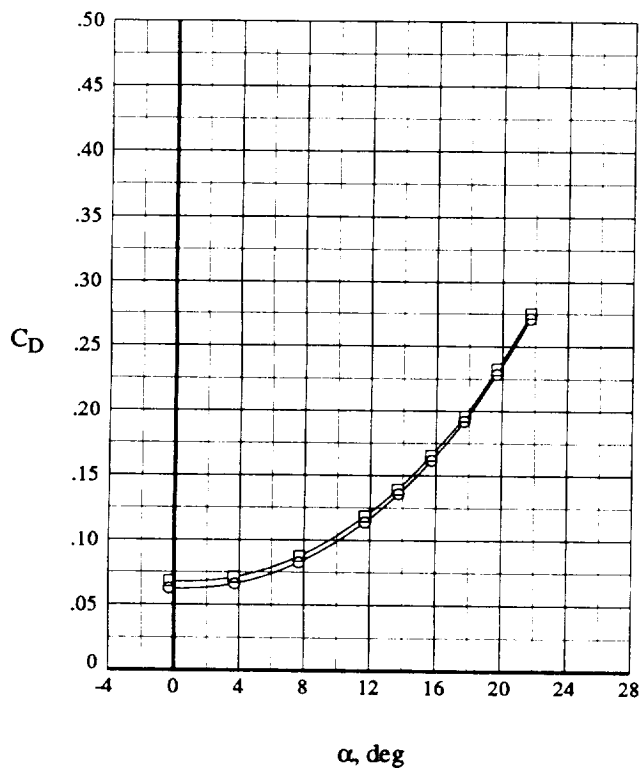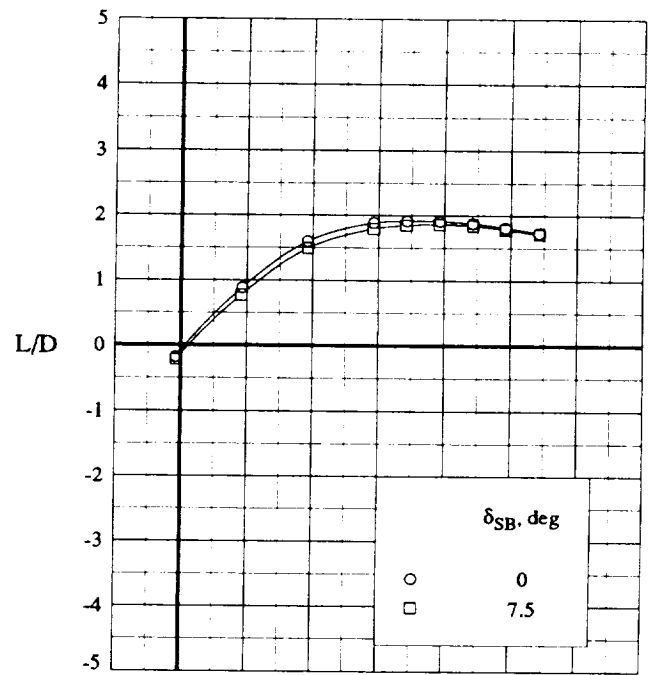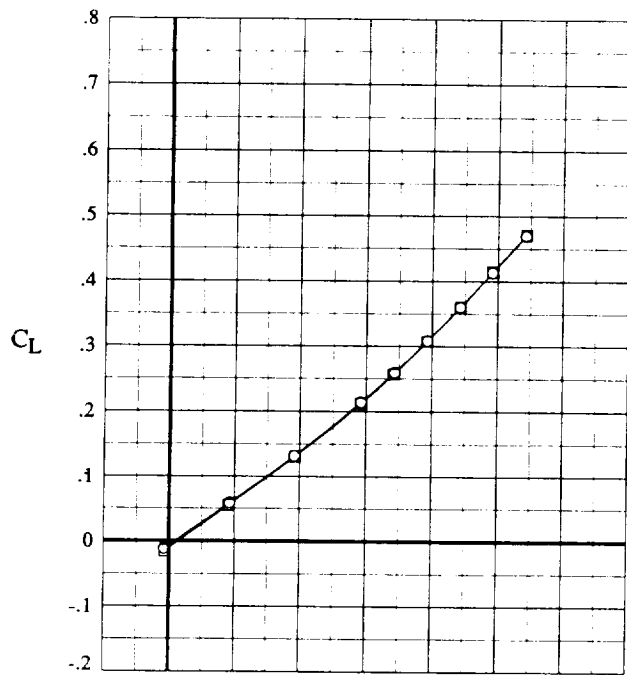
(e) M = 4.60.

Figure 7. Concluded.
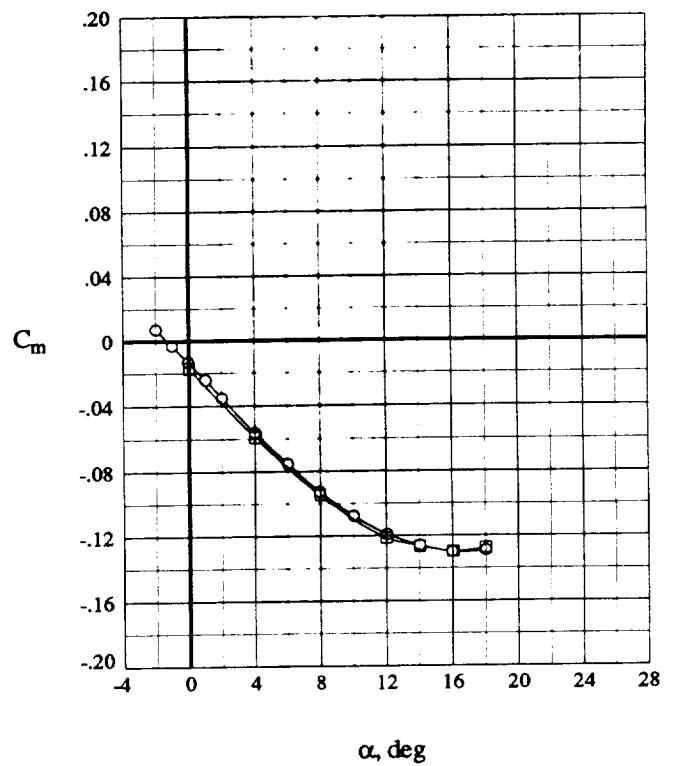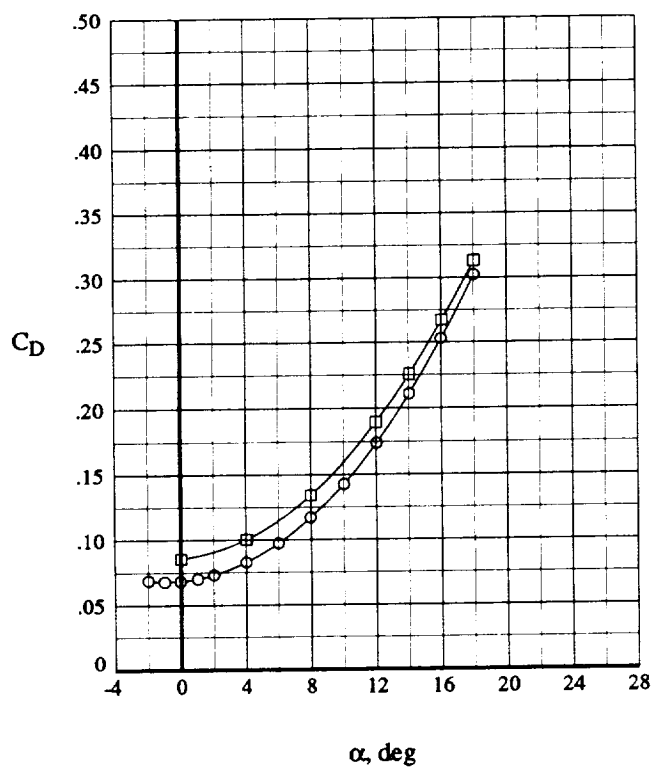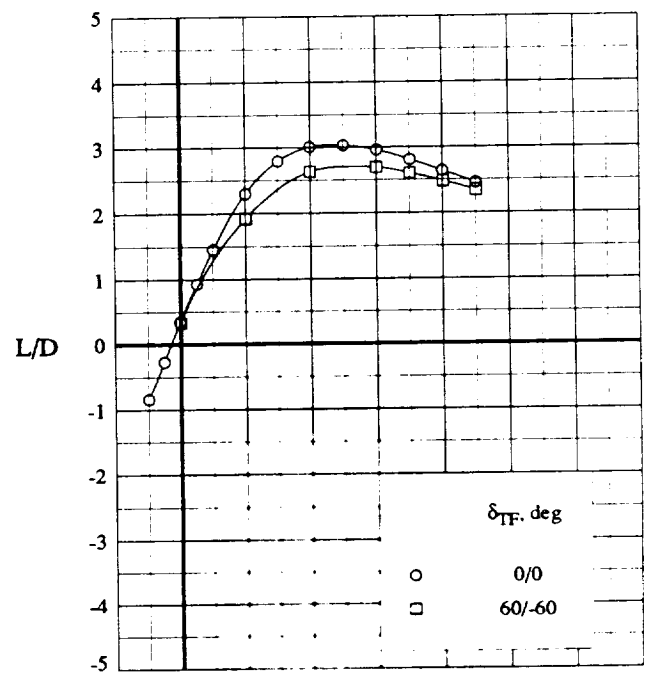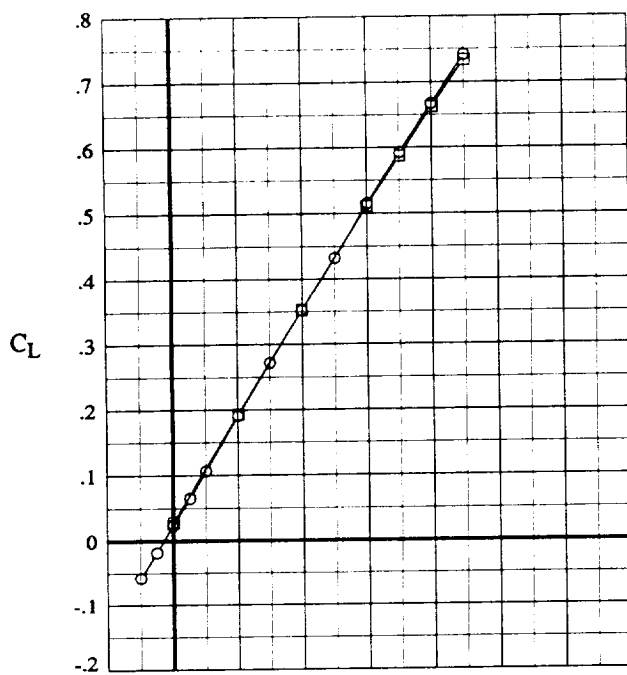
(a) M = 1.60.

Figure 8. Effect of speed brake deflection on longitudinal characteristics of circular body model with wingtip fins.
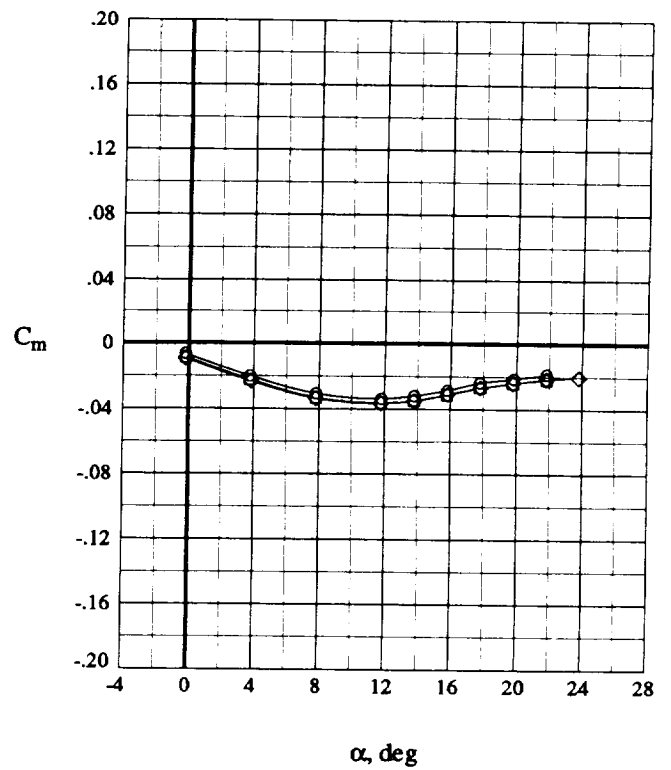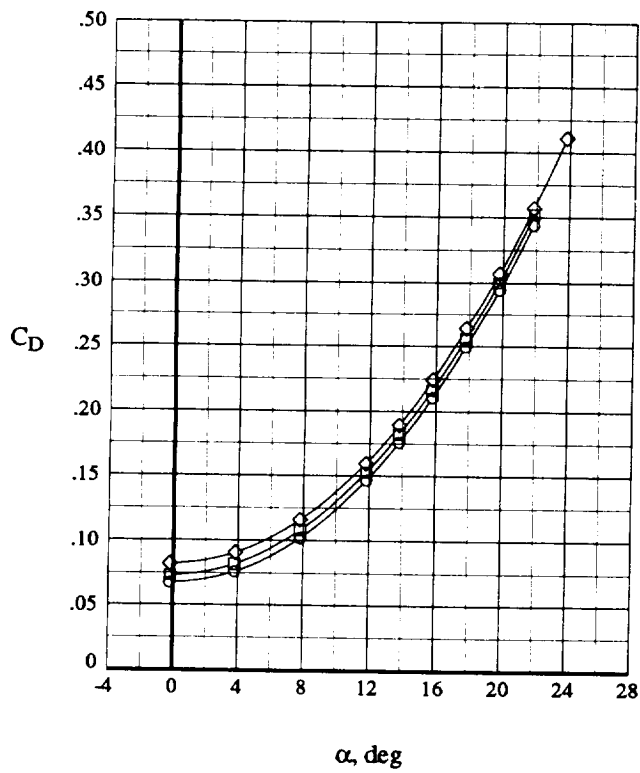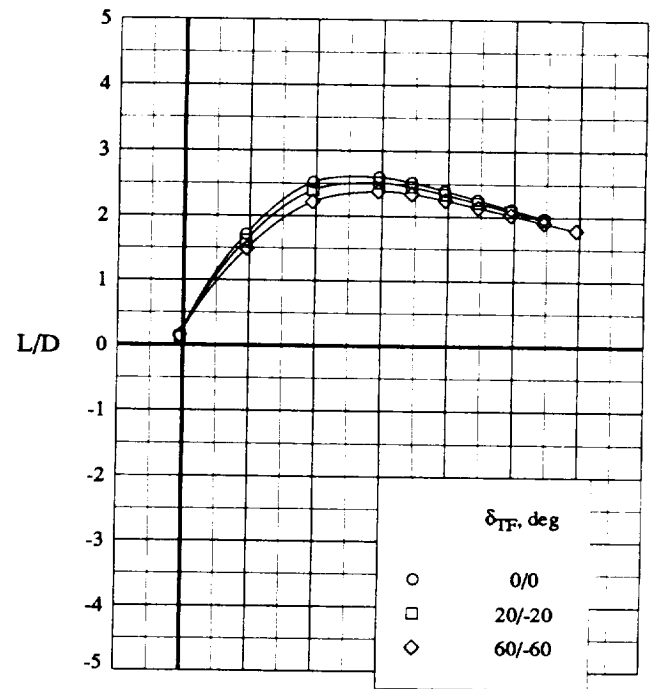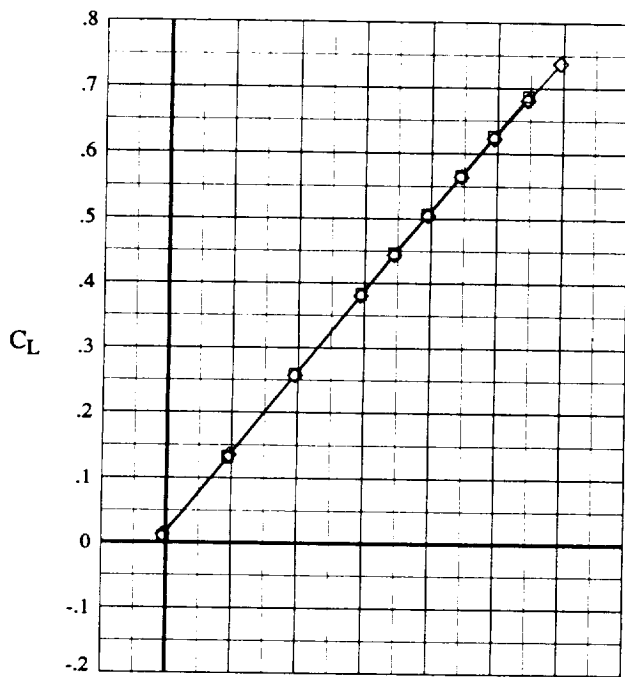
(b) M = 2.30.

Figure 8. Continued.
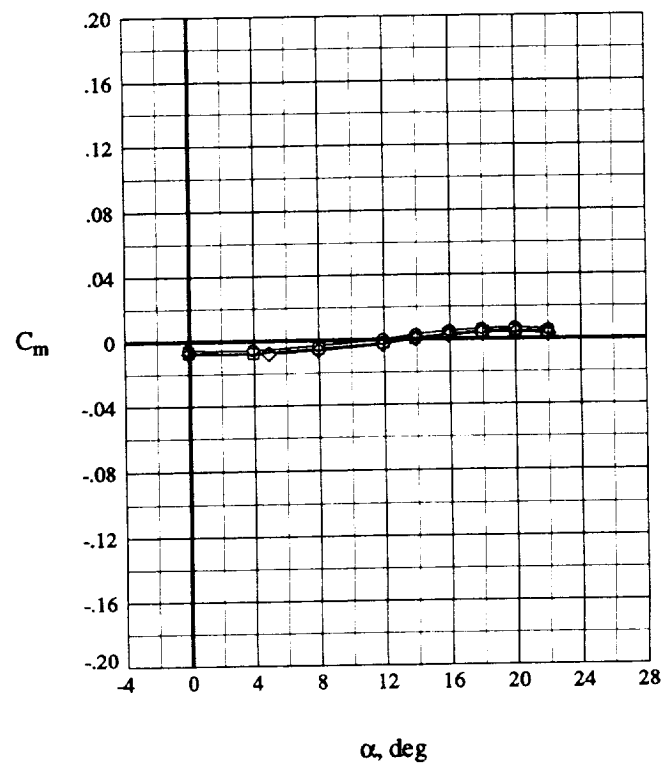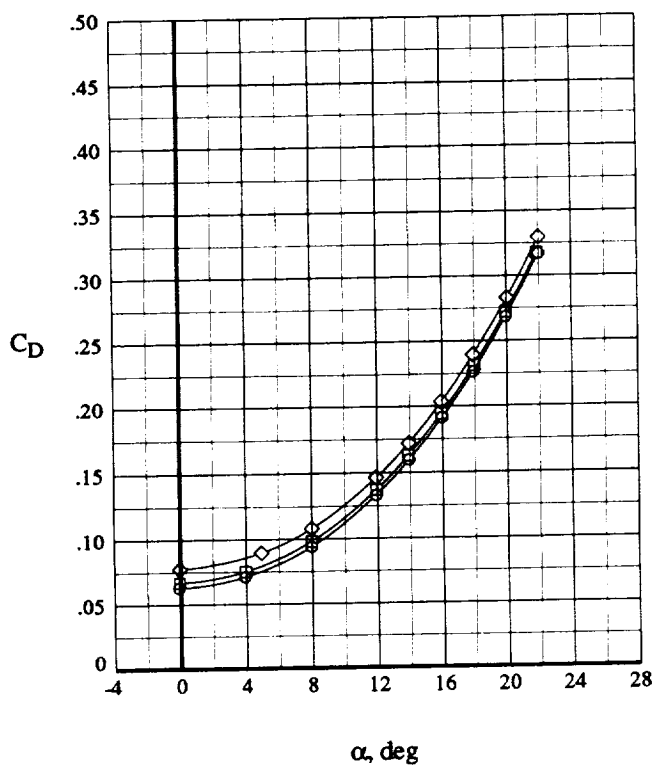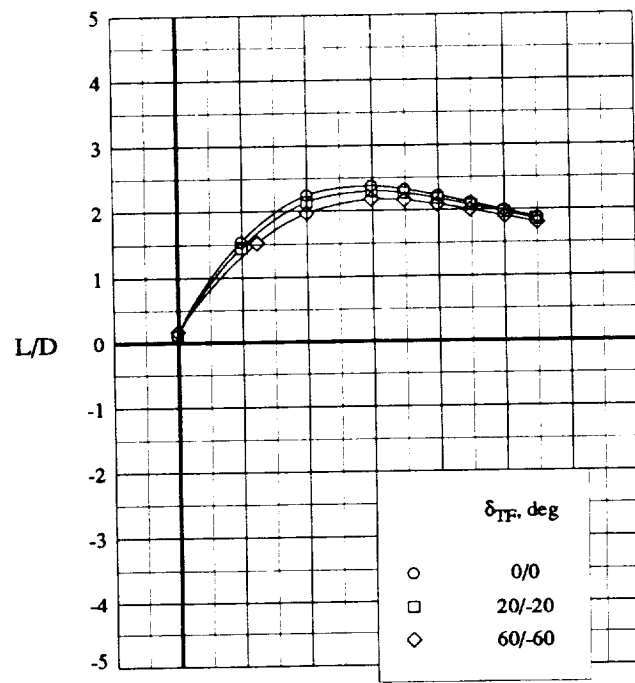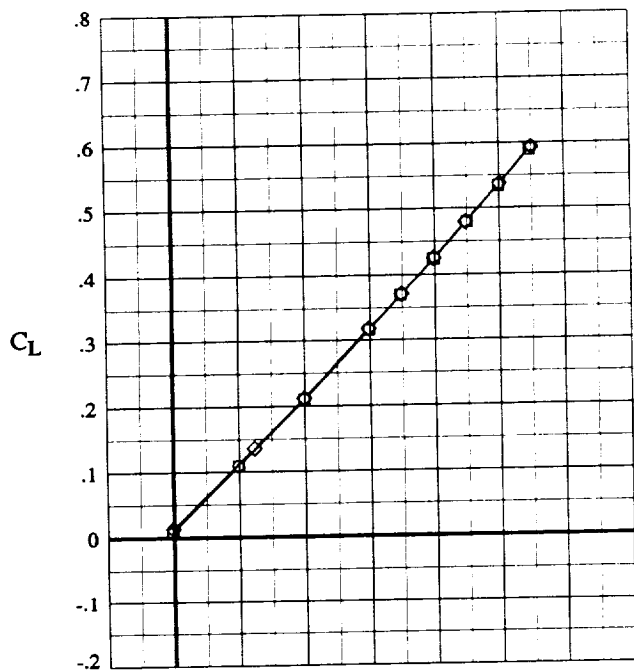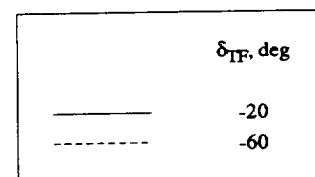
(c) M = 2.96.

Figure 8. Continued.
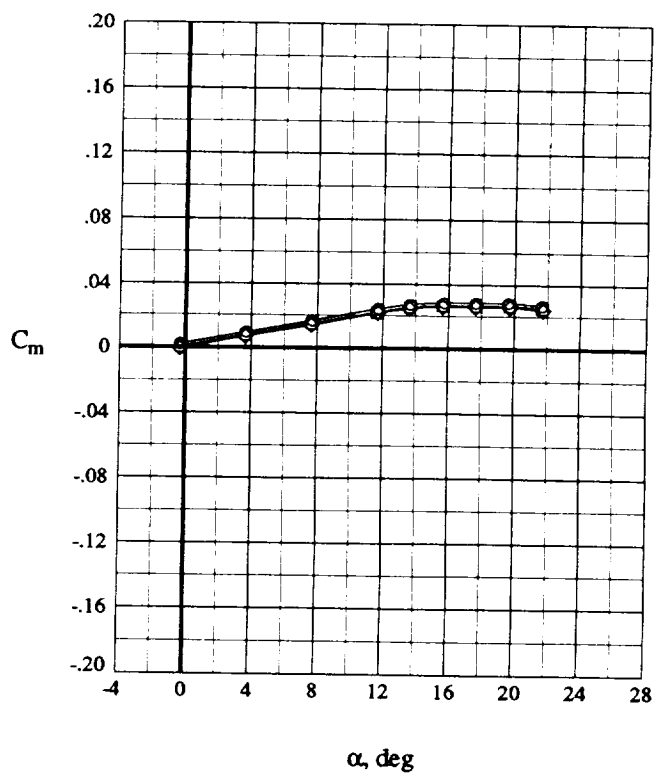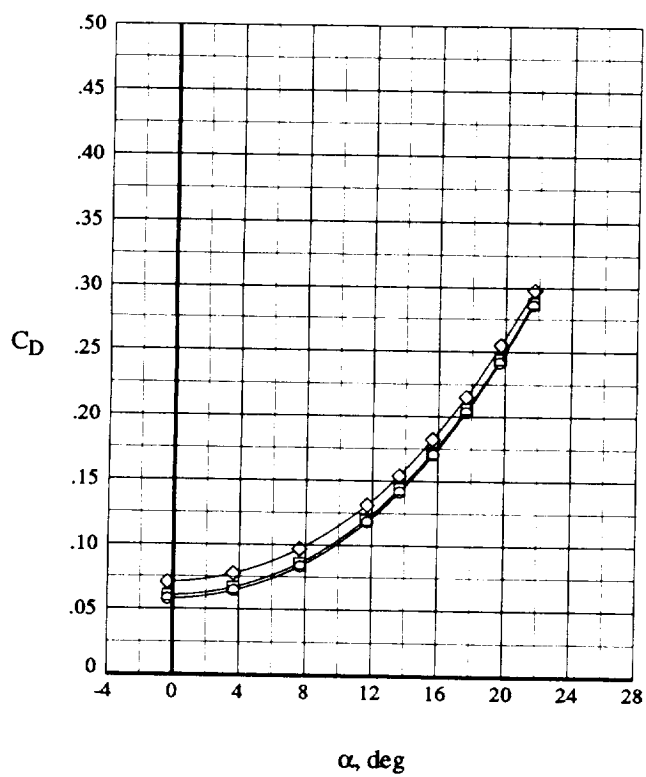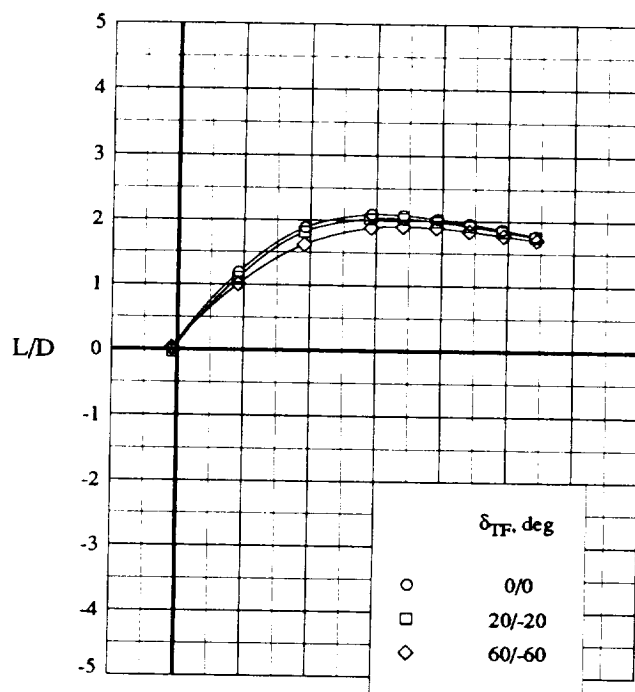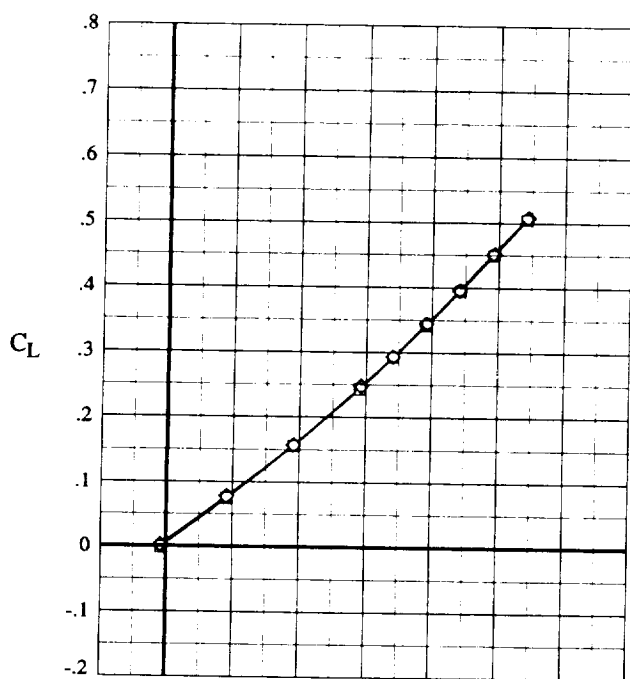
(d) M = 3.90.

Figure 8. Continued.
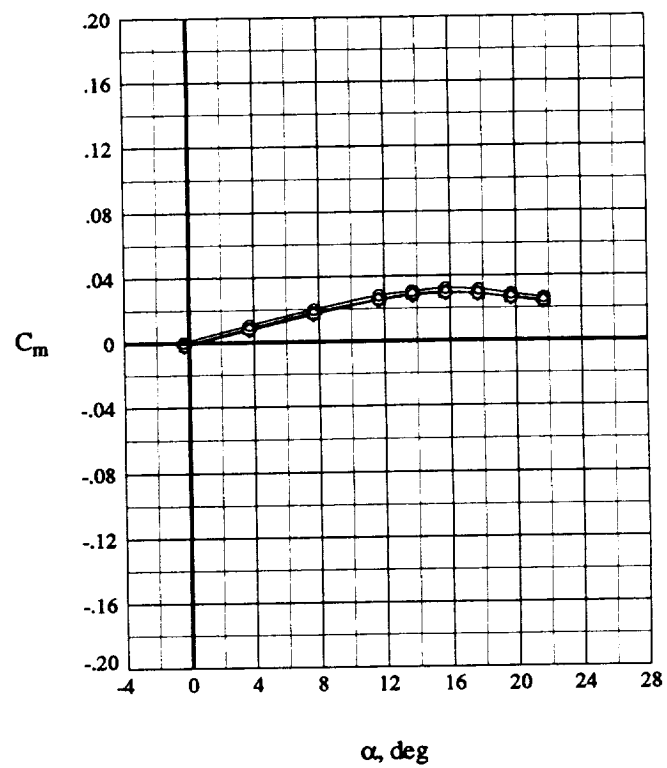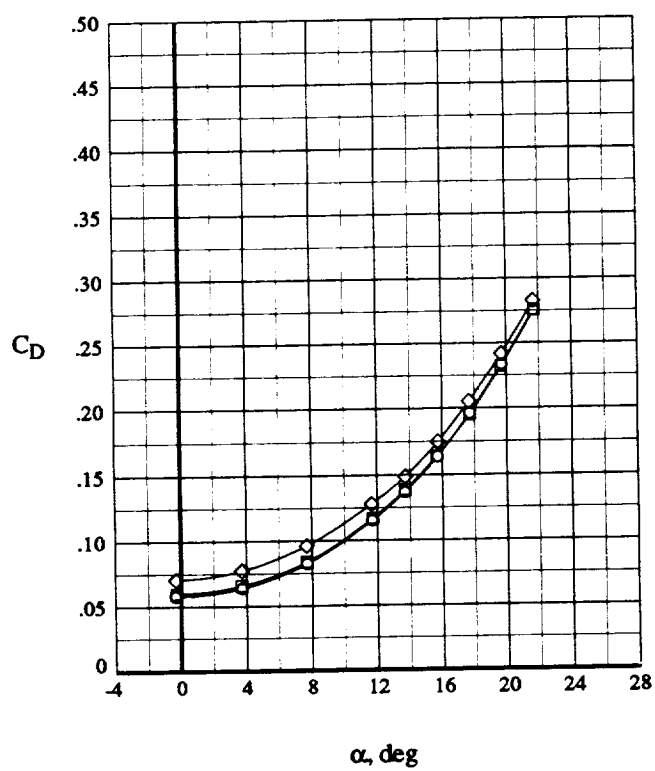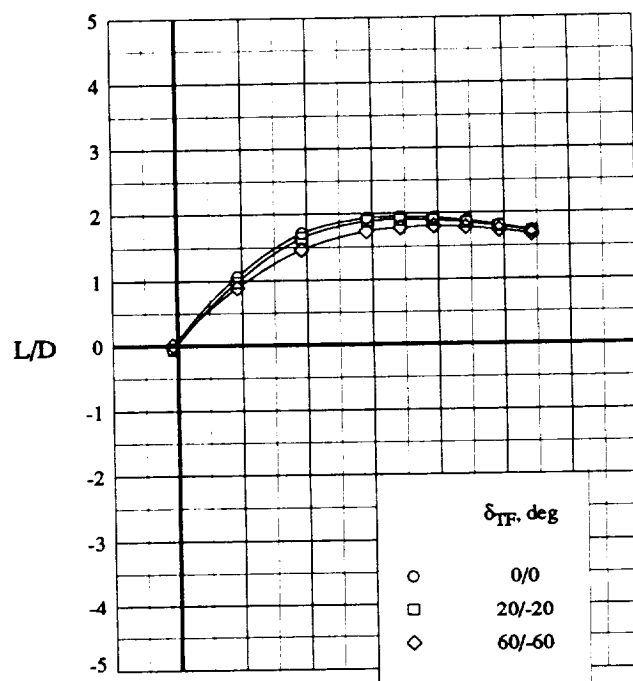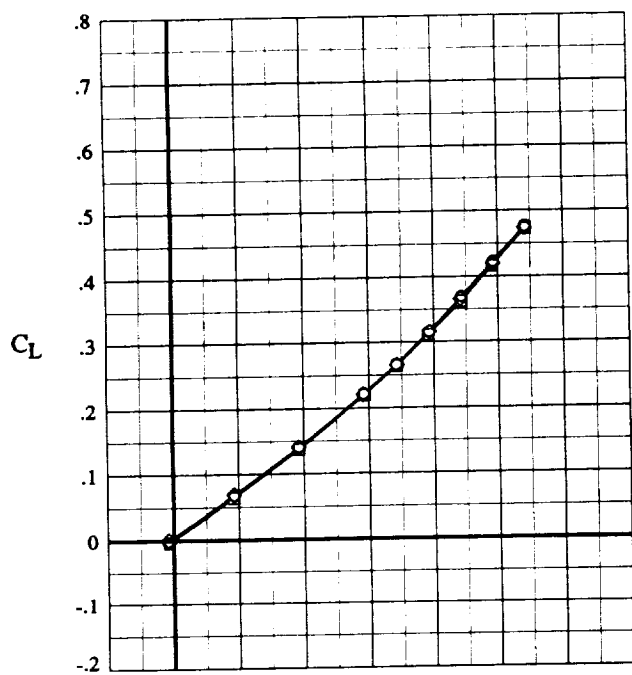
(e) M = 4.60.

Figure 8. Concluded.
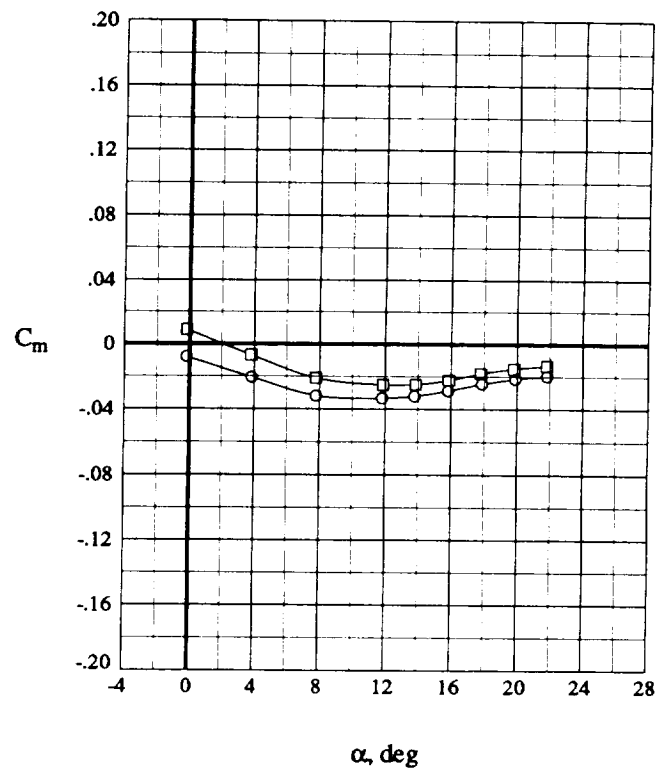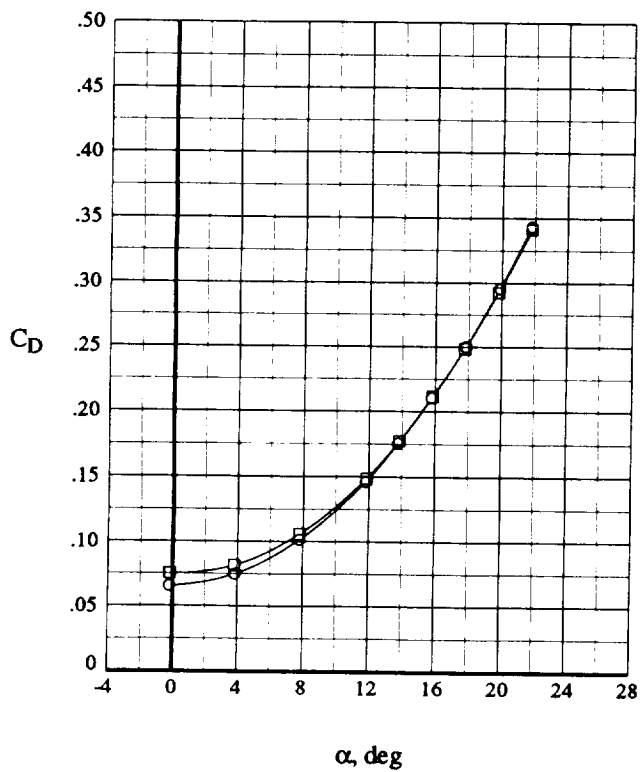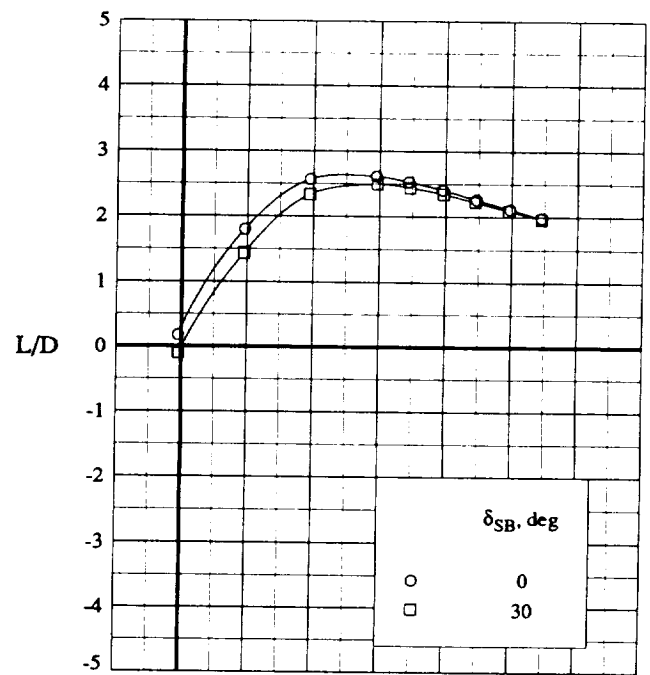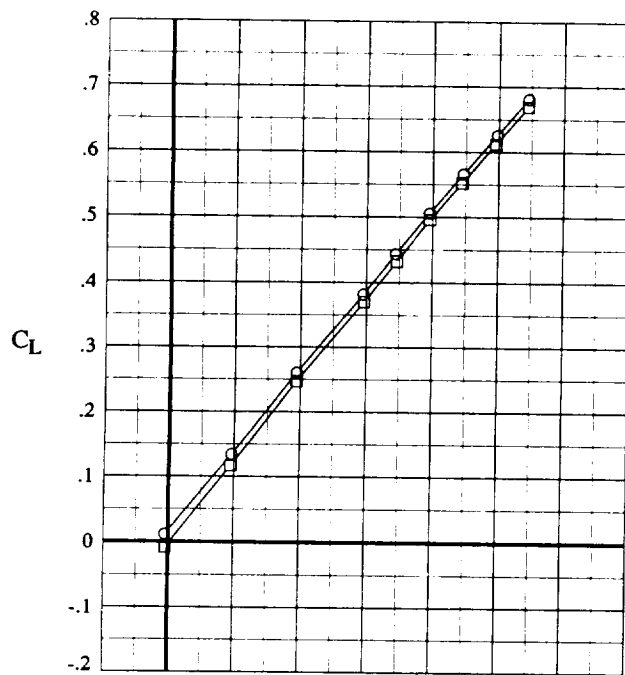
(a) M = 2.30.

Figure 9. Effect of speed brake deflection on longitudinal characteristics of circular body model with nose fin.
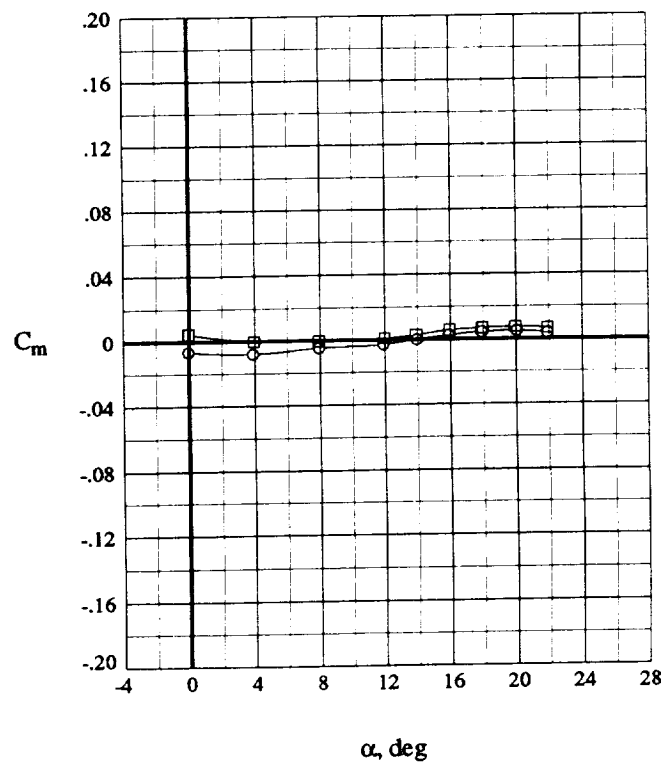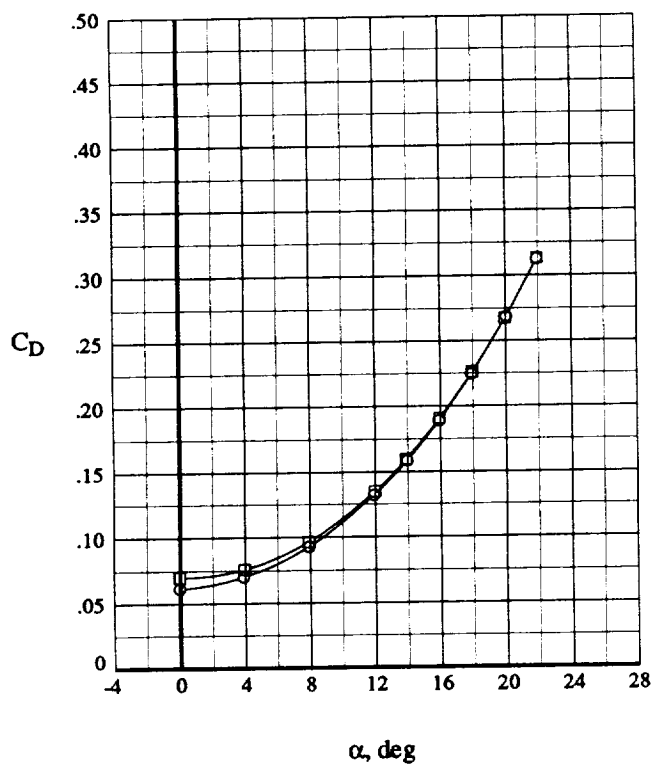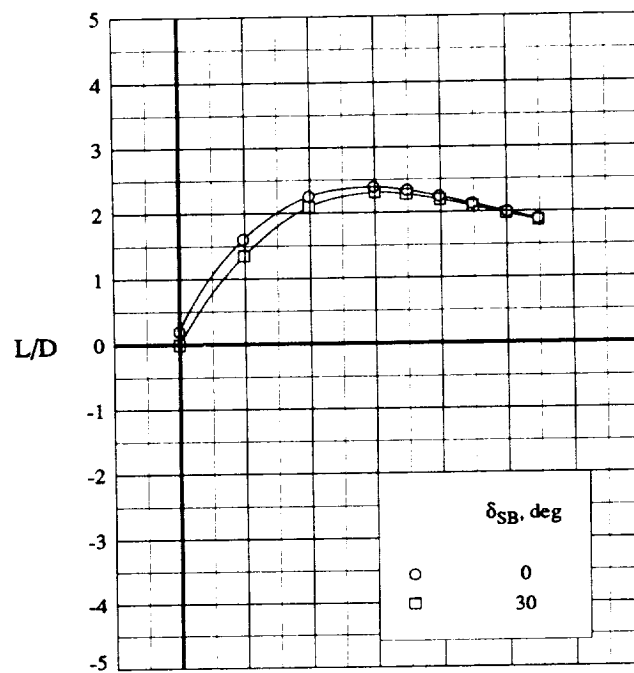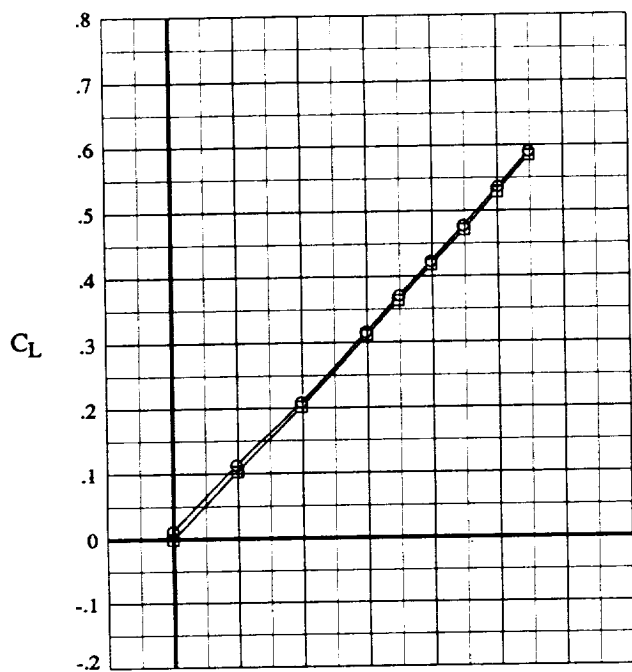
(b) M = 2.96.

Figure 9. Continued.
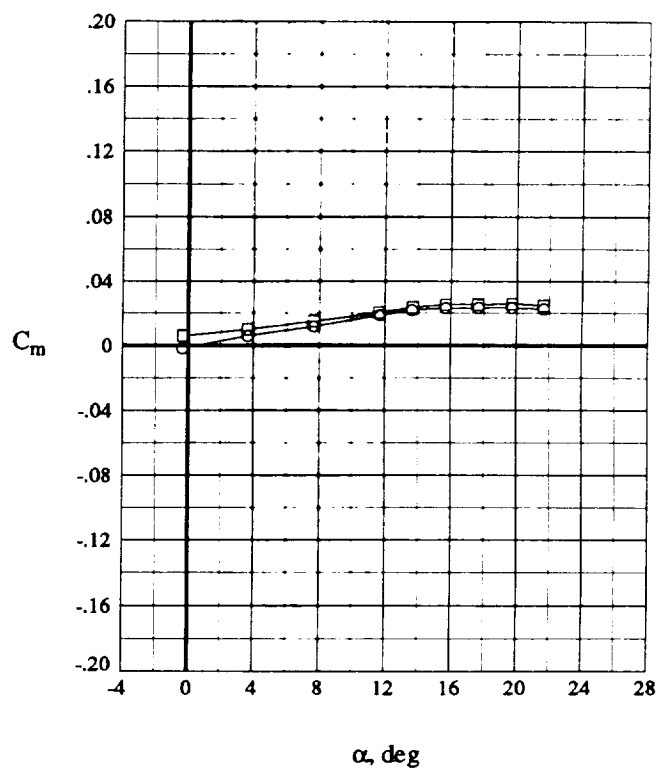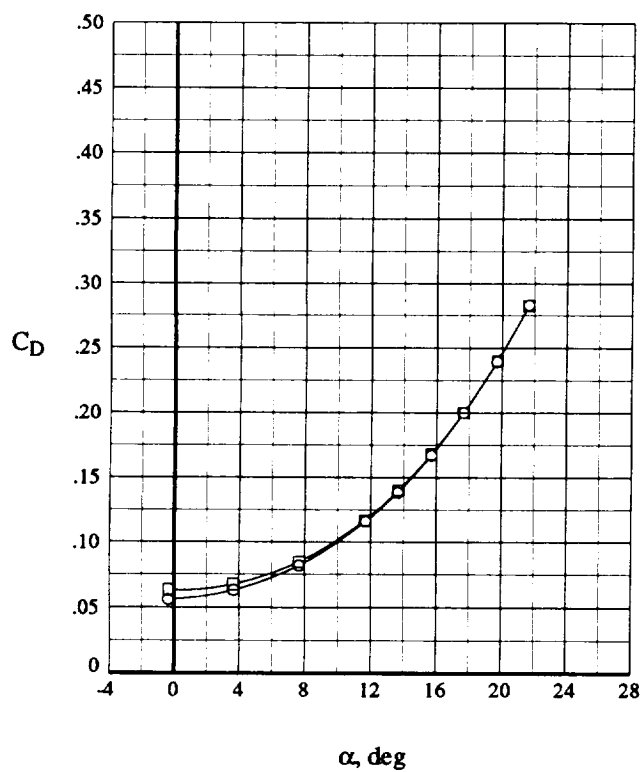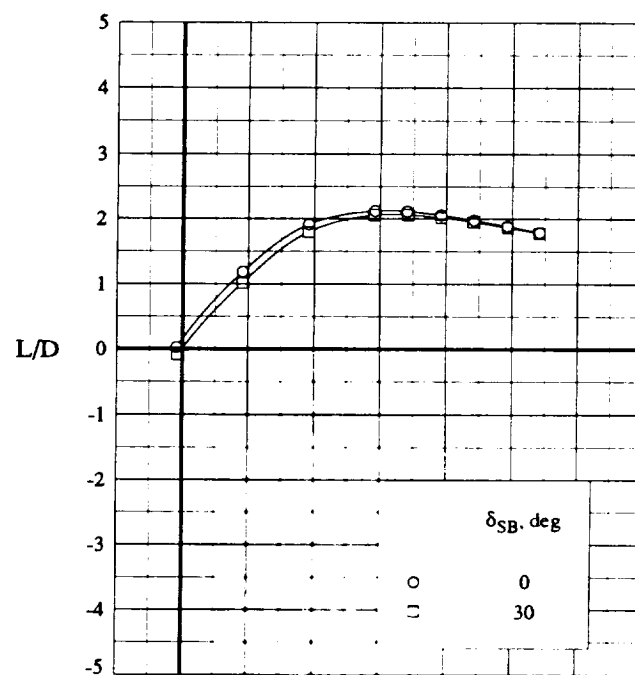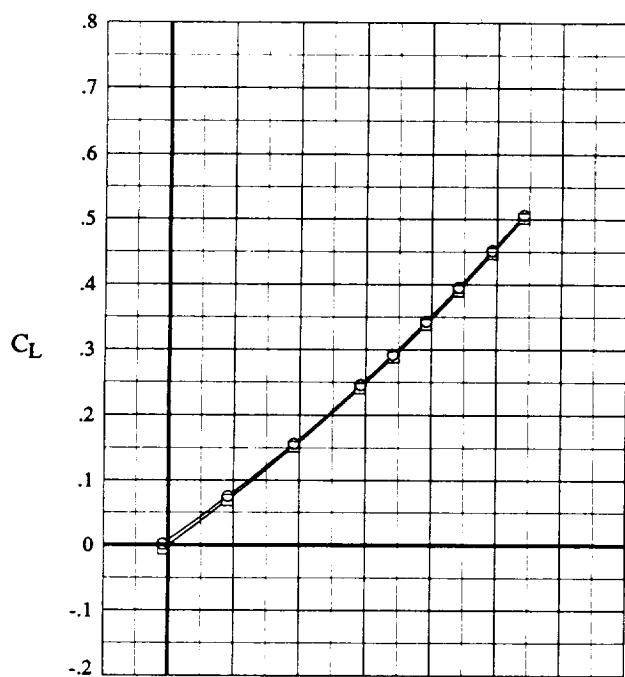
(c) M = 3.90.

Figure 9. Continued.
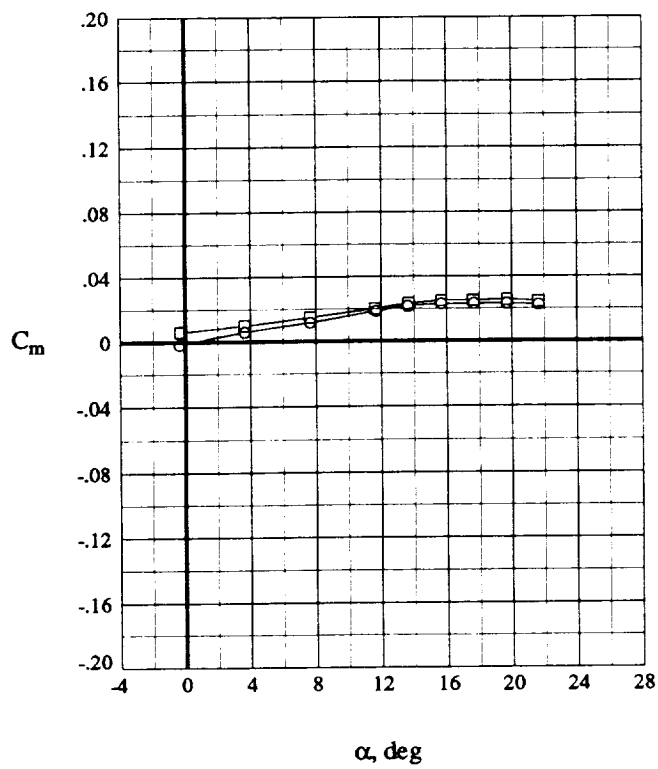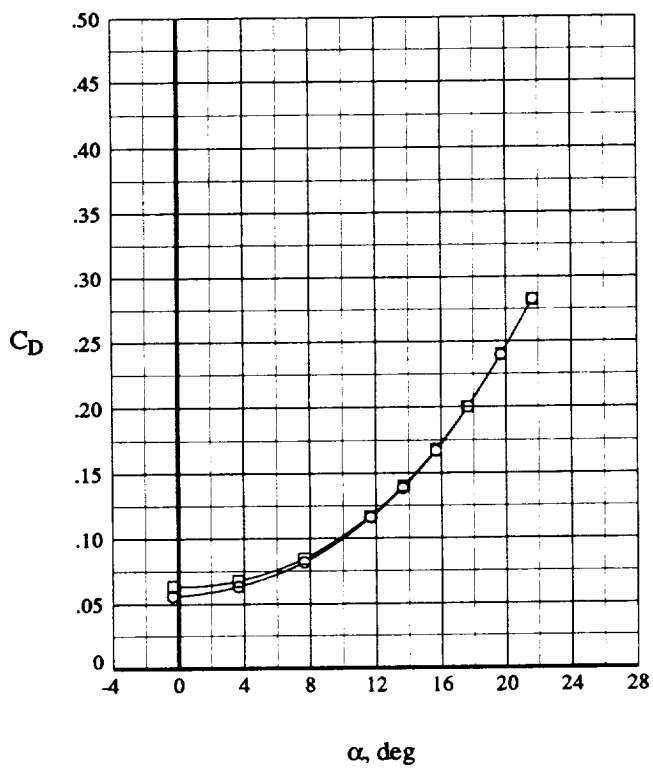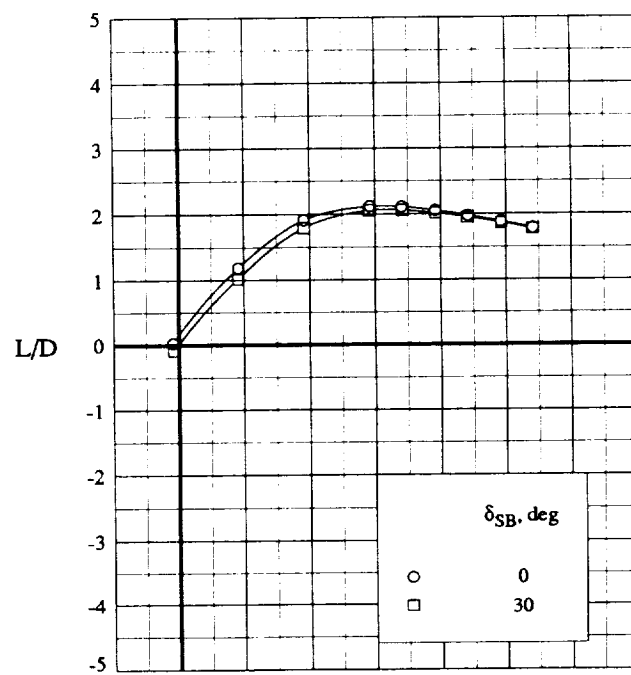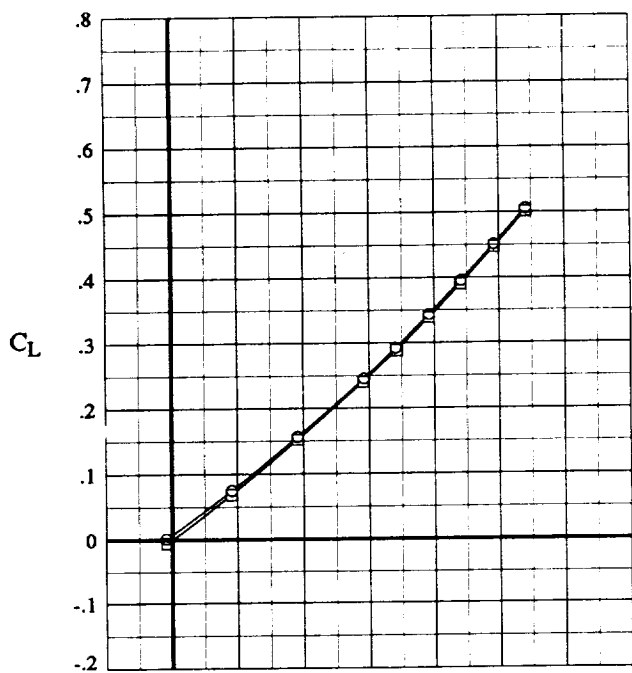
(d) M = 4.60.

Figure 9. Concluded.
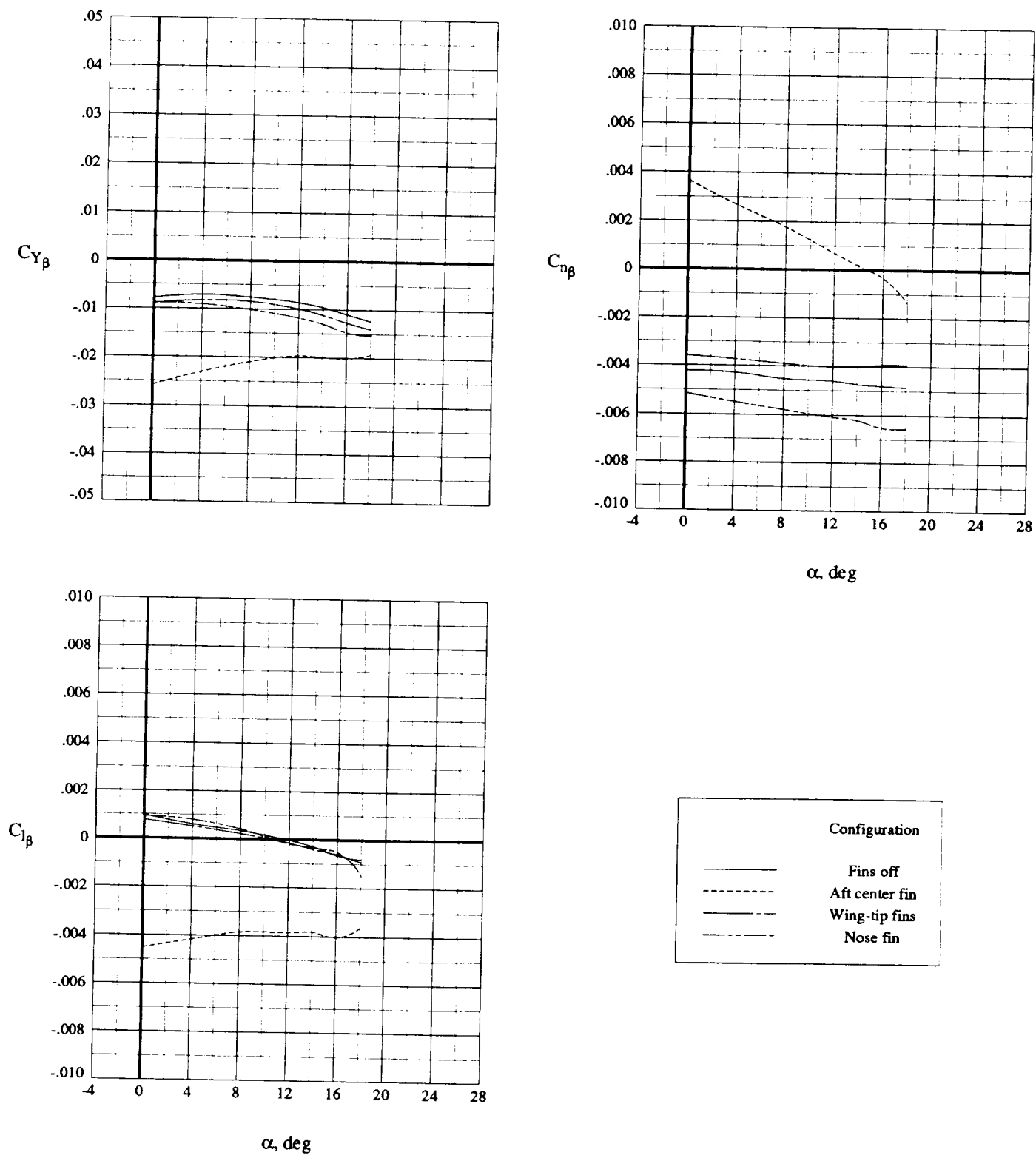
(a) M = 1.60.

Figure 10. Lateral-directional stability characteristics of circular body model with various fin arrangements.
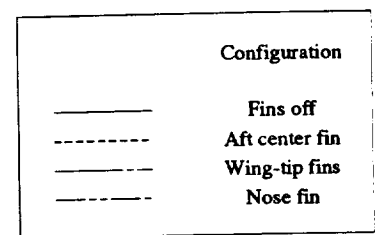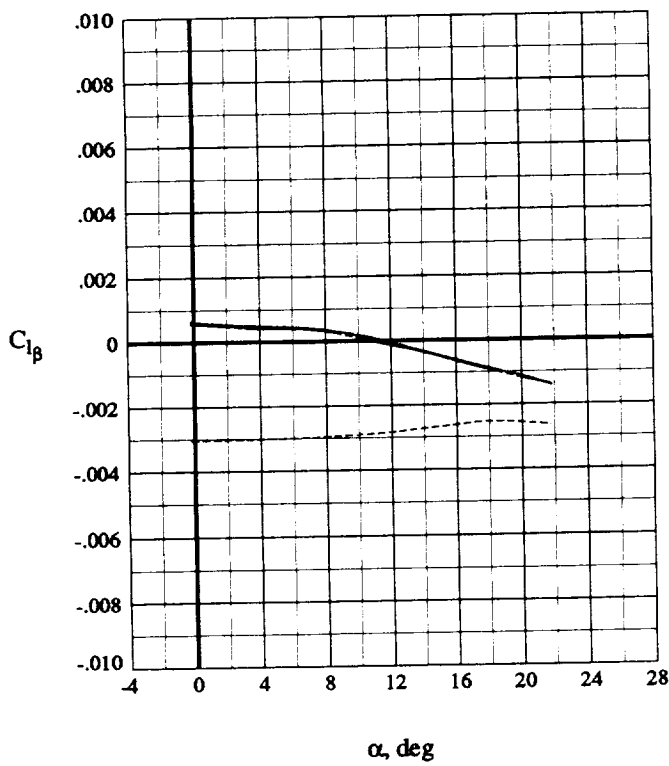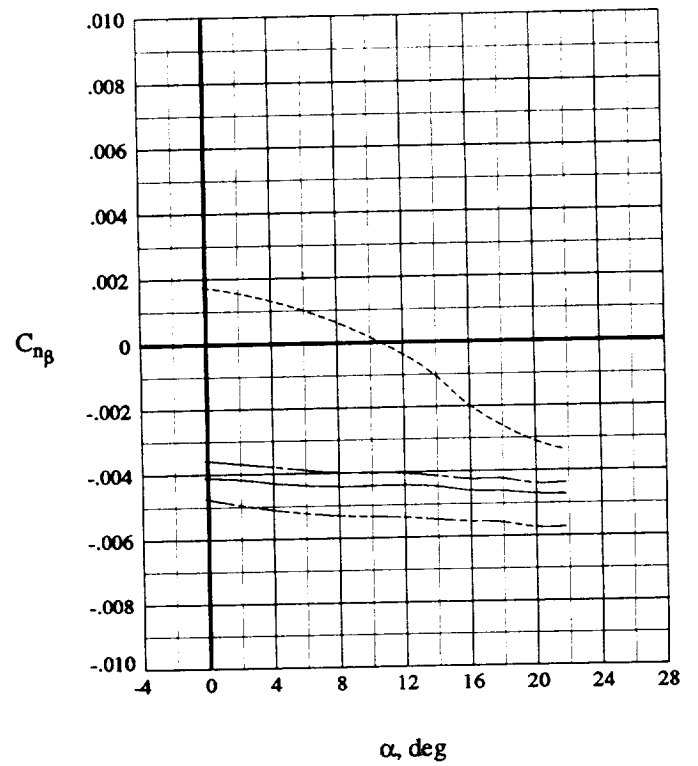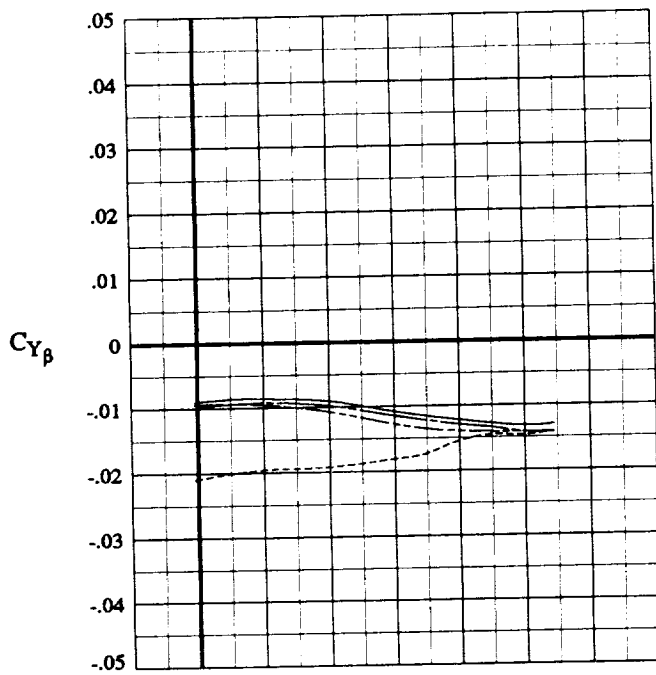
(b) M = 2.30.

Figure 10. Continued.

44

Figure 10. Continued.

(c) M = 2.96.

Configuration

-------	Aft center fin
—·—·—	Wing-tip fins
—··—··—	Nose fin

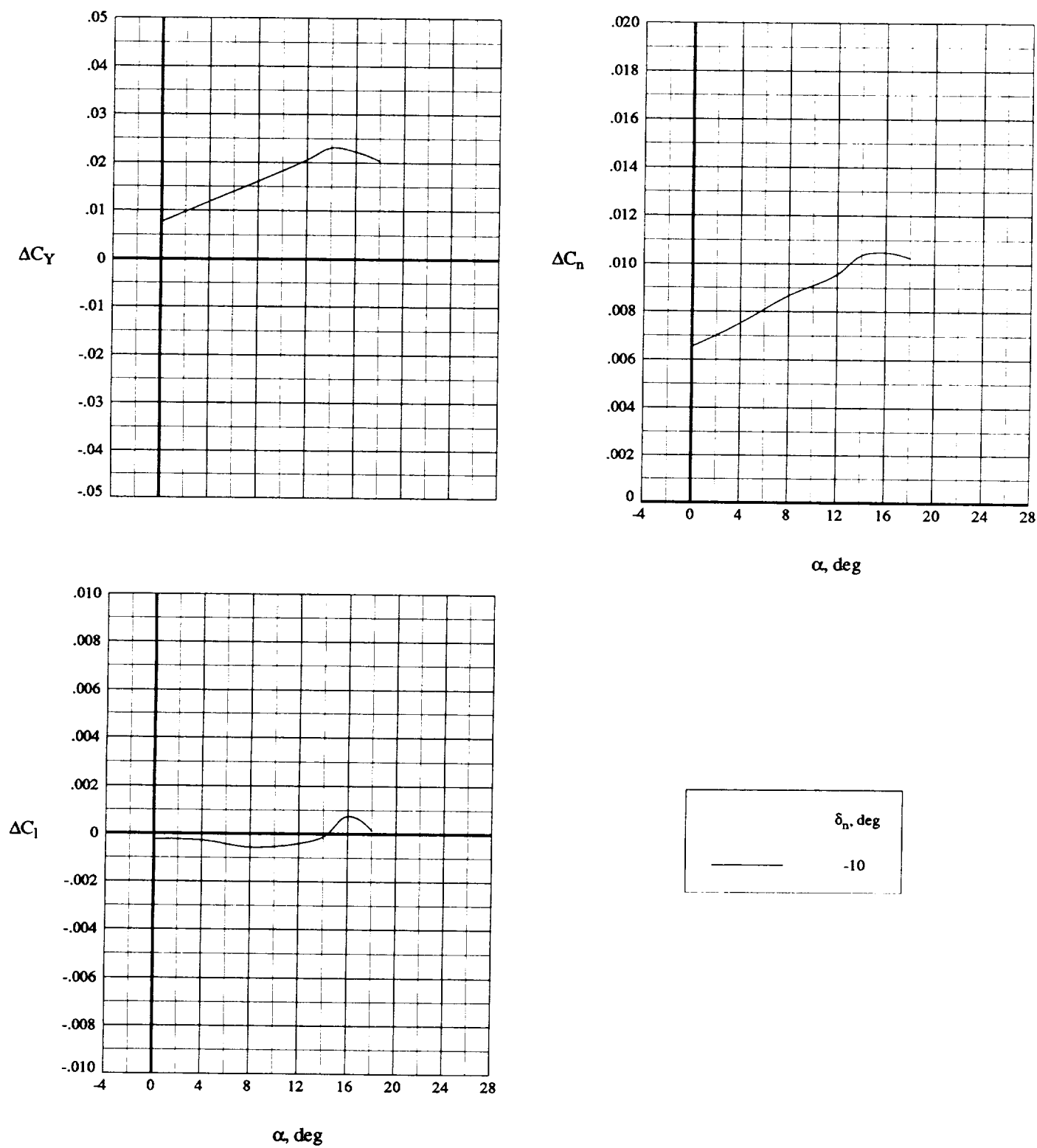(d) M = 3.90.

Figure 10. Continued.

Configuration

|	
———————	Fins off
- - - - - - -	Aft center fin
—— - —— - ——	Wing-tip fins
—— -- —— -- ——	Nose fin
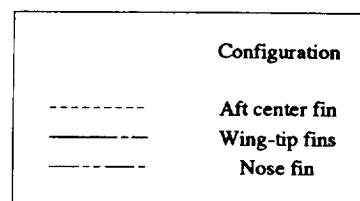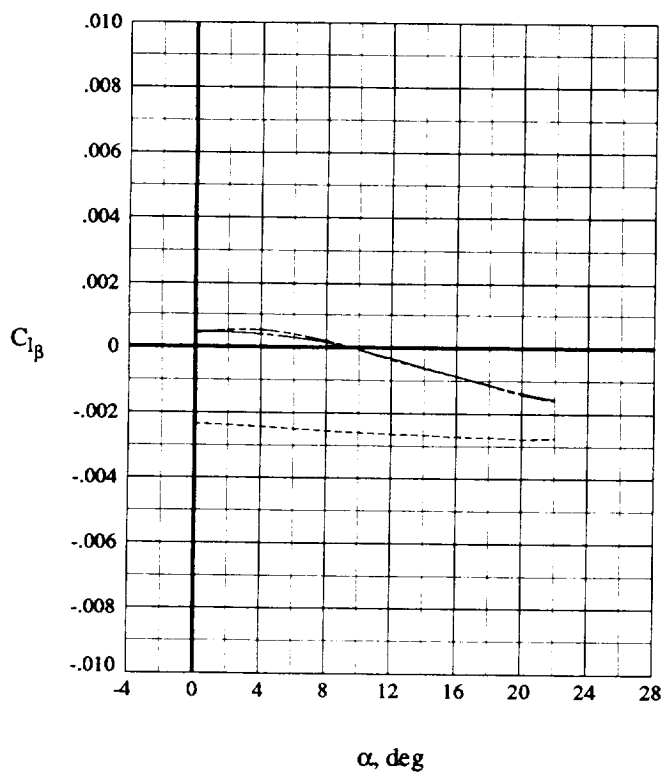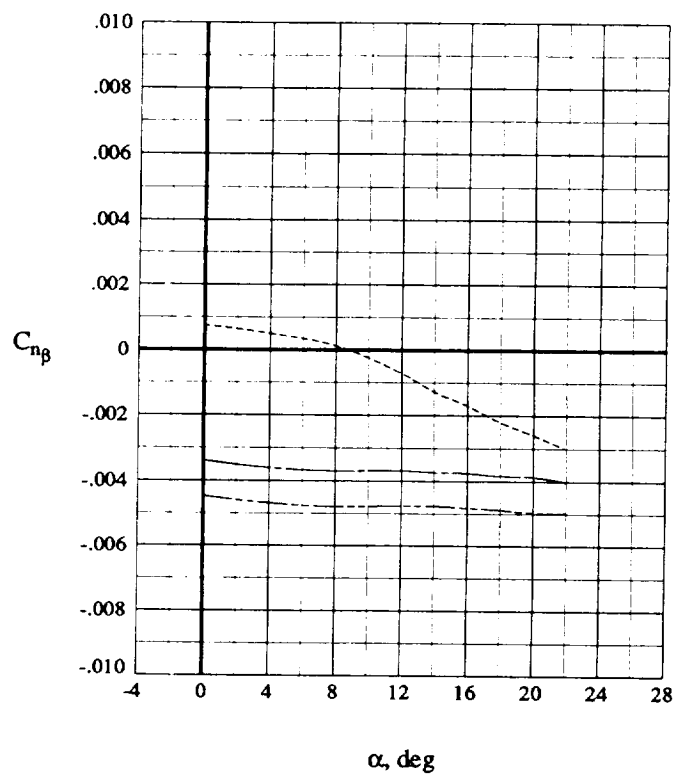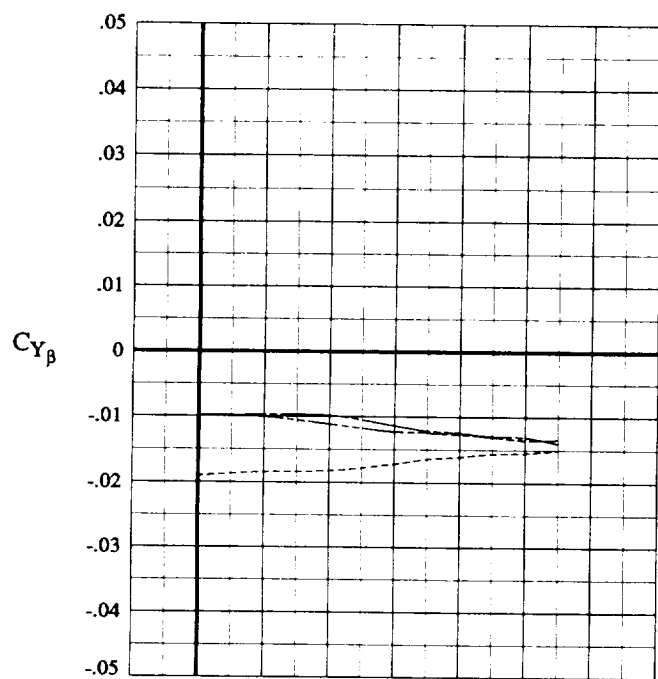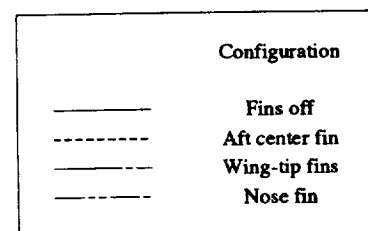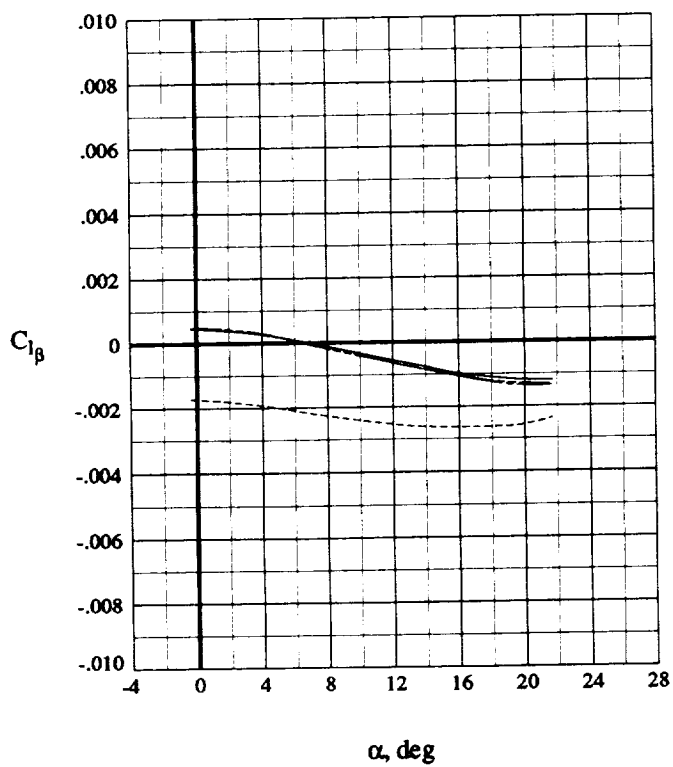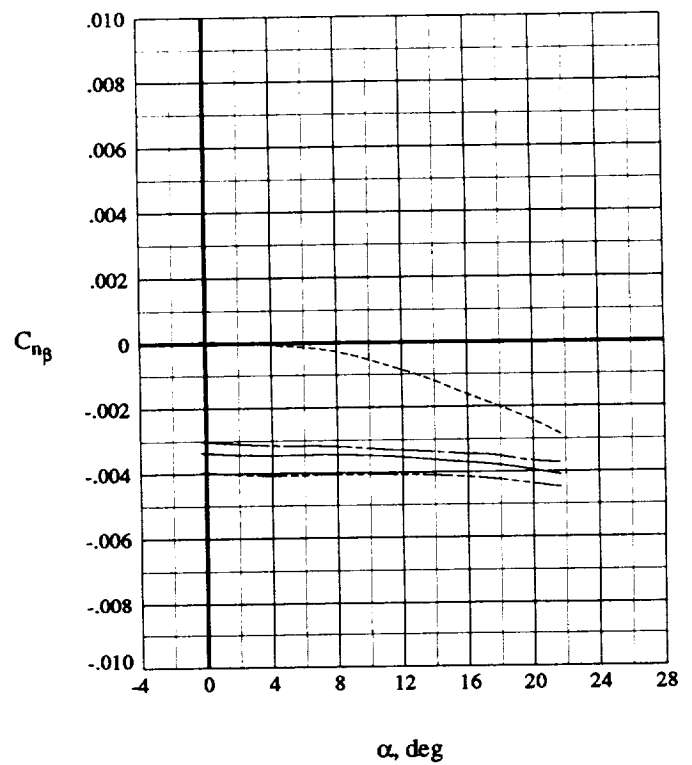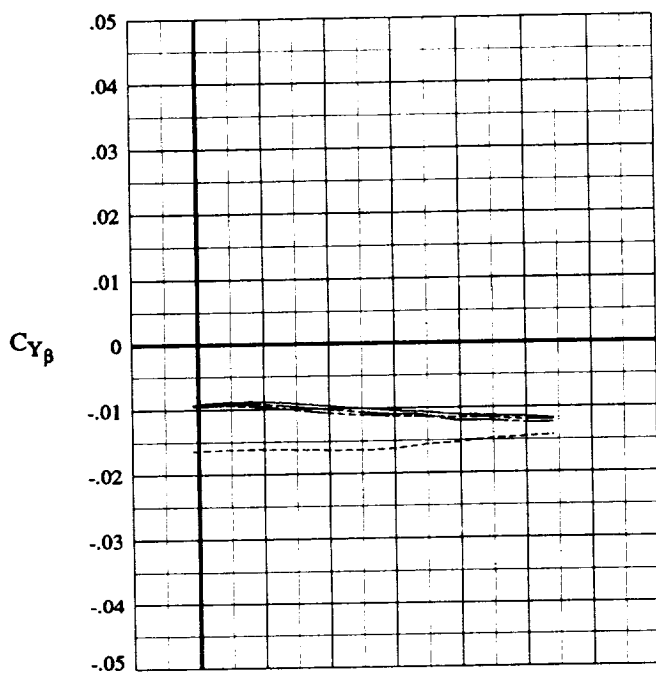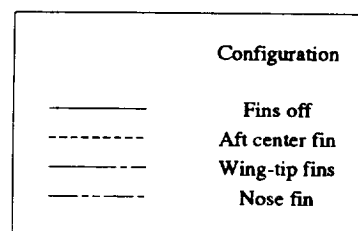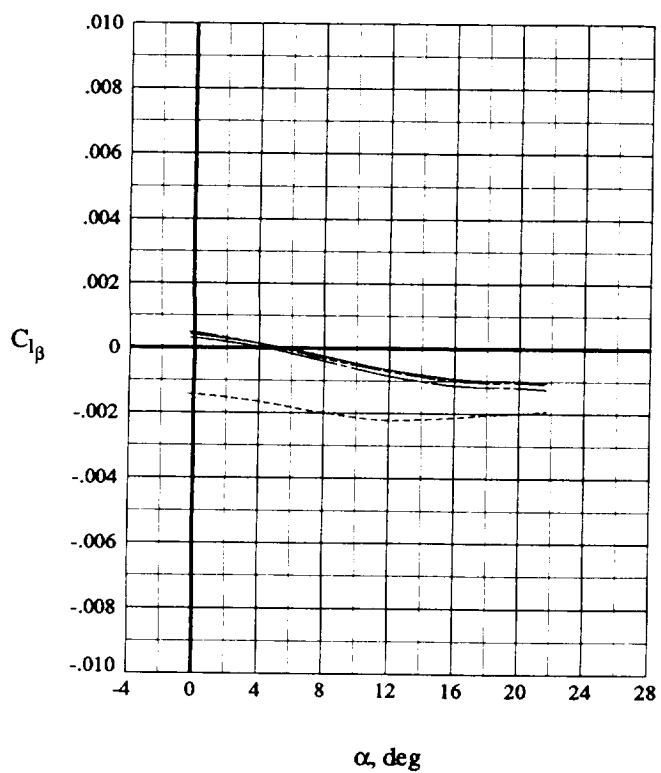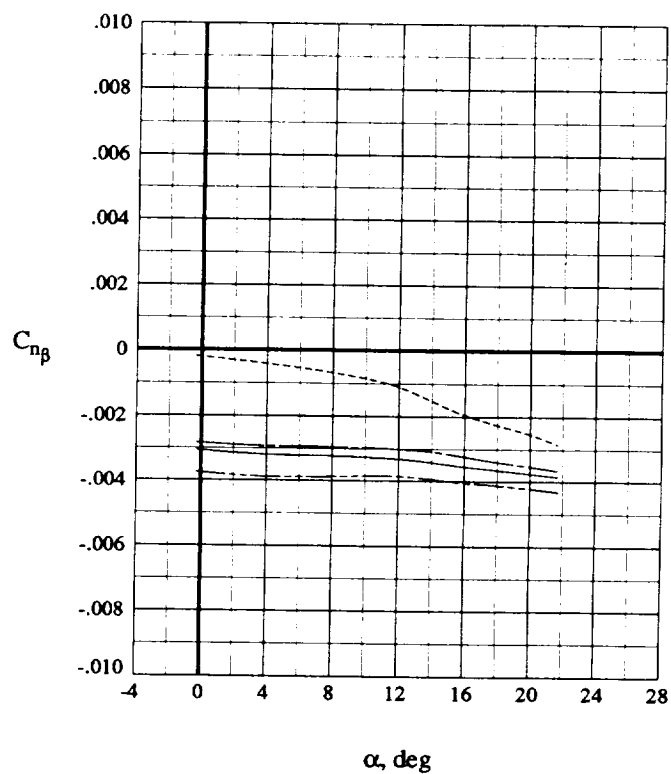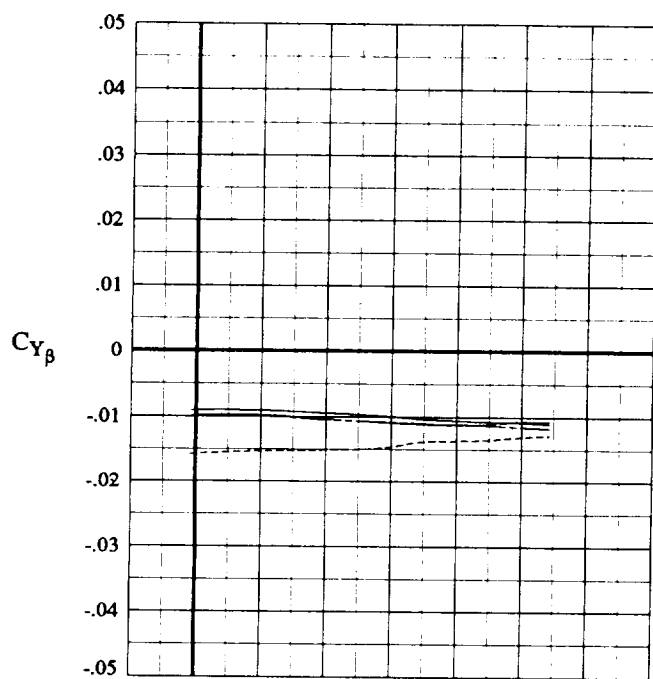
(e) M = 4.60.

Figure 10. Concluded.
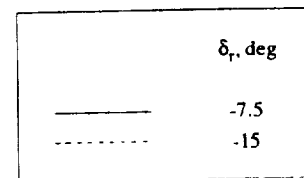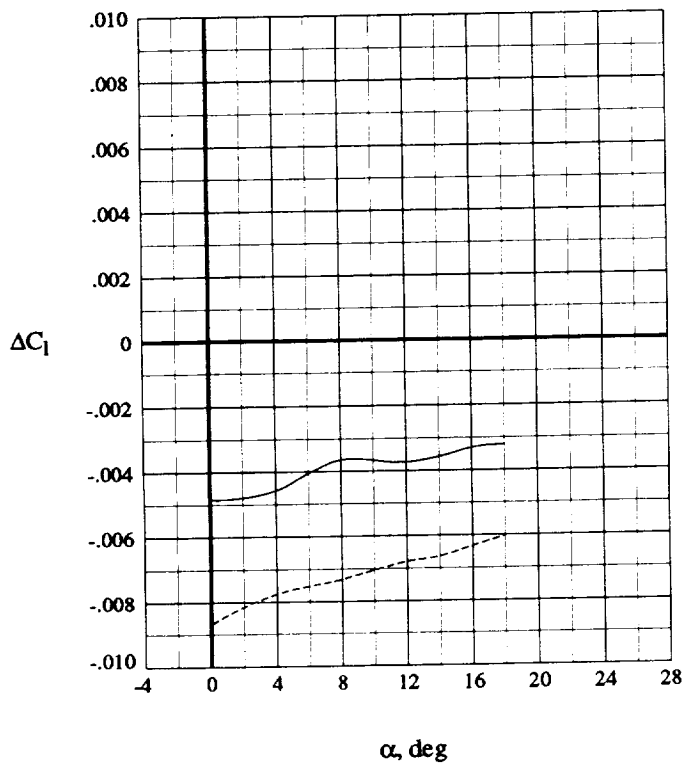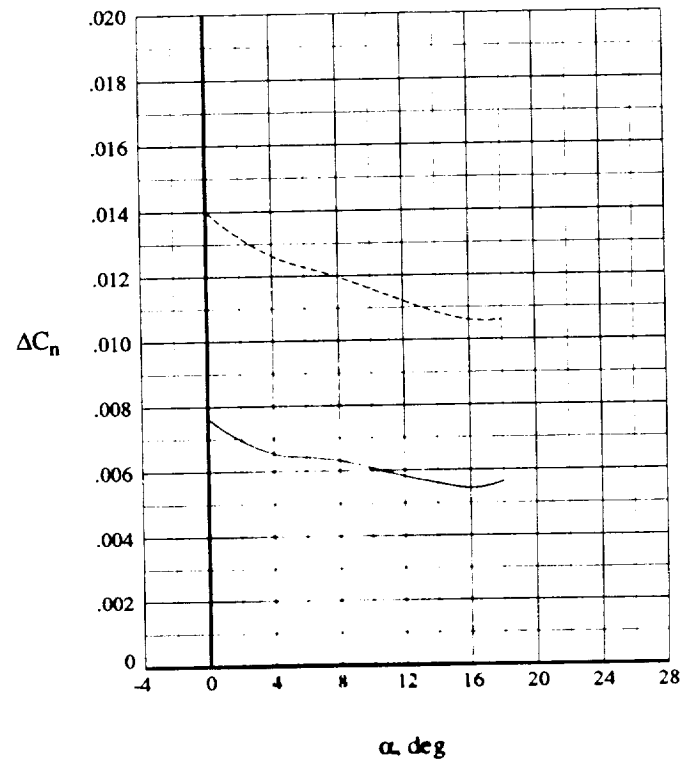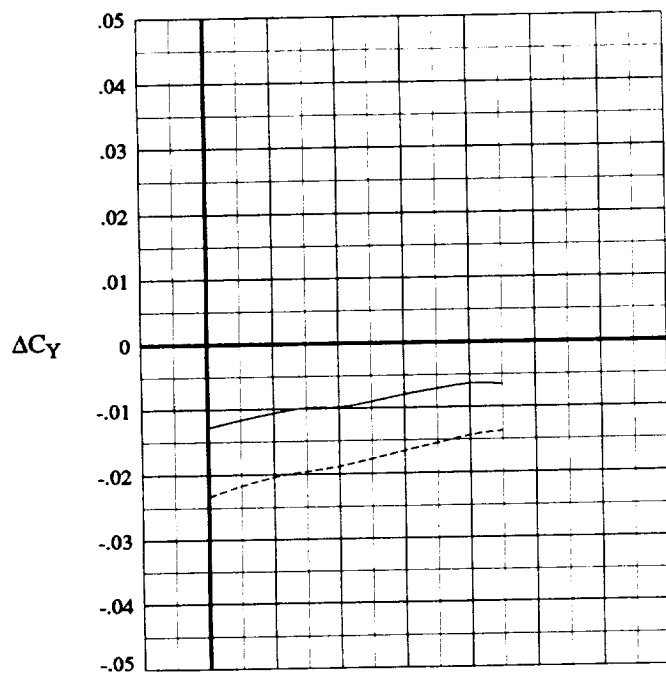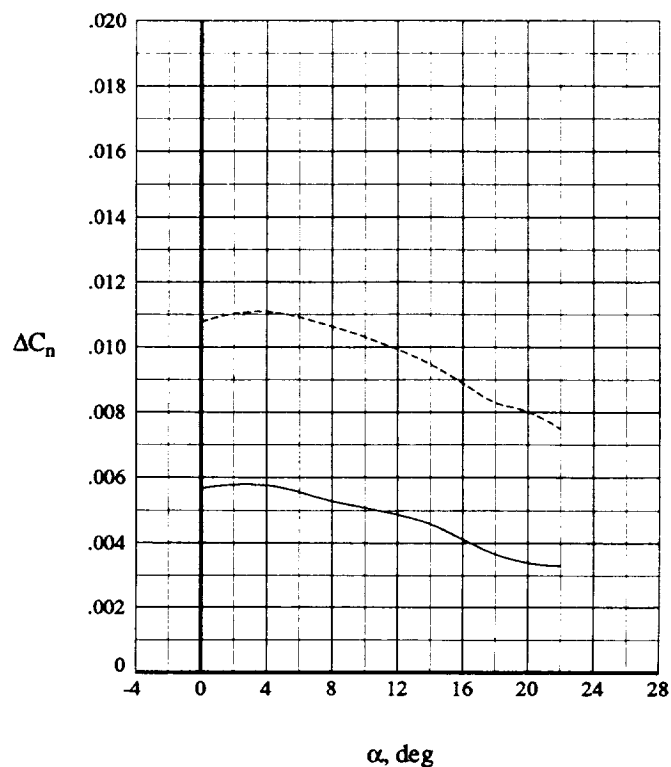
(a) M = 1.60.

Figure 11. Effect of rudder deflection as directional control for circular body model with aft center fin.
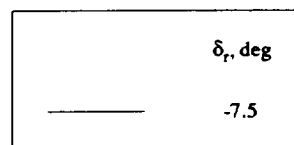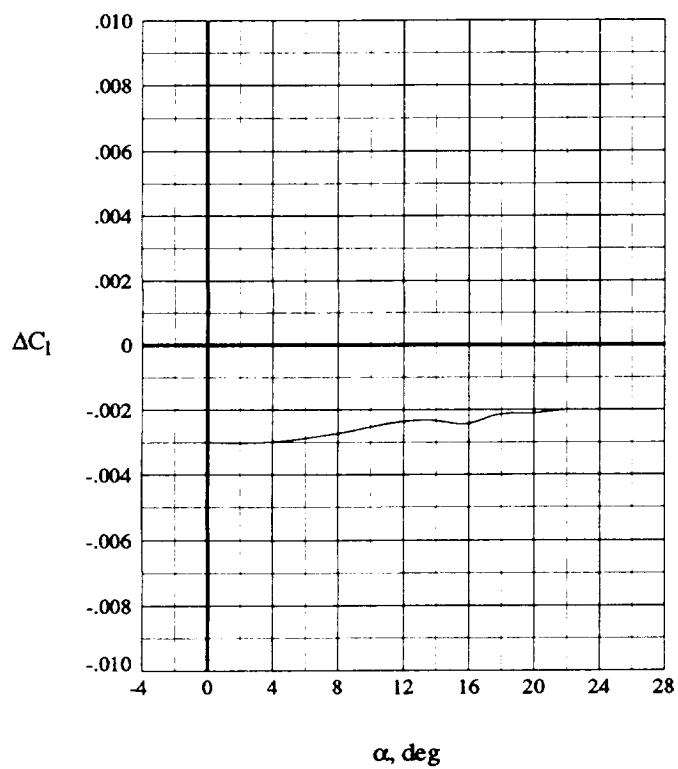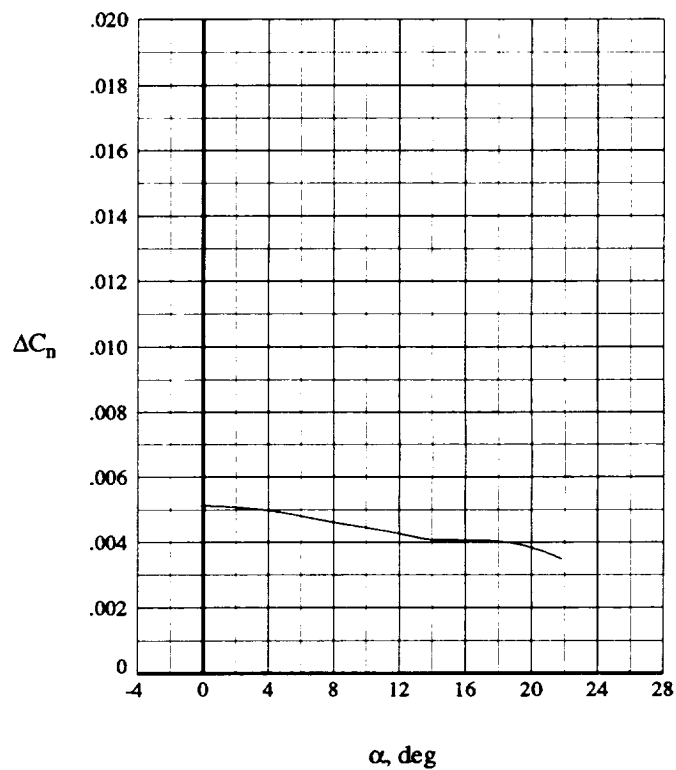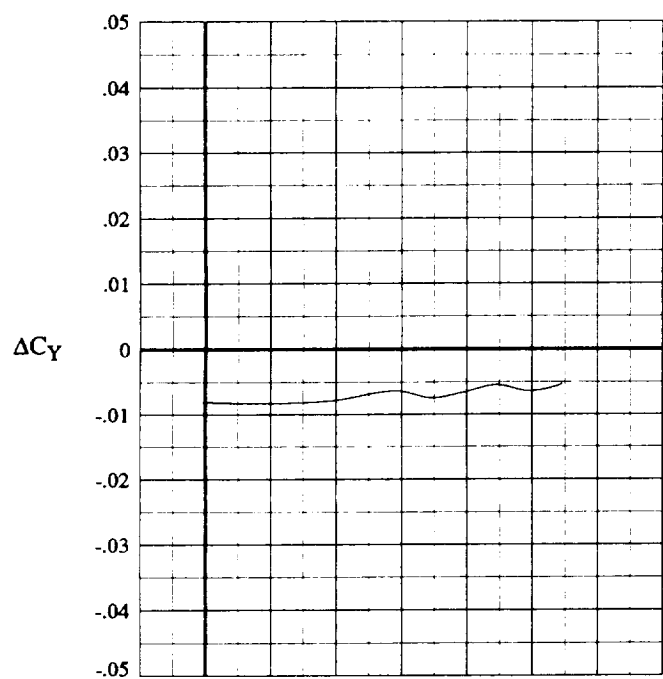
(b) M = 2.30.

Figure 11. Continued.

(c) M = 2.96.

Figure 11. Continued.

ΔC_Y

ΔC_n

α, deg

ΔC_l

α, deg

	δ_r, deg
———	-7.5
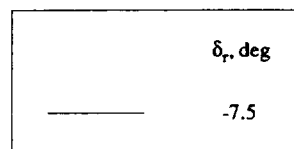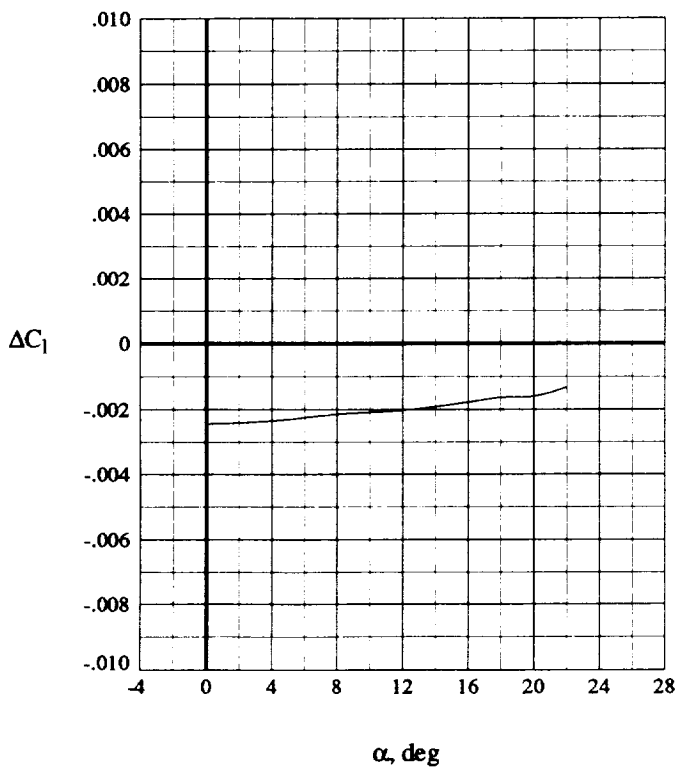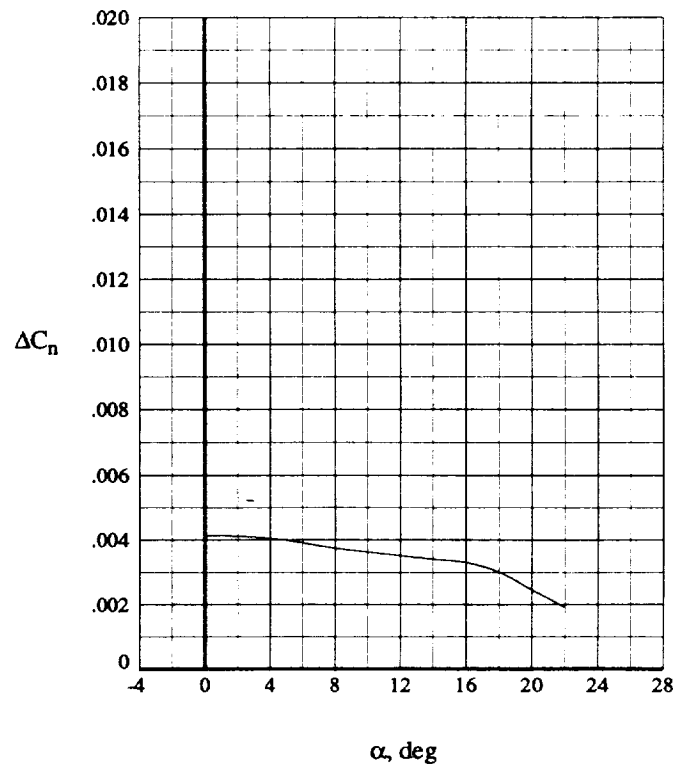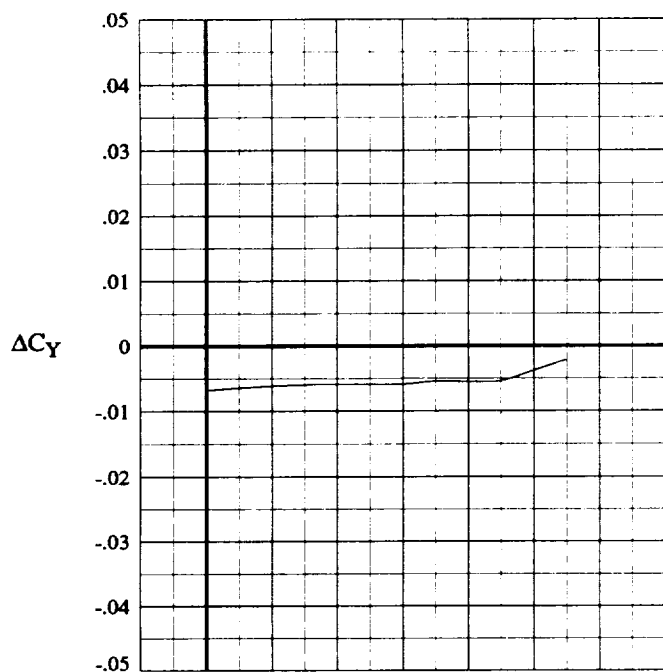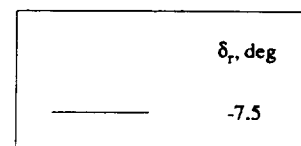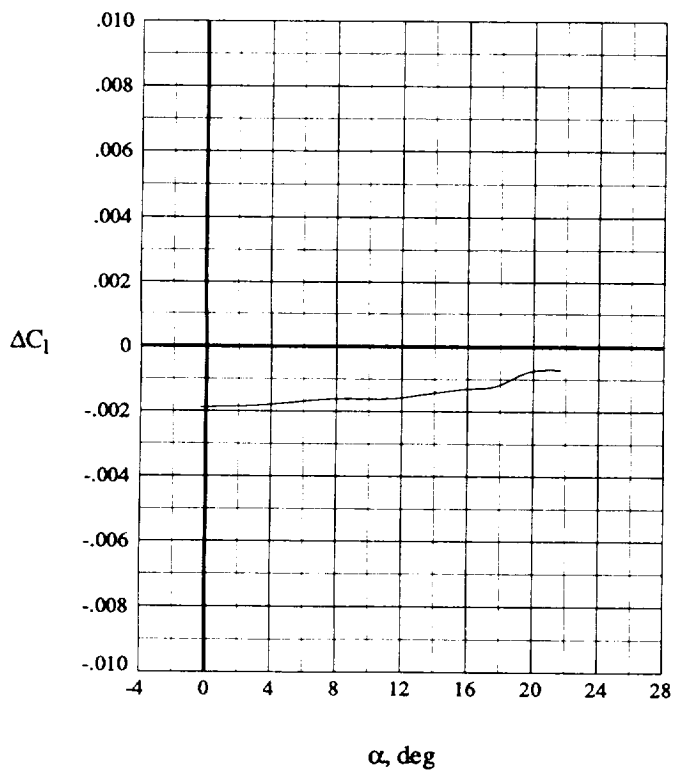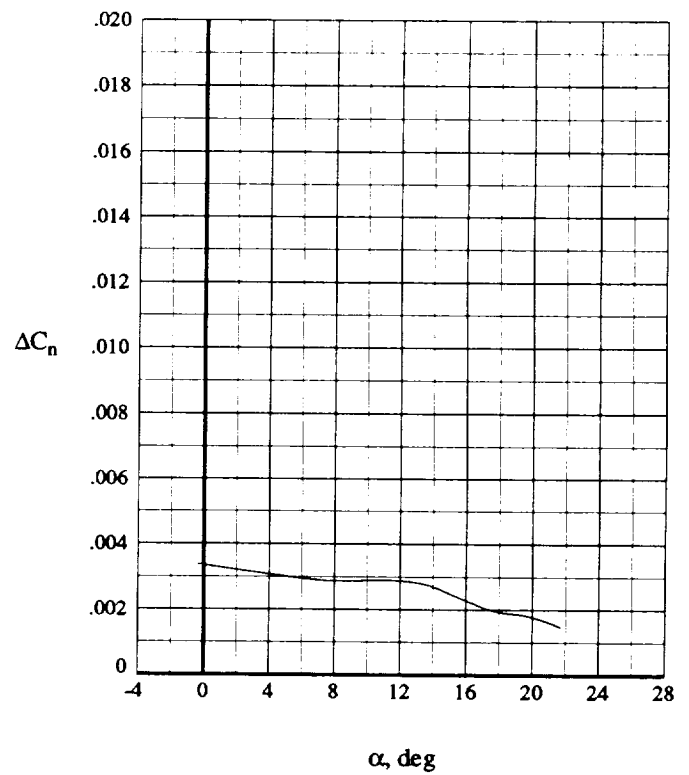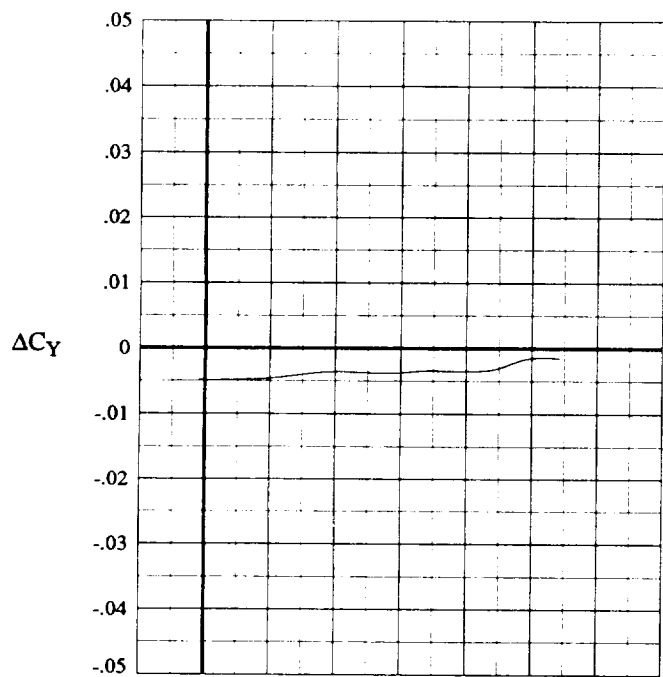
(d) M = 3.90.

Figure 11. Continued.
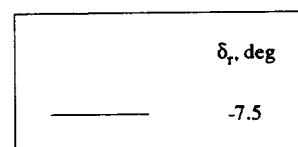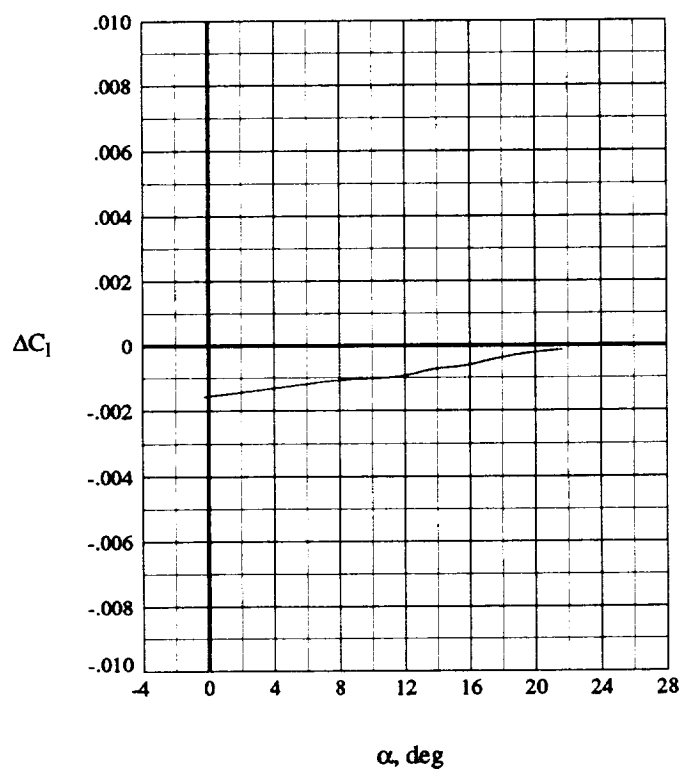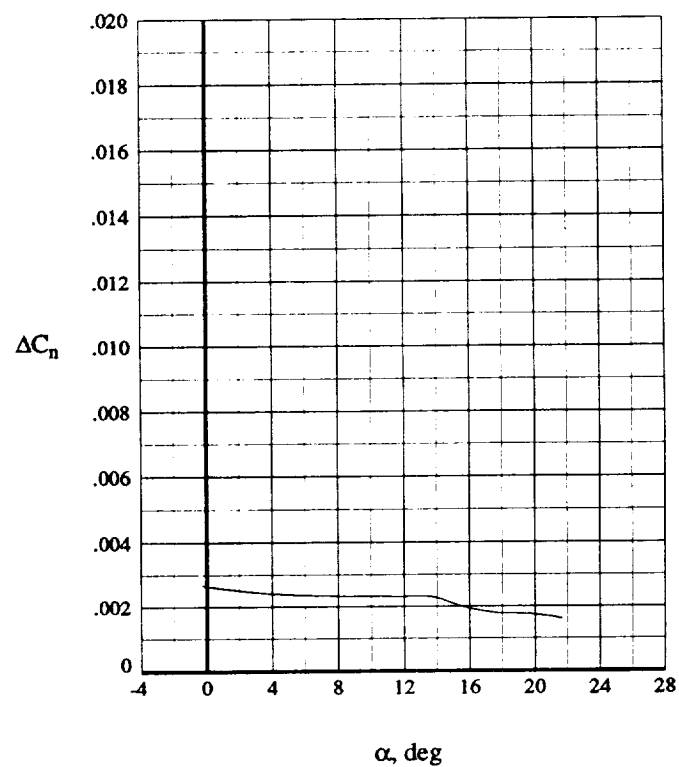
(e) M = 4.60.

Figure 11. Concluded.

(a) M = 1.60.

Figure 12. Effect of rudder deflection as directional control for circular body model with wingtip fins.

(b) M = 2.30.

Figure 12. Continued.
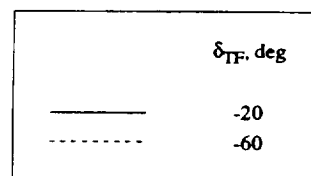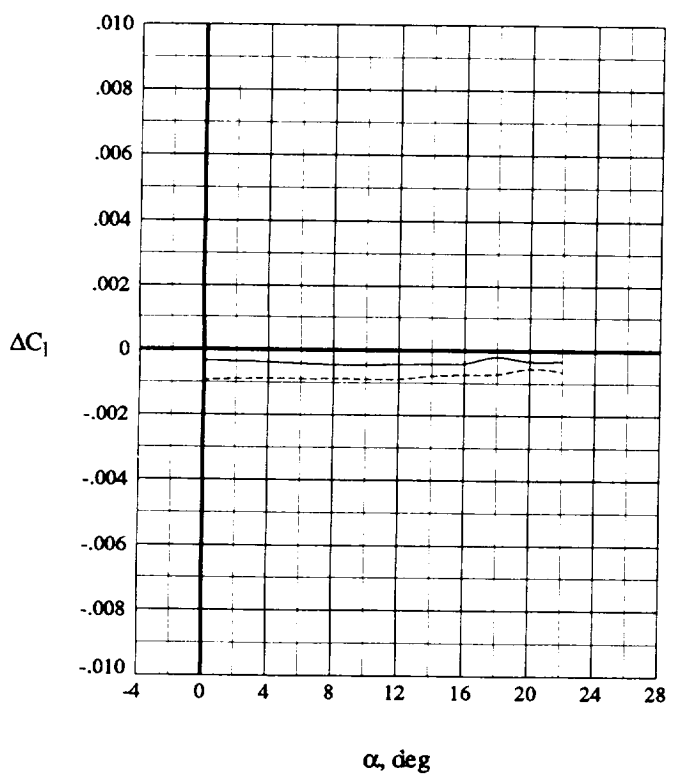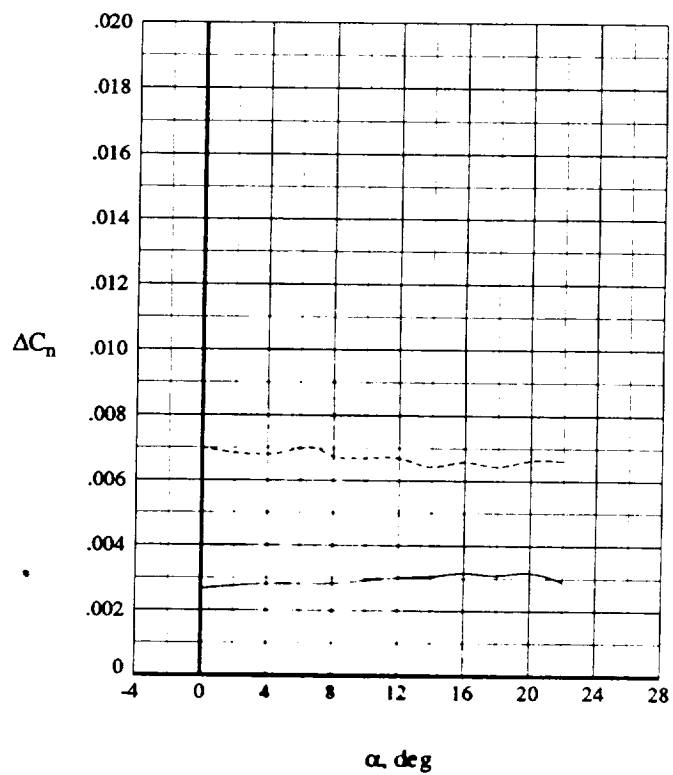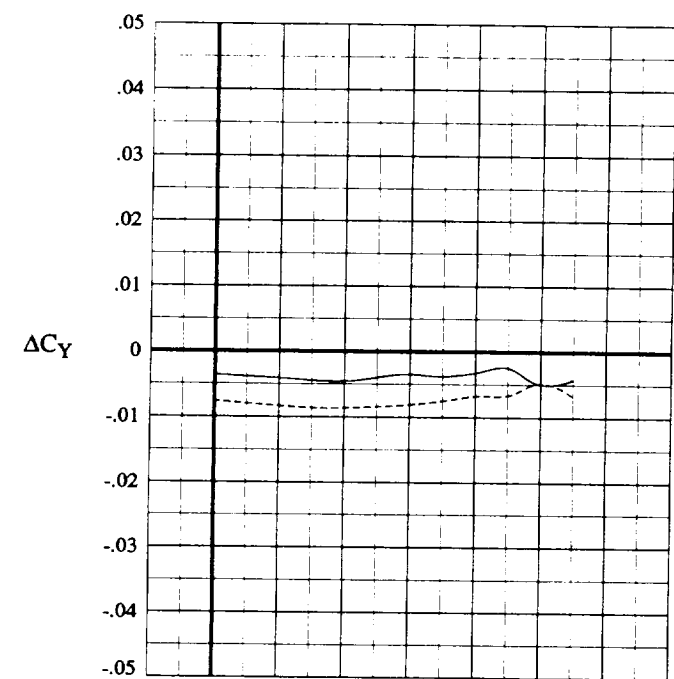
(c) M = 2.96.

Figure 12. Continued.
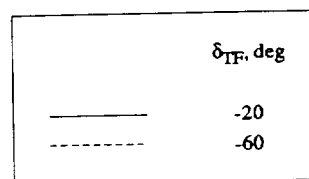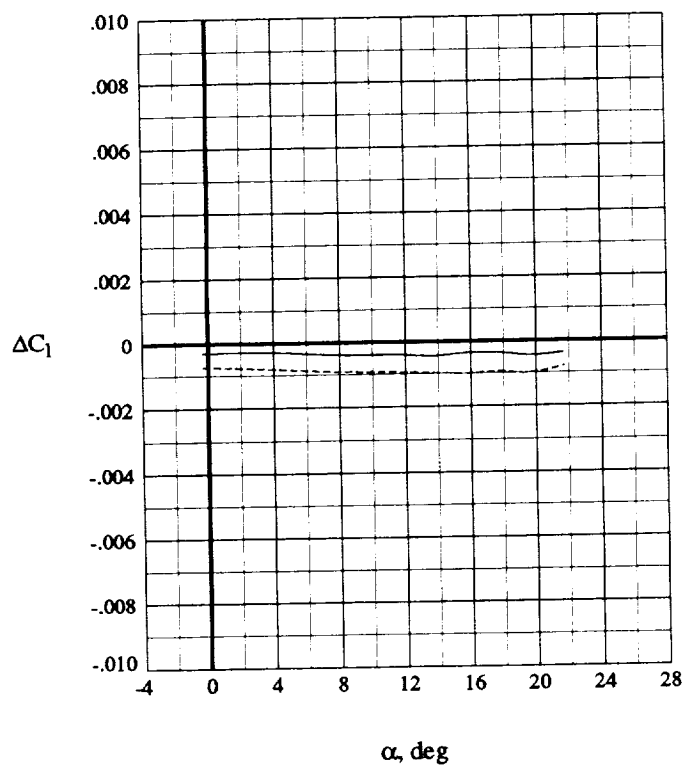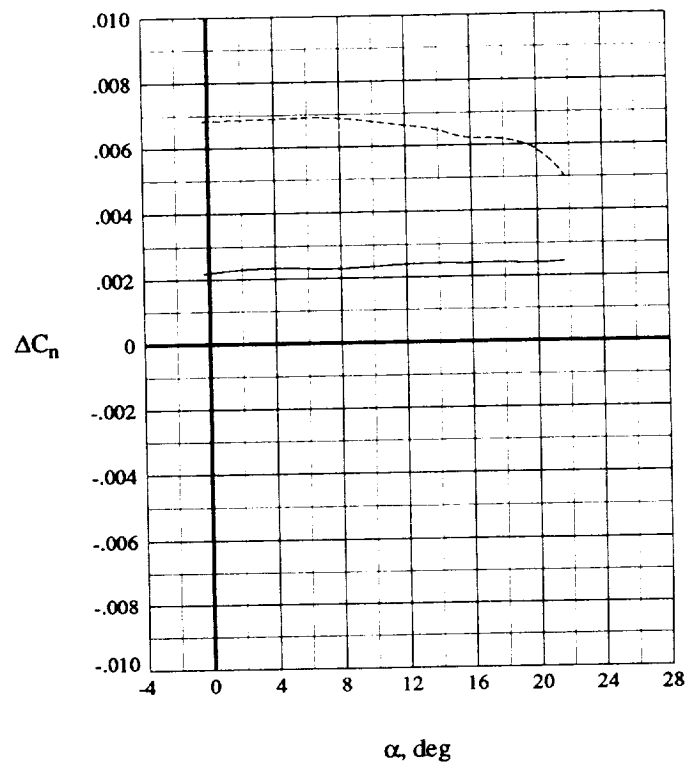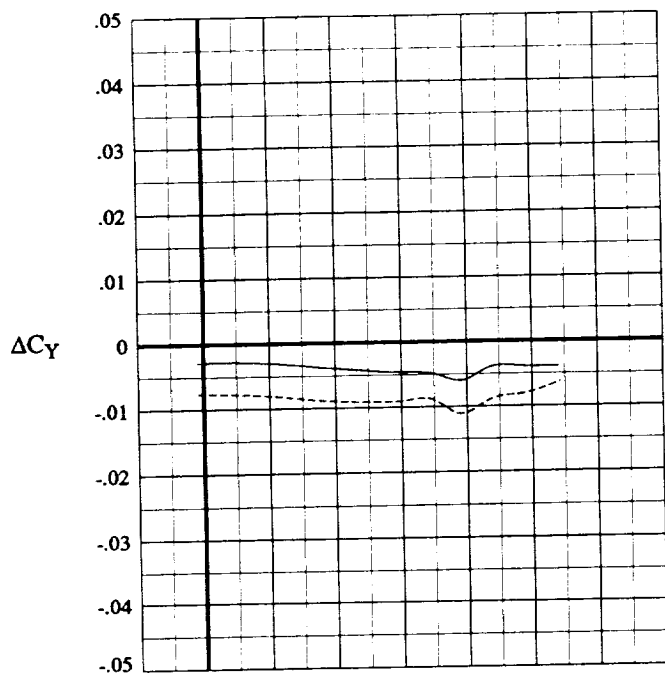
(d) M = 3.90.

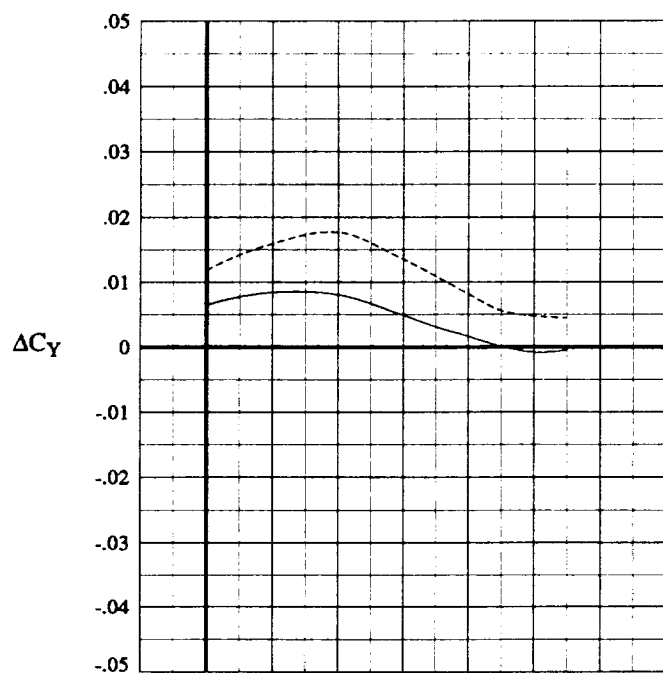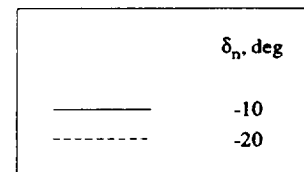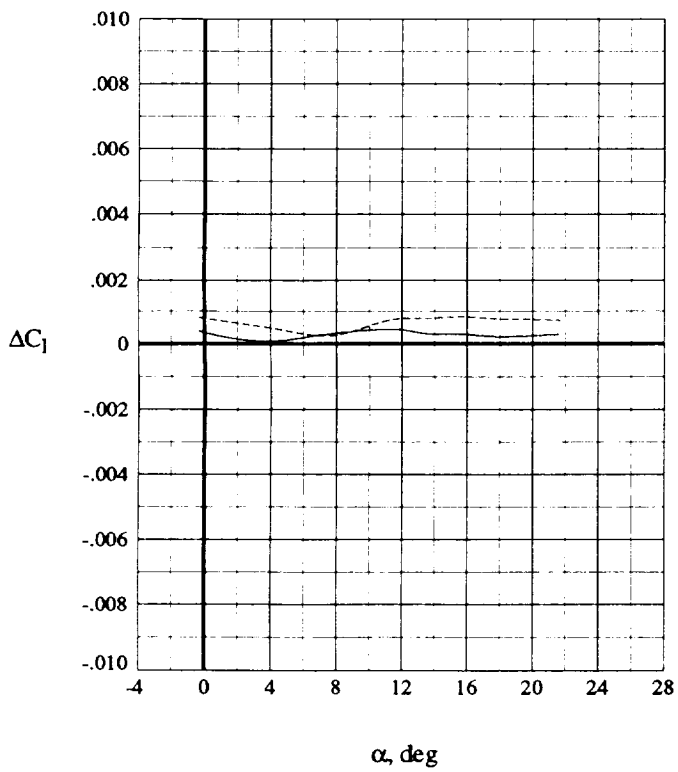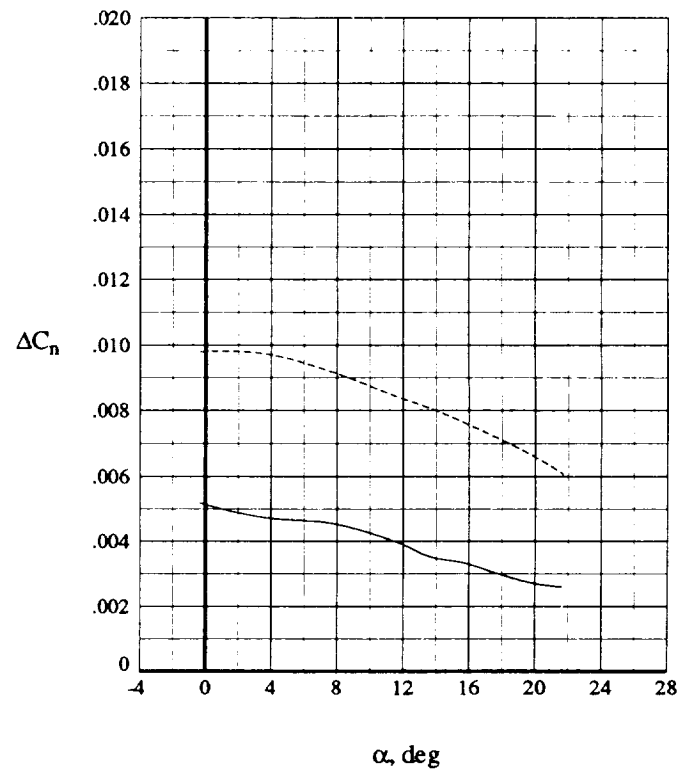Figure 12. Continued.
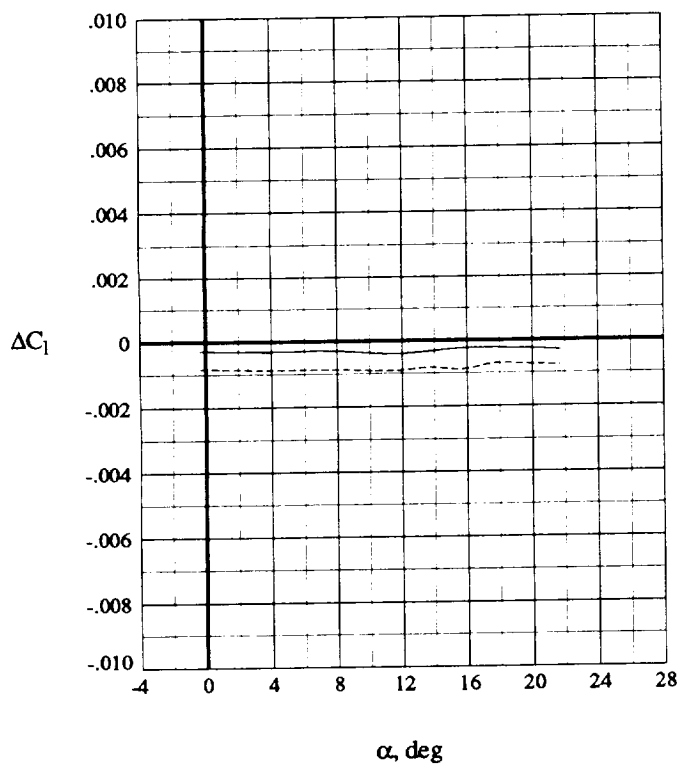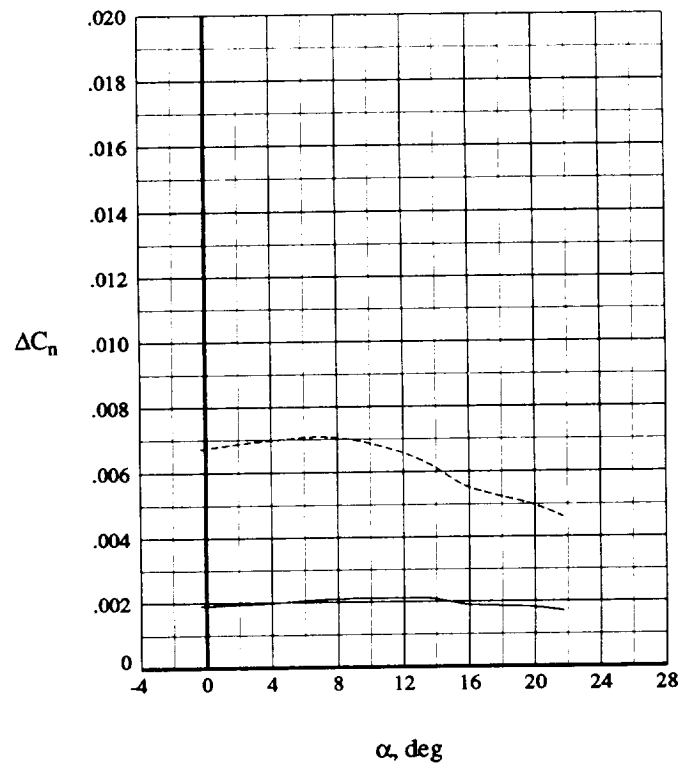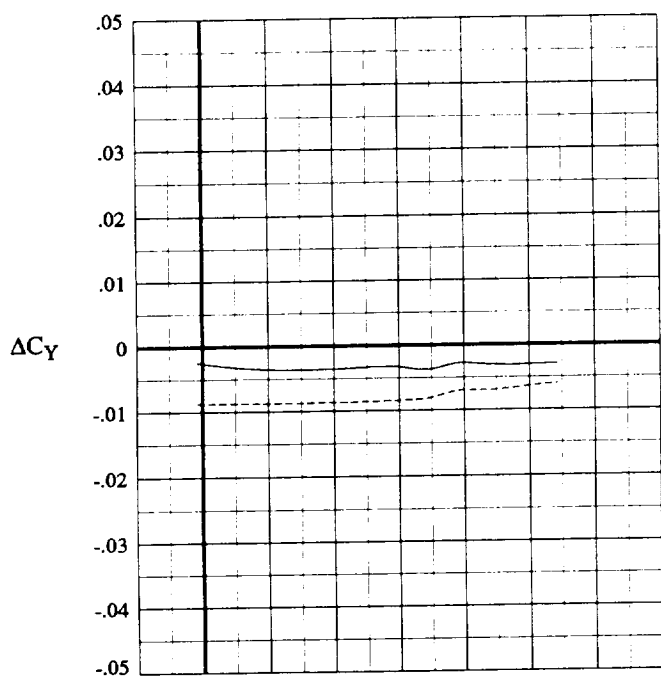
(e) M = 4.60.

Figure 12. Concluded.

(a) M = 1.60.

Figure 13. Effect of rudder deflection as directional control for circular body model with nose fin.
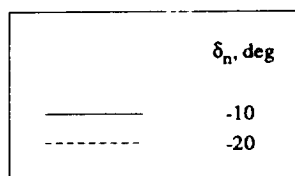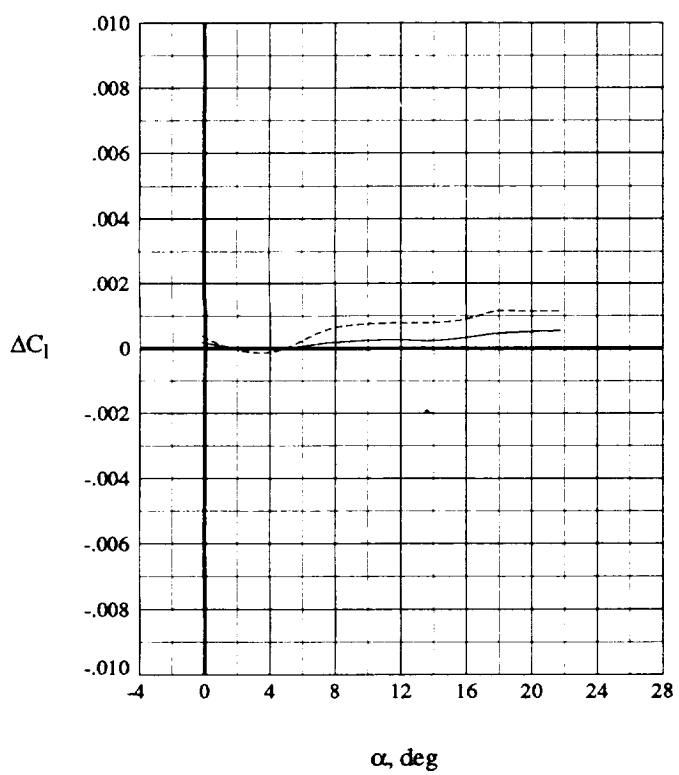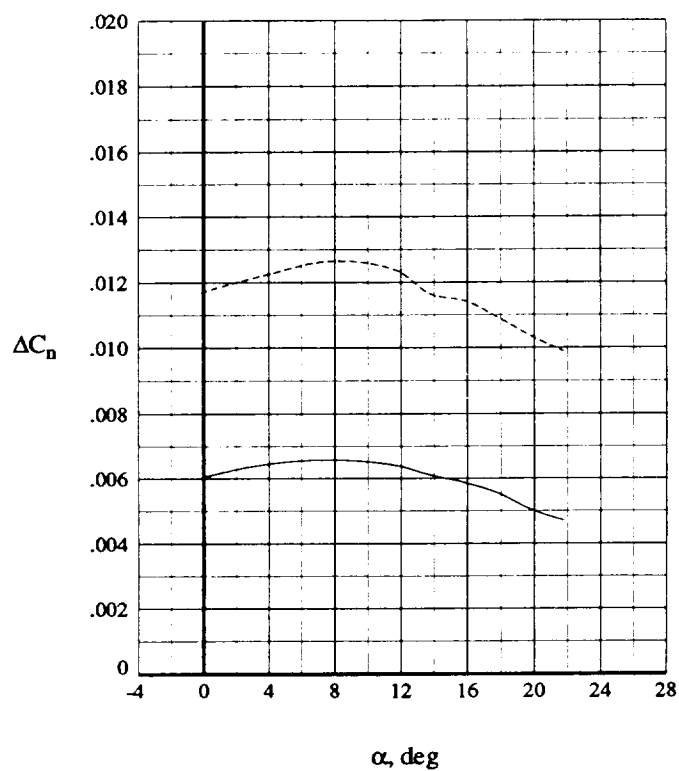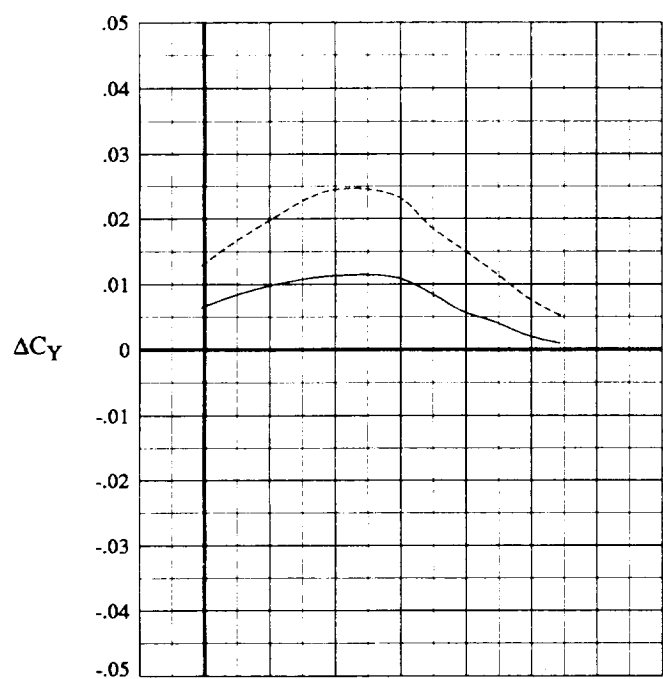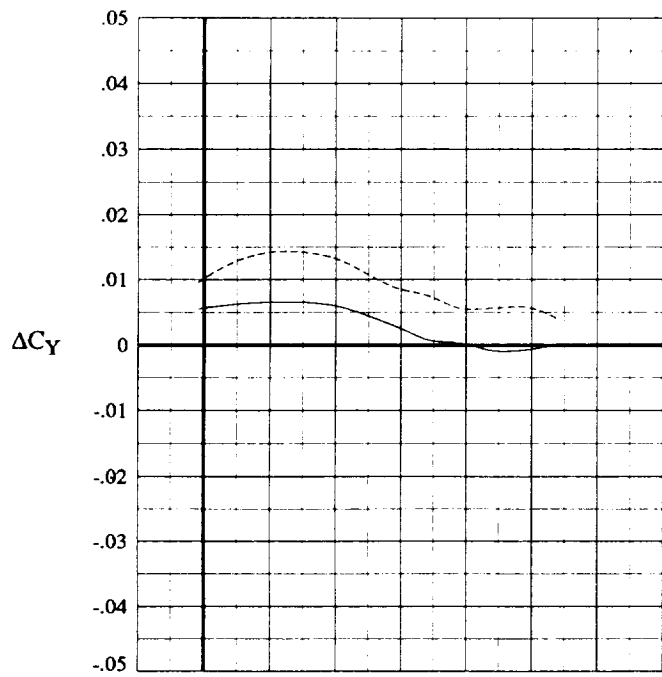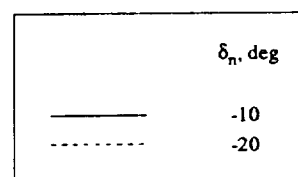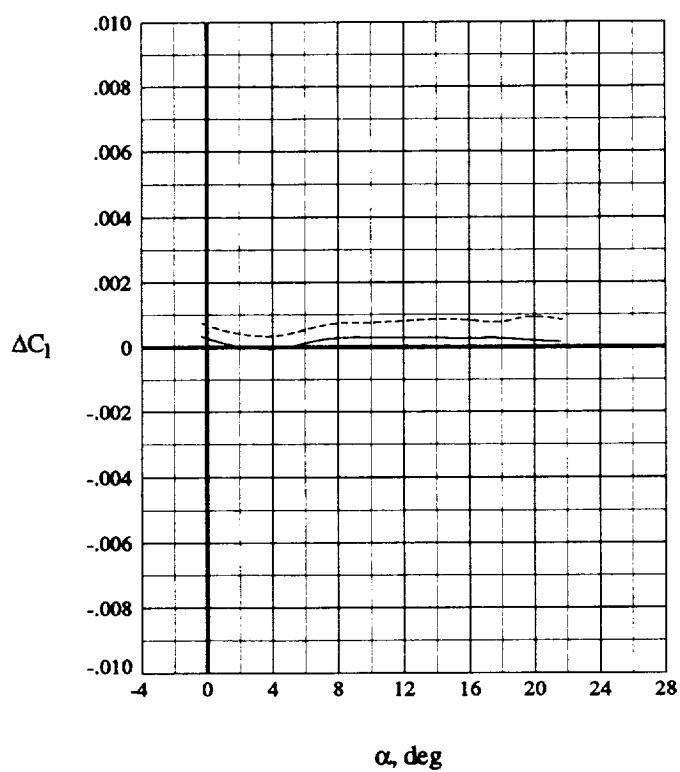
(b) M = 2.30.

Figure 13. Continued.

59
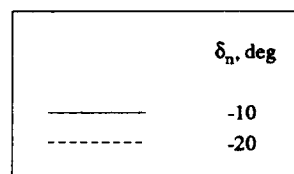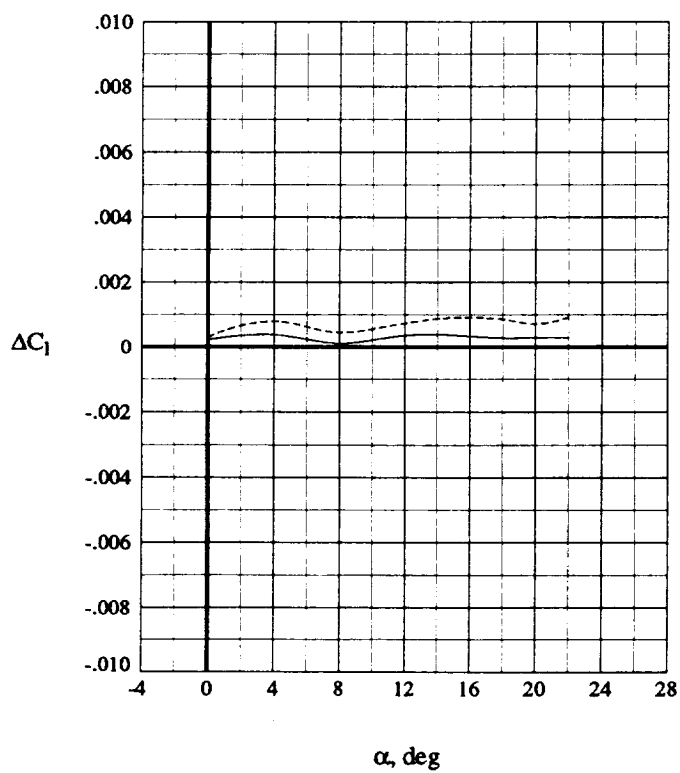
(c) M = 2.96.

Figure 13. Continued.

(d) M = 3.90.

Figure 13. Continued.

61

(e) M = 4.60.

Figure 13. Concluded.

(a) M = 1.60.

Figure 14. Effect of aileron deflection as roll control for circular body model with nose fin; nose-fin deflection angle is 10 degrees.
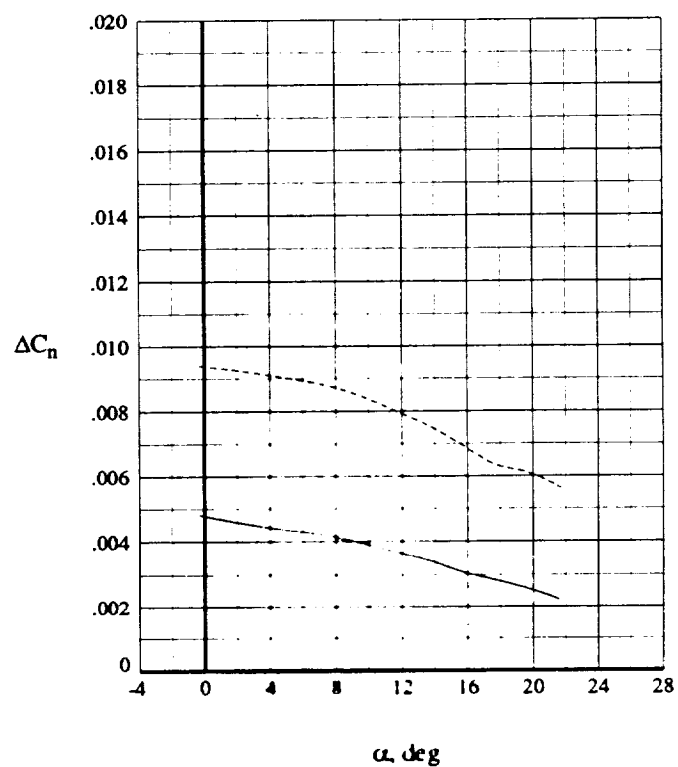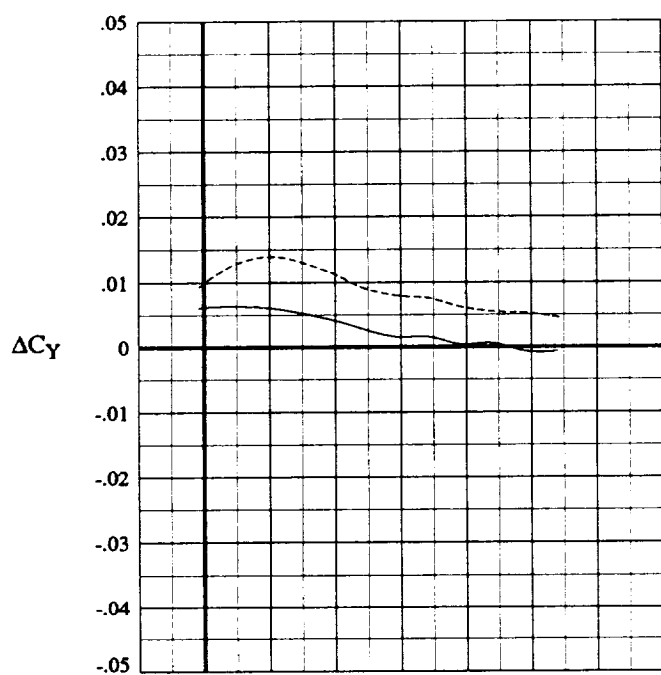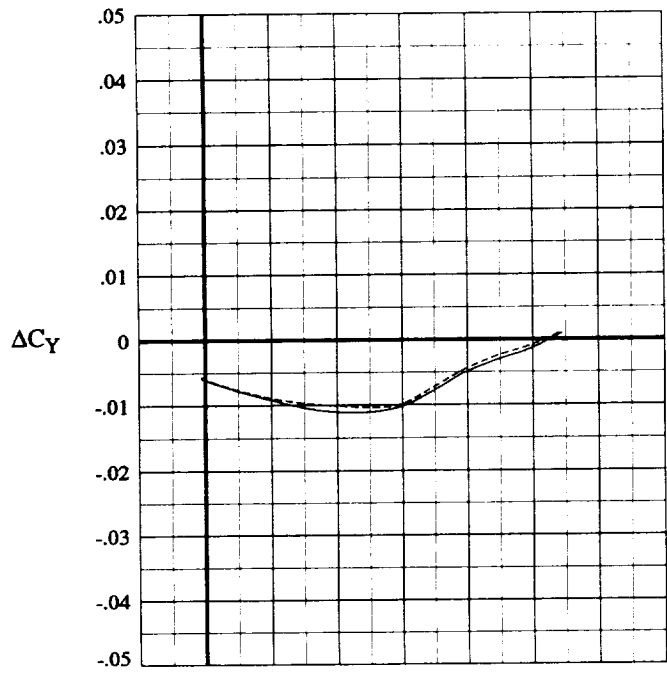
(b) M = 2.30.

Figure 14. Continued.

(c) M = 2.96.

Figure 14. Continued.

(d) M = 3.90.
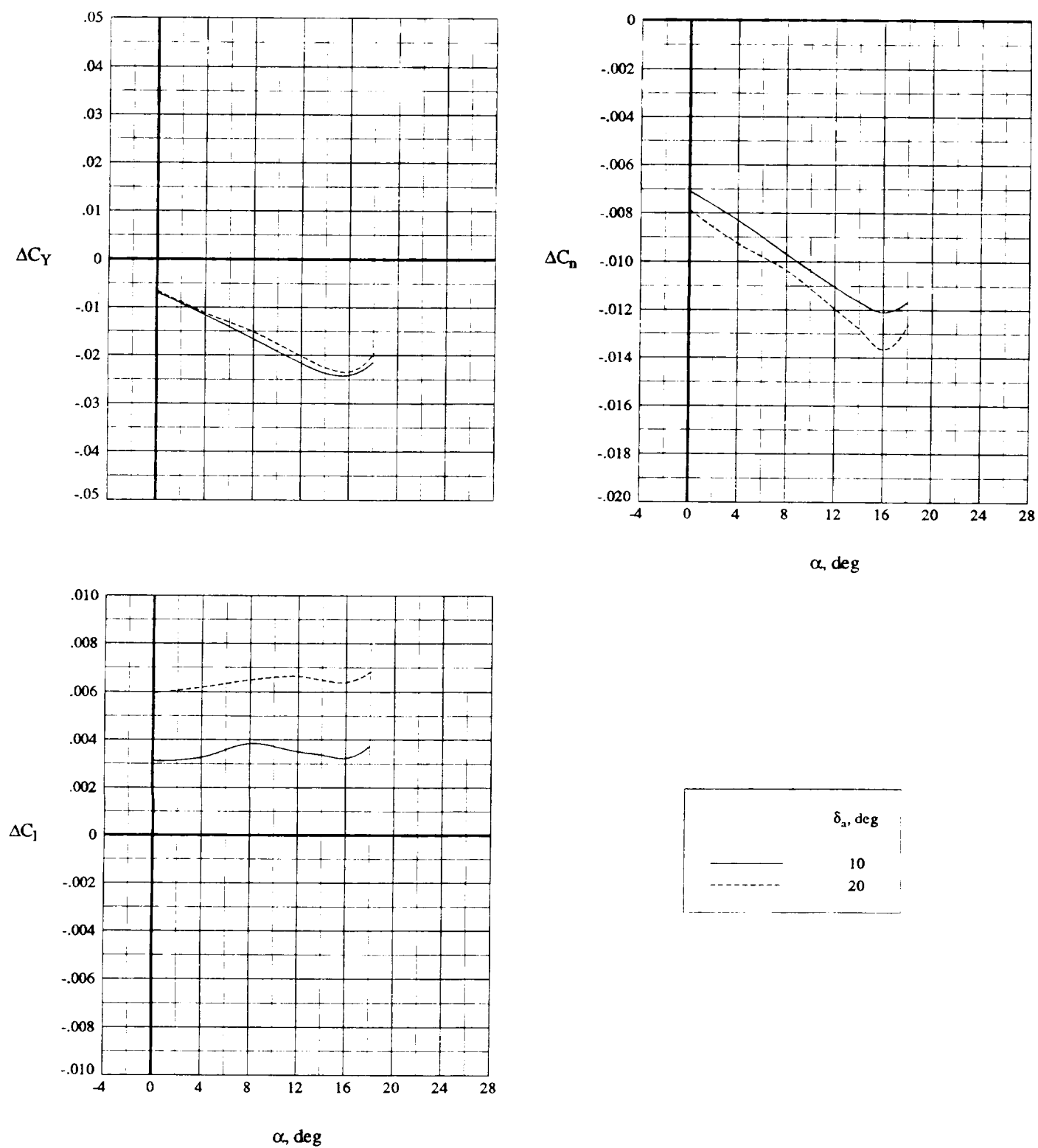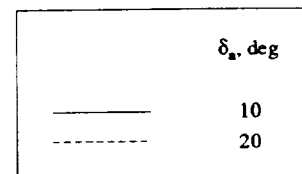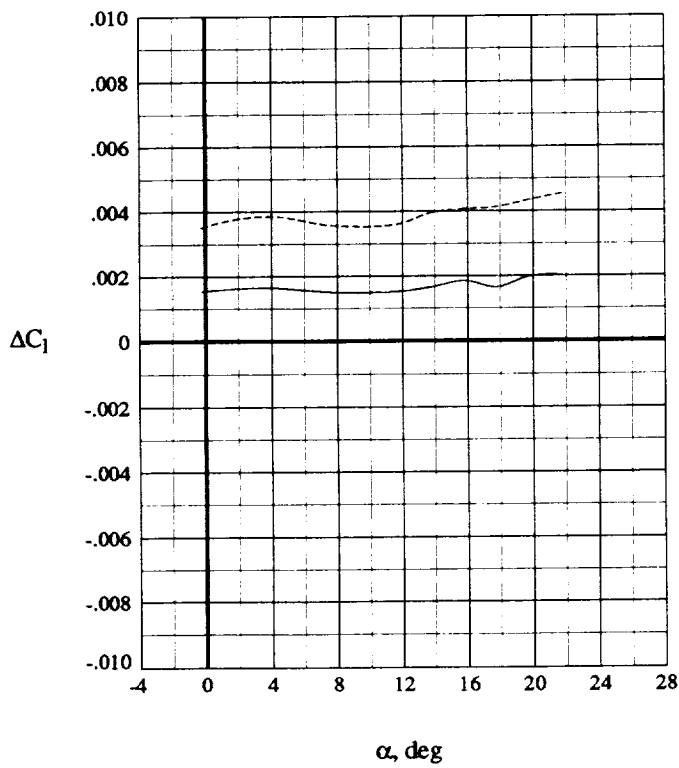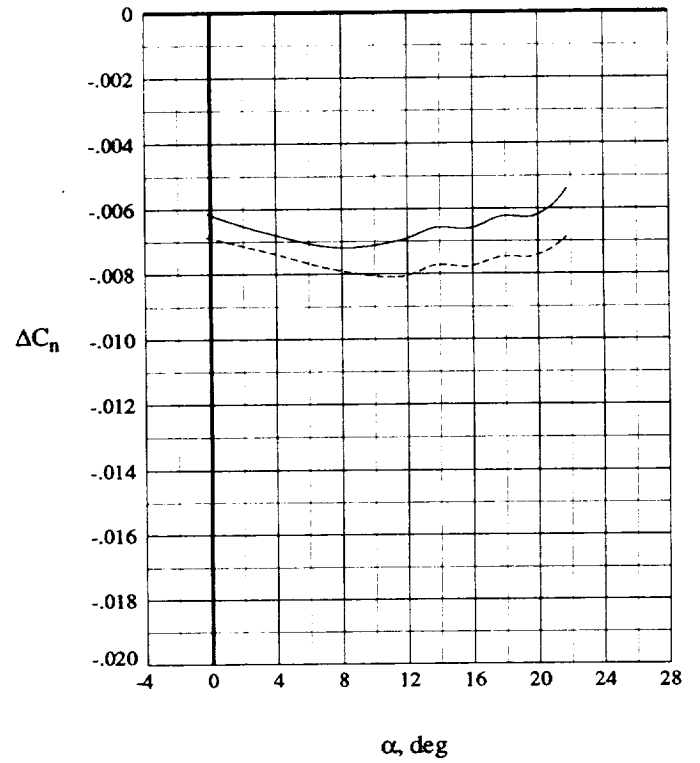
Figure 14. Continued.

(e) M = 4.60.

Figure 14. Concluded.

REPORT DOCUMENTATION PAGE

Public reporting burden for this collection of information is estimated to average 1 hour per response, including the time for reviewing instructions, searching existing data sources, gathering and maintaining the data needed, and completing and re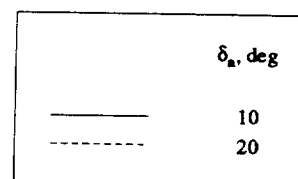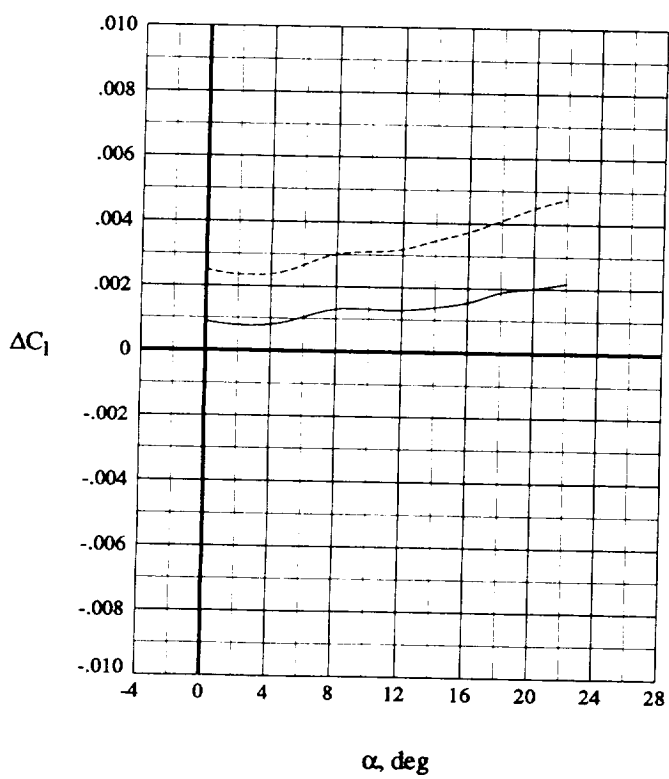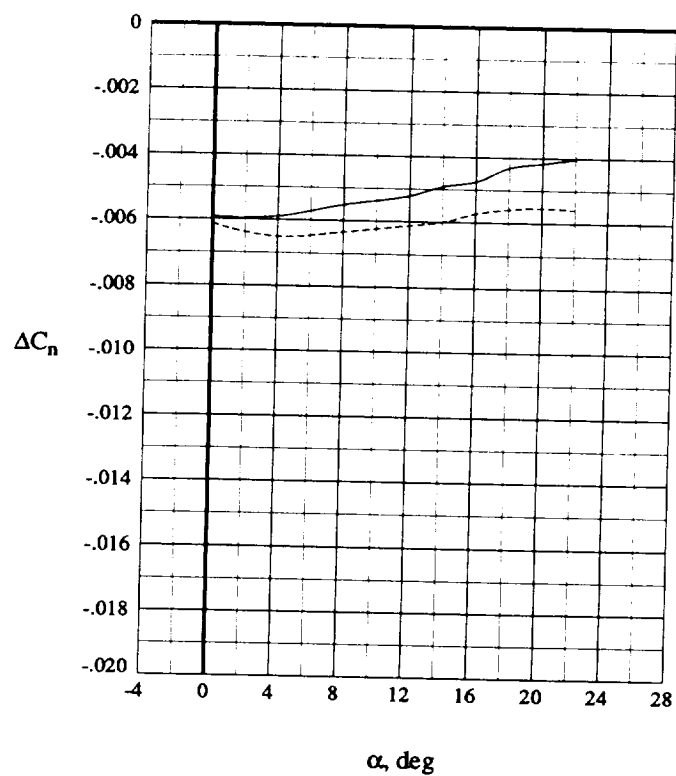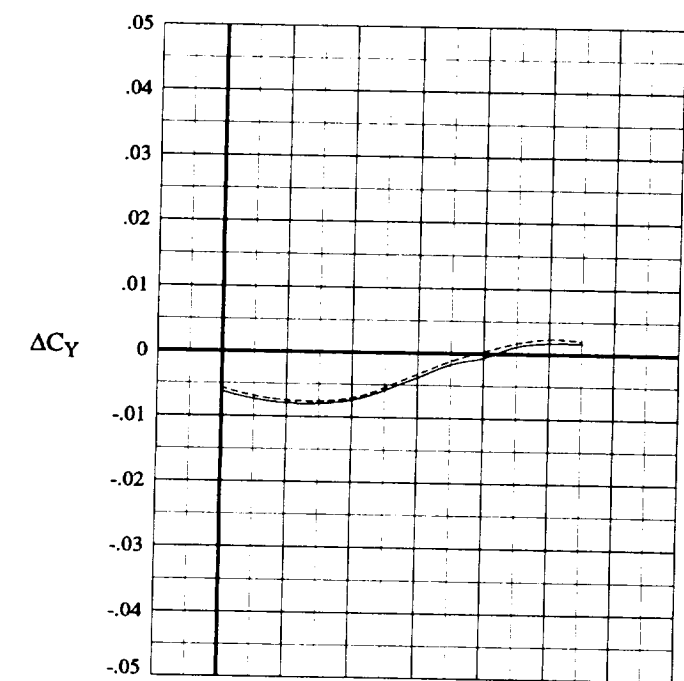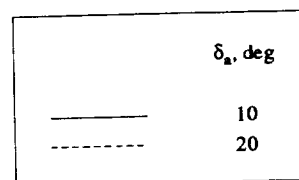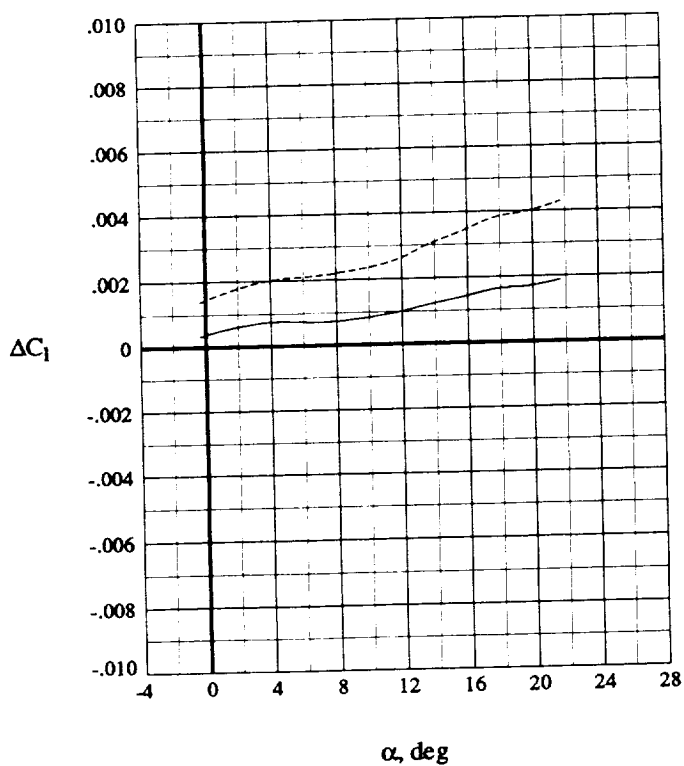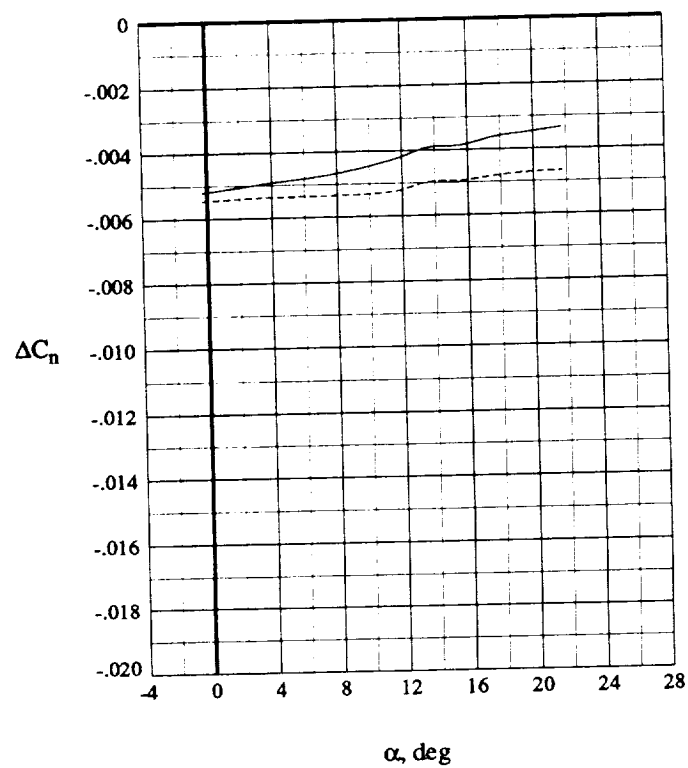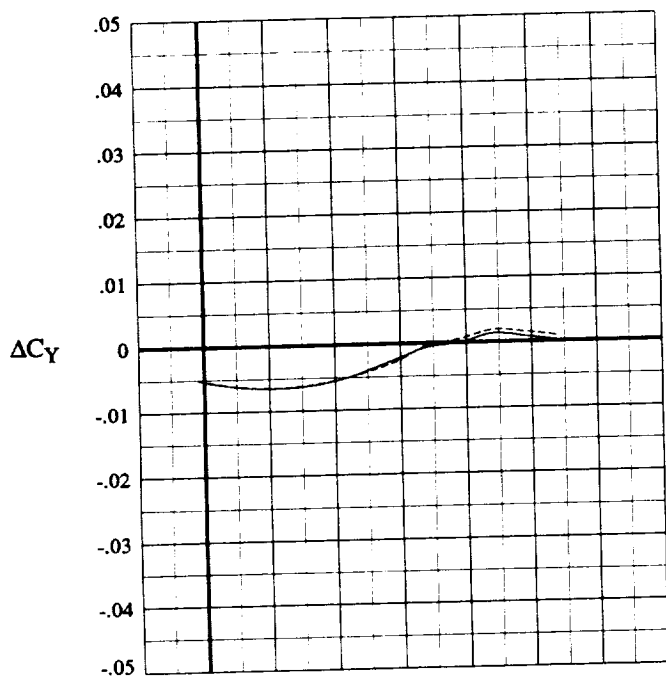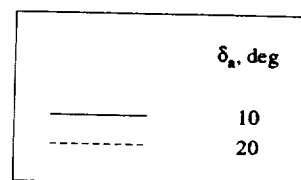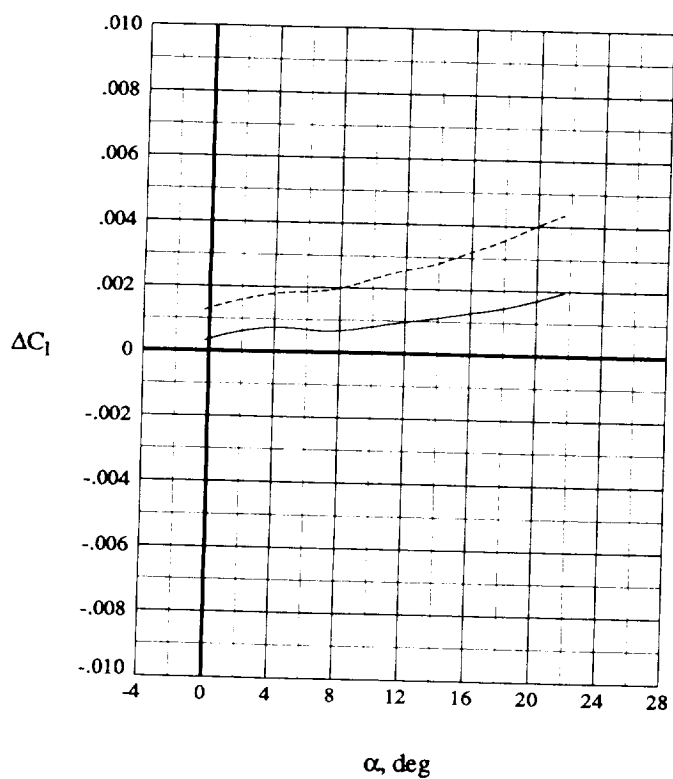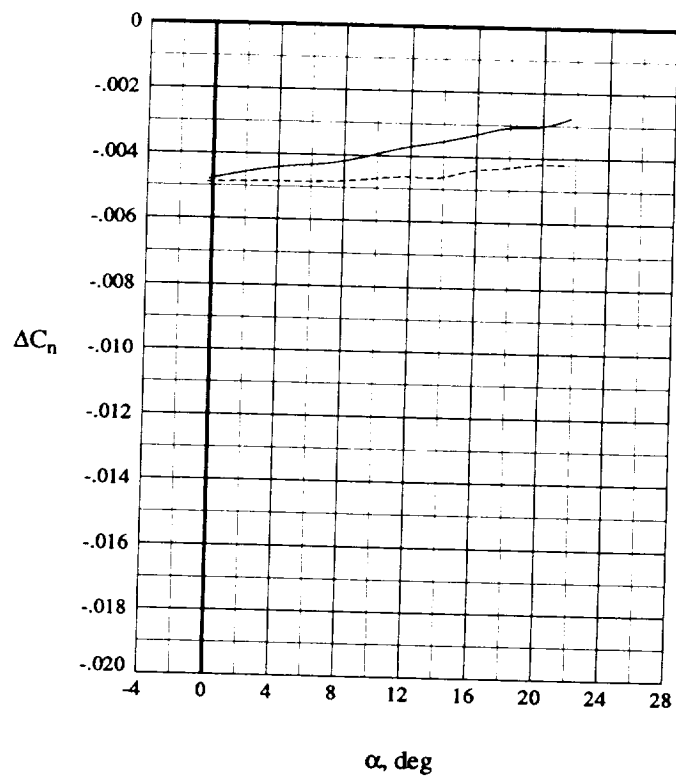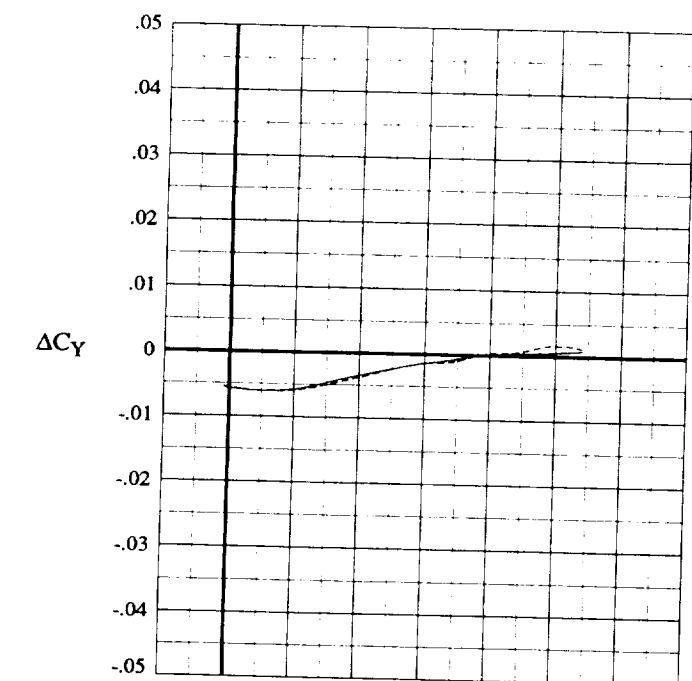viewing the collection of information. Send comments regarding this burden estimate or any other aspect of this collection of information, including suggestions for reducing this burden, to Washington Headquarters Services, Directorate for Information Operations and Reports, 1215 Jefferson Davis Highway, Suite 1204, Arlington, VA 22202-4302, and to the Office of Management and Budget, Paperwork Reduction Project (0704-0188), Washington, DC 20503

1. AGENCY USE ONLY*(Leave blank)*	2. REPORT DATE January 1994	3. REPORT TYPE AND DATES COVERED Technical Memorandum	

4. TITLE AND SUBTITLE
Supersonic Aerodynamic Characteristics of a Circular Body
Earth-to-Orbit Vehicle

5. FUNDING NUMBERS
WU 506-40-61-01

6. AUTHOR(S)
George M. Ware, Walter C. Engelund, and Ian O. MacConochie

7. PERFORMING ORGANIZATION NAME(S) AND ADDRESS(ES)
NASA Langley Research Center
Hampton, VA 23681-0001

8. PERFORMING ORGANIZATION REPORT NUMBER
L-17286

9. SPONSORING/MONITORING AGENCY NAME(S) AND ADDRESS(ES)
National Aeronautics and Space Administration
Washington, DC 20546-0001

10. SPONSORING/MONITORING AGENCY REPORT NUMBER
NASA TM-4533

11. SUPPLEMENTARY NOTES
Ware and Engelund: Langley Research Center, Hampton, VA; MacConochie: Lockheed Engineering & Sciences Company, Hampton, VA.

12a. DISTRIBUTION/AVAILABILITY STATEMENT

Unclassified Unlimited

Subject Category 02

12b. DISTRIBUTION CODE

13. ABSTRACT *(Maximum 200 words)*

The circular body configuration is a generic single- or multi-stage reusable Earth-to-orbit transport. A thick clipped-delta wing is the major lifting surface. For directional control, three different vertical fin arrangements were investigated: a conventional aft-mounted center fin, wingtip fins, and a nose-mounted fin. The tests were conducted in the Langley Unitary Plan Wind Tunnel. The configuration is longitudinally stable about the estimated center of gravity of 0.72 body length up to a Mach number of about 3.0. Above Mach 3.0, the model is longitudinally unstable at low angles of attack but has a stable secondary trim point at angles of attack above 30°. The model has sufficient pitch control authority with elevator and body flap to produce stable trim over the test range. The model with the center fin is directionally stable at low angles of attack up to a Mach number of 3.90. The rudder-like surfaces on the tip fins and the all-movable nose fin are designed as active controls to produce artificial directional stability and are effective in producing yawing moment. The wing trailing-edge aileron surfaces are effective in producing rolling moment, but they also produce large adverse yawing moment.

14. SUBJECT TERMS
Aerodynamics; Supersonic; Spacecraft; Booster

15. NUMBER OF PAGES
68

16. PRICE CODE
A04

17. SECURITY CLASSIFICATION OF REPORT Unclassified	18. SECURITY CLASSIFICATION OF THIS PAGE Unclassified	19. SECURITY CLASSIFICATION OF ABSTRACT	20. LIMITATION OF ABSTRACT